Segmentation of the Wasatch Fault Zone, Utah—Summaries, Analyses, and Interpretations of Geological and Geophysical Data

U.S. GEOLOGICAL SURVEY BULLETIN 1827

Segmentation of the Wasatch Fault Zone, Utah— Summaries, Analyses, and Interpretations of Geological and Geophysical Data

By RUSSELL L. WHEELER and KATHERINE B. KRYSTINIK

Descriptions, with supporting evidence, of segment boundaries as they are expressed in gravity, aeromagnetic, seismological, fault-geometric, topographic, and structural data

U.S. GEOLOGICAL SURVEY BULLETIN 1827

DEPARTMENT OF THE INTERIOR
DONALD PAUL HODEL, Secretary

U. S. GEOLOGICAL SURVEY
Dallas L. Peck, Director

UNITED STATES GOVERNMENT PRINTING OFFICE: 1988

For sale by the
Books and Open-File Reports Section
U.S. Geological Survey
Federal Center
Box 25425
Denver, CO 80225

Library of Congress Cataloging-in-Publication Data

Wheeler, Russell L.
Segmentation of the Wasatch fault zone, Utah—summaries, analyses, and interpretations of geological and geophysical data.
(U.S. Geological Survey bulletin ; 1827)
Bibliography: p.
Supt. of Docs. no.: I 19.3:1827
1. Faults (Geology)—Utah. I. Krystinik, Katherine B. II. Title. III. Title: Wasatch fault zone, Utah. IV. Series.
QE75.B9 no. 1827 557.3 s [551.8'7'097922] 87-600430
[QE606.5.U6]

CONTENTS

FIGURES

TABLES

CONVERSION FACTORS

For readers who wish to convert measurements from the metric system of units to the inch-pound system of units, the conversion factors are listed below.

Metric unit	Multiply by	To obtain inch-pound unit
meter (m)	3.281	foot (ft)
kilometer (km)	0.6214	mile (mi)
square kilometer (km^2)	0.3861	square mile (mi^2)

Segmentation of the Wasatch Fault Zone, Utah—Summaries, Analyses, and Interpretations of Geological and Geophysical Data

By Russell L. Wheeler *and* Katherine B. Krystinik

Abstract

The Wasatch fault zone of central Utah has been hypothesized to be segmented into lengths that tend to rupture independently of each other, with large seismic ruptures tending not to cross boundaries between segments. Validity of the segmentation hypothesis would affect estimates of seismic hazard for the urban corridor that contains most of Utah's population. Our evaluation of the hypothesis concentrates on detecting segment boundaries. To form a basis for this search, we examined six data types for anomalies that might record the presence and locations of segment boundaries that could influence the next few large seismic ruptures on the fault zone.

Mapped Bouguer gravity values define saddles, east-trending gradients, ends of north-trending gradients, and ends of north-trending highs and lows that together identify 10 transverse anomalies. Mapped aeromagnetic intensities show east-trending gradients and belts of small, intense highs that define three other transverse anomalies. Earthquake and microearthquake epicenters identify another four anomalies, as places where recent seismic activity along and near the trace of the fault zone changed markedly northward or southward along the zone. Geometry of the fault zone defines four more anomalies, which are large footwall salients around which the fault trace bows westward. Smoothed topography of the upthrown Wasatch Range and San Pitch Mountains defines two topographic anomalies. Consideration of pre-Cenozoic structures and geologic history identifies the Uinta aulacogen and two large, north-dipping lateral ramps in thrust sheets as three structural anomalies.

Each data type and its anomalies satisfy seven criteria that insure that the anomalies are pertinent to identification of segment boundaries and the evaluation of seismic hazard, and are reliable. The 26 anomalies appear to be concentrated in two narrow sections and one wide section of the fault zone, each of which might contain one or more segment boundaries.

This report is the second of three. The first described numerical methods for evaluating anomaly concentrations like those described in this report. The third report describes the application of the numerical methods to these concentrations, and the use of the results to help evaluate seismic hazard of the Wasatch fault zone.

INTRODUCTION

About two-thirds of Utah's 1.5 million people live within 25 km of the trace of the north-striking Wasatch fault zone (fig. 1; 1980 Census data). Large, young fault scarps along the fault zone indicate that seismic slip in the fault zone has continued through the late Pleistocene and Holocene and will probably continue into the future (Cluff and others, 1970, 1973, 1974, 1975; Cluff and Slemmons, 1972; Bucknam and others, 1980; Algermissen and others, 1982). The potential for future damaging earthquakes constitutes a hazard that needs to be assessed (Hays and Gori, 1984).

Swan and others (1980) and Schwartz and Coppersmith (1984) hypothesized that the fault zone is segmented into lengths that tend to rupture independently of each other. If their segmentation hypothesis is valid, large ruptures would tend not to cross boundaries between segments, so that most ruptures would stop at segment boundaries. The strained rock in a boundary at the end of a recent rupture would be a likely place for the next rupture to nucleate, so ruptures would also tend to start at segment boundaries (King and Nabelek, 1985). If ruptures tend not to cross boundaries, then segment lengths would provide an upper limit on potential rupture length, and hence on earthquake size. Thus, the validity of the segmentation hypothesis will influence estimates of possible mainshock locations and maximum sizes, both of which are important parameters in the probabilistic estimation of ground motion (Algermissen and others, 1982). Maps of estimated ground motion are widely used components of hazard assessment. The maps are often incorporated into building codes, seismic design criteria, analyses of potential losses, and other applications (Hays, 1979, p. 2, 20).

Accordingly, evaluation of the segmentation hypothesis as it applies to the Wasatch fault zone is an important part of hazard assessment for Utah (Wheeler, 1984). Our strategy for this evaluation is to seek evidence of segment boundaries that have persisted through

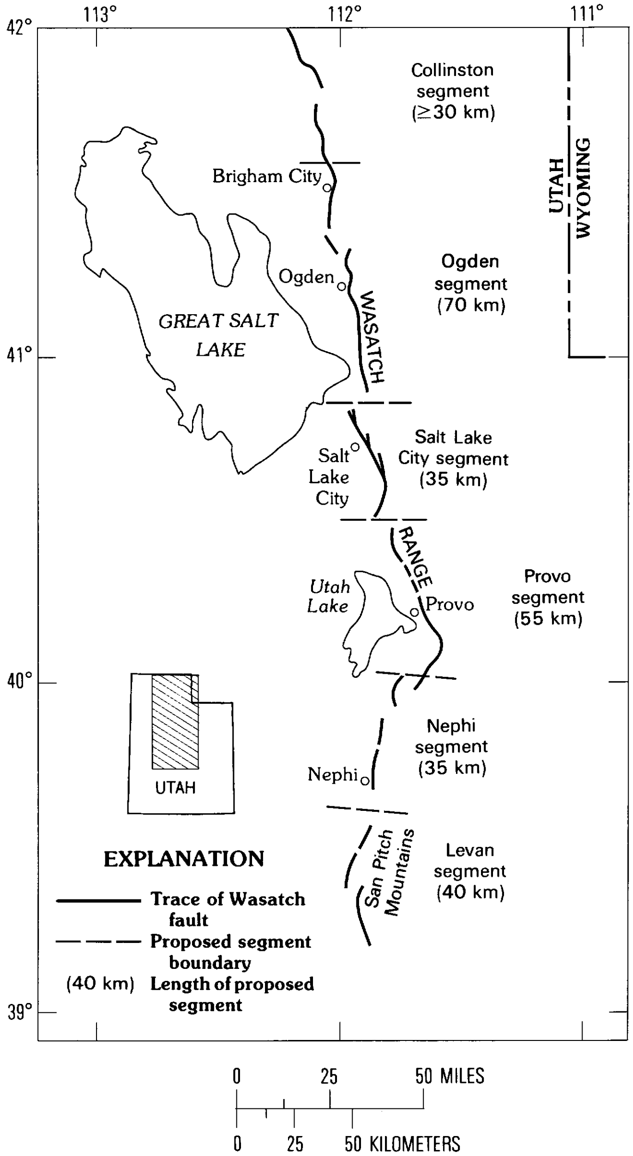

Figure 1. Index map of the Wasatch fault zone in northern central Utah, showing selected features along the Wasatch Front. The Wasatch Front is usually taken to include the populated valleys that lie along and immediately west of the trace of the Wasatch fault (Mabey, 1987) and which include most of the population of Utah. The high ground and mountains that border the fault on the east are called the Wasatch Range south to Nephi and the San Pitch Mountains south of there. Lat 42° N. marks the Utah-Idaho border. Segment boundaries are those of Schwartz and Coppersmith (1984), from whose figure 1 this map is modified.

enough of the geologic past that they are likely to continue to affect large ruptures through the next few centuries or millenia, the time span of interest in hazard assessment. We examined six types of data along and near the fault zone, seeking the kinds of anomalies that a persistent segment boundary should produce in each data type. Other processes than segmentation might produce similar anomalies in one or more data types. Where more anomalies coincide than would be expected by chance, and where these other processes can be ruled out on geologic grounds, we will have identified a persistent segment boundary.

The area studied stretches along the north-trending fault zone from central Utah at lat 39° N. to the Idaho-Utah border at lat 42° N. The study area has no fixed width, because for each data type the examined area extends east and west of the trace of the fault zone as far as is necessary to identify and characterize anomalies.

In this report we cannot present all aspects of our investigations. Here we describe the anomalies in each data type, demonstrate their validity, and estimate the locational uncertainty of each anomaly. Wheeler and Krystinik (1987a) described the statistical and related methods that we used to analyze the set of anomaly locations, and Wheeler and Krystinik (1987b, c, d) applied the methods to the anomalies and interpreted the results in terms of segment boundaries.

This report uses more diverse kinds of information than two authors could pretend to understand alone. We are unusually deeply indebted to topical and regional specialists for discussions, preprints, sharing of unpublished data and maps, and informal reviews of parts of the manuscript. These generous colleagues include W.J. Arabasz, R.L. Bruhn, Bruce Bryant, P.A. Cashman, T.G. Hildenbrand, R.M. Kligfield, D.R. Mabey, M.N. Machette, A.R. Nelson, C.G. Oviatt, S.F. Personius, W.E. Scott, Alain Villien, and M.L. Zoback. The entire manuscript was improved by the comments of M.N. Machette, A.R. Nelson, and K.M. Shedlock.

CRITERIA THAT THE DATA MUST SATISFY

Each of the six types of data that we examined, or the anomalies in a data type, must meet seven criteria. Criteria 1–4 were imposed by the geological aspects of the segmentation hypothesis. Criteria 5–7 were imposed by requirements of the statistical and related analyses of Wheeler and Krystinik (1987a).

The first criterion is that data must have a resolution that would enable them to show something the size of a segment boundary. For example, the distribution of earthquakes of magnitude 5 or greater along the Wasatch fault zone could not resolve segment boundaries because there have been too few such earthquakes in historic times. However, the many hundreds of closely spaced measurements of Bouguer gravity that have been collected by many workers and plotted and contoured by Zoback (1983) constitute data that have sufficient resolution potentially to detect segment boundaries.

Second, data must be capable of delineating whatever structures are likely to be responsible for large earthquakes along the Wasatch fault zone. We do not require that the data actually identify the causative structures of large earthquakes, but only that the data are likely to be useful in some future identification. For example, some measure of the youthfulness or abundance of fault scarps could be used, if such a measure could be made continuously or at intervals of a few kilometers along the fault zone. However, estimates of depth to the base of the crust are unlikely to be useful because most earthquakes along the fault zone take place at shallower depths (Arabasz and others, 1980).

Third, data must be likely to indicate the presence of a segment boundary by forming an anomaly whose relationship to the boundary can be explained. For example, Zoback (1983) noted that the contoured gravity values show several closed, elongate lows along the west side of the Wasatch fault zone. She argued that these lows correspond to low-density, sedimentary fillings of young basins that formed in the hanging-wall block during normal faulting. At several places along the fault zone such closed gravity lows are separated by gravity saddles or steep, east-trending gravity gradients that Zoback (1983) interpreted as indicating boundaries between adjacent basins of different depths.

The explanation of the gradients as indications of segment boundaries begins with the assumption that sediments of about the same age will have about the same densities in adjacent basins. Adjacent basins that have had similar depositional and subsidence histories will have similar gravity signatures, and thus will not be separated by a gravity gradient. Steep gradients between basins therefore record different times of basin formation, different amounts of downdropping of the basin floors, or both. Because the basins formed by motion on the Wasatch fault and associated faults, and because that motion can be assumed to have been mostly seismic, the steep gradients between closed gravity lows are likely to indicate boundaries between parts of the fault zone with different seismic histories. These parts would be segments. However, if the gravity data contained no steep, east-trending gradients, or if the gradients could not be explained in terms of possible segment boundaries, then the gravity data would not be a useful tool with which to evaluate segmentation.

Fourth, the data must record processes that operate over times that allow inferences to be drawn about the expected seismicity of the next decades to millenia. Accordingly, information on Precambrian structures would not be useful unless it can be shown that such structures were active during the late Pleistocene and Holocene, or influenced such young activity. Recently active structures are more likely to continue their activity into the near future than are structures that have been inactive for a long time. Elevations of the Bonneville shoreline east of the Wasatch fault zone could record segment boundaries because such elevations record uplift of the east wall of the fault zone since the shoreline formed about 15 ka. If adjacent segments had different amounts of uplift since the shoreline formed, then shoreline elevations east of the fault zone would vary more across segment boundaries than within the segments themselves. Unfortunately remnants of the shoreline on the east wall are too few to be able to resolve segment boundaries (Currey, 1982; Wheeler, 1984).

Fifth, identification of anomalies is a subjective procedure, so the anomaly locations must be shown to be reliable. For most data types we demonstrated reliability by showing that identical anomaly locations have been inferred by two independent workers. Underlying such a demonstration is the assumption that independent observers are unlikely to make the same error of interpretation by inferring the existence of an anomaly at the same place, if none exists there. Less preferably, if no second worker has analyzed the data, we demonstrated reliability by describing the identification of the anomalies in sufficient detail that an independent worker would be likely to reproduce the anomalies.

Sixth, the identification of the anomalies in any one data type must occur without reference to any other data type. If identification of anomalies in one data type were influenced by examination of a second type of data, then the anomalies in the first data type would contain information from the second. However, the statistical and related procedures of Wheeler and Krystinik (1987a) require that each data type be examined separately for anomalies, in order to determine where along the fault zone the data types have coincident anomalies.

Seventh, the anomalies must be identifiable without reference to the proposed segment boundaries of Schwartz and Coppersmith (1984). Otherwise, efforts to identify anomalies would be distorted by this prior inspection of the boundaries (Hicks, 1973, p. 15–16; Freedman and others, 1978, p. 494; Moore, 1979, p. 294–295; Wheeler, 1985). This seventh criterion does not duplicate the sixth, because we did not use the proposed segment boundaries as a data type.

BOUGUER GRAVITY DATA

Introduction

Zoback (1983) mapped, contoured, and interpreted complete Bouguer gravity data that had been collected, reduced, and compiled by many previous workers (for example, Cook and Berg, 1961; Cook and Montgomery, 1972, 1974; Cook and others, 1975). The area studied by Zoback spans long 111°–113° W. and lat 39°00′–42°15′ N. This area includes the Wasatch Front and Wasatch fault zone (fig. 1). Zoback (1983, fig. 3) interpreted her gravity map in terms of fault-bounded basins filled by low-density Cenozoic sediments and sedimentary rocks. The basins inferred from the gravity data correspond to those known from geologic mapping and subsurface investigations. The inferred basins trend north-south, and their gravity expressions are interrupted by transverse zones that Zoback (1983) interpreted as ends of basins or abrupt changes in basin depth. Several of the transverse zones also have recognizable expressions in surface geology (Zoback, 1983, p. 9, figs. 3–4).

In the study of gravity and magnetic data, the term anomaly has several established meanings (Gary and others, 1972; Bates and Jackson, 1980). We use the term anomaly to refer to unusual aspects of various types of geological or geophysical data that characterize some small parts of the Wasatch fault zone and distinguish them from nearby, less anomalous lengths of the fault zone. To avoid confusion between this usage of anomaly and those usages that are common in the study of gravity and magnetic data, this section and the section on aeromagnetic data refer to anomalies as transverse anomalies, following Zoback (1983). The word transverse does not imply that a transverse anomaly has an east-west extent that is larger than its north-south extent along the Wasatch fault zone. Some transverse anomalies are elongate east-west, but others represent just the north or south ends of gravity features that extend for several tens of kilometers along the fault zone. In particular, the presence of a transverse anomaly by itself does not justify the inference of an east-striking fault (Zoback, 1983, p. 3, 9).

The complete Bouguer gravity map of Zoback (1983) constitutes one type of data that can be examined along the Wasatch fault zone for transverse anomalies that might coincide with the proposed segment boundaries of Schwartz and Coppersmith (1984). The transverse zones of Zoback (1983) are candidates for these transverse anomalies, and indeed both Zoback (1983, p. 3) and Schwartz and Coppersmith (1984, p. 5688) noted that some transverse zones appear to coincide with some proposed segment boundaries.

Procedures

M.L. Zoback (written and oral communs., 1984) supplied copies of the gravity map used by Zoback (1983). The map, which was machine contoured at intervals of 2.5 mGal, is at a scale of 1:500,000 and shows only the isogals, station locations, and latitude and longitude marks at intervals of 0.5°. Thus, geologic, geographic, or geophysical information that might bias interpretation is not shown. In the several months before our analysis of the gravity map we took care not to compare the maps of Zoback (1983) and Schwartz and Coppersmith (1984), in order to reduce distortion of our interpretation by prior inspection.

Zoback (1983) and Mabey (1987) interpreted much the same gravity data and produced different sets of transverse anomalies. In order to determine which, if either, set to use, we must determine whether we can independently reproduce one of the sets. We demonstrate the credibility of our analysis by describing it in enough detail that a sufficiently determined reader could likely reproduce our results. Without the next three paragraphs a critical reader would have no reason to accept our set of transverse anomalies and therefore no basis for choosing the set of Zoback (1983) or that of Mabey (1987).

Using only the 1:500,000 gravity map as a base, we prepared four colored working maps (R.L. Wheeler, unpublished maps, 1986). The working maps cannot be reproduced here because color and large size are essential to their use. However, examples of most of the kinds of features described below are visible in figure 2 and in figures 2 and 4 of Zoback (1983). The procedures by which the working maps were prepared are more important than the maps themselves. If the procedures are accepted as reliable, then their results are reliable and the working maps are unnecessary for the acceptance of the transverse anomalies of figure 2.

The area covered, which is the central half of that mapped by Zoback (1983), spans long 111°30′–112°30′ W., a strip about 85 km wide that is roughly centered on the north-trending Wasatch fault zone (fig. 1). The working maps were designed to abstract and emphasize aspects of the complete Bouguer gravity field that best identify and locate structures like steep normal faults, low-density sediments that fill basins bounded by such faults, and north-south changes in the geometries of such faults and basins.

Of the four working maps, map 1 is a colored version of the contoured Bouguer gravity map and shows general features of the gravity field such as regional gradients and groups of connected lows and highs. Features seen on map 1 aided preparation of map 2, which shows shapes of inferred basins and intervening horsts. Features that we drew first on map 2 are trough and crest lines of elongate gravity lows and highs. We infer the lows to represent basins filled by low-density sediments, so the trough lines are interpreted as running approximately along the deepest parts of the basins. We infer the highs to represent bedrock horsts between basins, so the crest lines are interpreted as running approximately along the highest parts of the horsts. Map 2 also identifies saddles in the contoured surface that is represented by the gravity values of map 1. To avoid saddles that are minor, caused by single spurious values, or artifacts of the contouring algorithm, map 2 shows only saddles that are

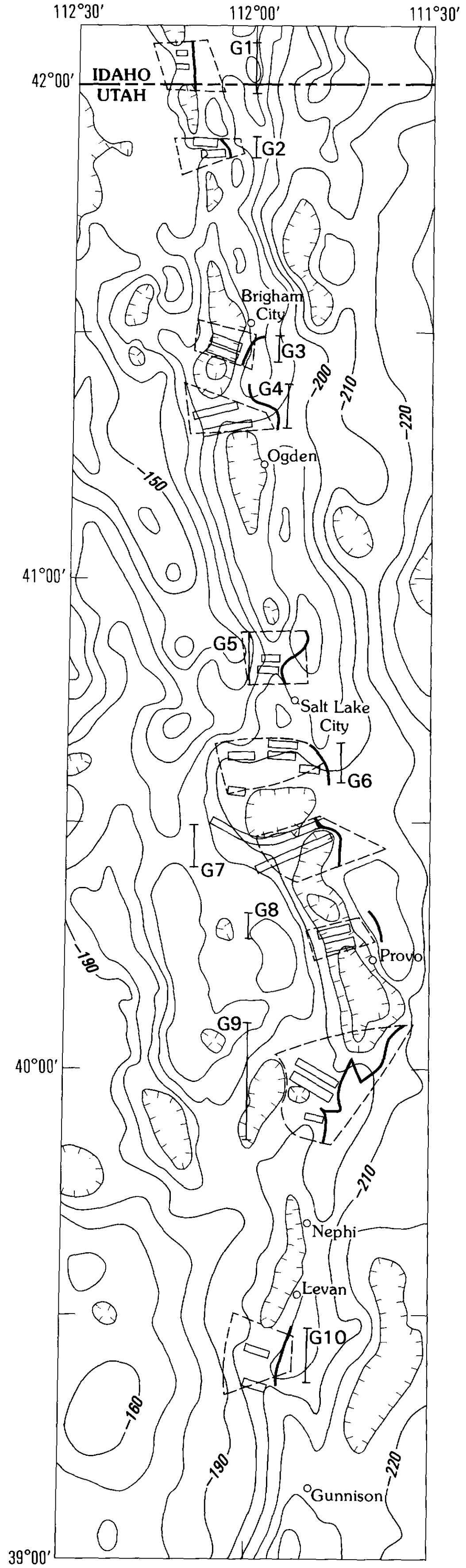

EXPLANATION

—200— Contour, in mGal, on complete Bouguer gravity field. Contour interval is 10 mGal. Hachures identify contour around closed gravity low. Gravity contours were traced and simplified from an enlarged clear-film version of the gravity map of Zoback (1983, fig. 2), which M.L. Zoback supplied at a scale of 1:500,000 and a contour interval of 2.5 mGal

Transverse zone as drawn by Zoback (1983, fig. 3). Only those transverse zones that lie along the Wasatch fault zone are shown

Transverse anomaly drawn by procedures described in text

Section of Wasatch fault zone that is intercepted by a transverse anomaly or its eastward projection. Fault traces simplified for clarity

G1 North-south extent of transverse anomaly G1, as projected east or west onto long 112° W. Projections of anomalies G3, G4, G6, G7, and G10 are offset from long 112°W. for clarity

0 10 20 30 MILES

0 10 20 30 KILOMETERS

Figure 2. Transverse anomalies (G) identified from map of complete Bouguer gravity field. The north-trending alignment of closed gravity lows, which have cities and towns along their eastern edges, marks the sediment-filled valleys that lie at the western base of the Wasatch Range and San Pitch Mountains.

controlled by more than three stations and outlined by more than two isogals, or which are defined by a trough line that crosses a crest line. We interpret saddles to represent either ends of basins or horsts, or places where basin depth or horst height is less than to the north and south in the same basin or horst. Map 3 shows inferred faults, as drawn along the steepest parts of long, moderately straight gradients in the gravity field. If the faults are assumed to be steep normal faults, then the sides toward the bounding gravity lows have dropped down. Ends of pairs of inferred faults that face each other and ends of gravity lows that are controlled by several stations were interpreted as representing the ends of fault-bounded basins.

Comparison of colored maps 1–3 allowed inference of block-faulted structure. Separate and explicit representation of the various features shown on maps 1–3 greatly aided identification of ends of fault-bounded basins and of abrupt steps along strike in basin depth or horst height. Inferred ends of basins and horsts, inferred steps, and saddles were compiled on map 4. Thus, map 4 shows gravity saddles, north- and south-facing gravity gradients, north and south ends of east- or west-facing gravity gradients, and north and south ends of elongate gravity highs and lows. Map 4 is simplified as figure 2.

Results

The structure interpreted by Zoback (1983, fig. 3) and that interpreted independently by us are essentially identical (fig. 2). All large fault-bounded basins mapped in either analysis were also mapped in the other. There are small differences in the degree to which basins are connected and in details of the shapes of inferred bounding faults. Each analysis mapped one small basin not mapped by the other; neither small basin lies along the fault zone. Along the fault zone, Zoback mapped transverse zones or groups of transverse zones at ten places. We mapped ends or steps in fault-bounded basins at these same ten places, and only there. In an independent study of much the same Bouguer gravity data, Mabey (1987) inferred block boundaries at six of these ten places and nowhere else along the fault zone.

The transverse zones of Zoback (1983) identify centers of transverse anomalies. However, we identified the boundaries of transverse anomalies. Boundaries have estimated accuracies of 1–2 km in most cases and less than 5 km in all cases. Most boundaries of transverse anomalies have estimated accuracies of 11–22 percent of the median width of the transverse anomalies. Transverse anomalies as identified in map view were projected onto a north-south line running along long 112° W. (fig. 2, table 1). Such a projection aids comparison of several data types and does not distort shapes of transverse anomalies much because the Wasatch fault zone also runs north-south (fig. 1). Schwartz and Coppersmith (1984) defined their segments only in Utah. However, our northernmost transverse anomaly extends 10 km north of the Utah-Idaho border at lat 42° N. (fig. 2); data north of the border will not be used.

The transverse anomalies obtained from analysis of the gravity data satisfy all seven of the criteria previously listed. First, the transverse anomalies have the necessary resolution to detect segment boundaries because transverse anomalies and segment boundaries (Schwartz and Coppersmith, 1984) have similar sizes and spacings along the Wasatch fault zone. Second, the transverse anomalies can show whatever structures are responsible for large earthquakes along the Wasatch Front, because scarps from such earthquakes are present on the Wasatch fault zone, and the transverse anomalies record different blocks in the hanging wall of the fault zone. Third, the transverse anomalies can indicate the presence of a segment boundary in an explainable way. The transverse anomalies delineate boundaries between basins of different depths in the hanging wall of the fault zone. Differences along strike in the amplitudes of the gravity lows record different thicknesses of sedimentary fillings of the basins, and different sedimentary thicknesses record different ages or rates of faulting. The faulting occurred seismically. Therefore, the transverse anomalies may be interpreted as separating segments of the fault zone whose hanging walls have had different seismic histories. Fourth, the transverse anomalies are products of faulting and sedimentation that have occurred more or less continually over the last several million years, that continue today as expressed in seismicity, and that therefore may be expected to continue into the next decades to millenia. Fifth, the transverse anomalies are reproducible because Zoback (1983) and we separately produced transverse zones or anomalies that are essentially identical (fig. 2). Mabey (1987) separately reproduced six of the ten transverse anomalies. Sixth, the transverse anomalies were derived without reference to any other data type of this report. Seventh, the transverse anomalies were derived without reference to the proposed segment boundaries of Schwartz and Coppersmith (1984).

AEROMAGNETIC DATA

Introduction

As is the case for gravity data, the term anomaly has several established usages in the study of magnetic data (Gary and others, 1972; Bates and Jackson, 1980). To avoid confusion with these established usages, we define a transverse anomaly in the magnetic data as a feature, usually a gradient or belt of narrow highs, and

Table 1. Locations of transverse anomalies interpreted from gravity data
[n.a., not applicable. Study area is 332 km long, north to south]

Transverse anomaly number	North end of transverse anomaly[1]	South end of transverse anomaly[1]	Transverse anomaly width (km)	Distance to next transverse anomaly to south (km)
G1	[2]-10	2	[2]2	10
G2	12	17	5	40
G3	57	63	6	5
G4	68	78	10	45
G5	123	135	12	13
G6	148	157	9	9
G7	166	175	9	11
G8	186	192	6	19
G9	211	237	26	42
G10	279	292	13	[3]40
Sum	n.a.	n.a.	98	234

[1]Distance south of Utah-Idaho border, in kilometers.

[2]Zoback (1983, fig. 2) showed that anomaly G1 extends 10 km north of Utah-Idaho border (north end of anomaly shown as negative number). Data north of border lie outside study area and are not used in this report, so width of G1 is taken as 2 km.

[3]Distance to south edge of study area at lat 39° N.

usually east-trending, that distinguishes a small part of the Wasatch fault zone from adjoining parts of the zone.

Various workers have mapped total magnetic intensity for north-central Utah and surrounding regions (Mabey and others, 1964; Zietz and others, 1976; Stewart and others, 1977; Mabey and others, 1983). The digital magnetic data set of Mabey and others (1983) has its eastern edge as much as 30 km west of the Wasatch fault zone, and so cannot be used here, but the other maps show a general northward rise in total magnetic intensity along the Wasatch Front. Superimposed on this rise are east-trending gradients and east-trending belts of high-amplitude, short-wavelength magnetic highs. Three of these east-trending features cross the Wasatch fault zone or abut it from the west.

Total magnetic intensity can be examined along the Wasatch Front for transverse anomalies that might coincide with proposed segment boundaries and with transverse anomalies in other data types. The east-trending magnetic features are candidates for transverse anomalies.

Procedures

Mabey and others (1964) and Stewart and others (1977) noted a south-facing magnetic gradient near the south end of Great Salt Lake and attributed the small, intense magnetic highs north of the gradient to Precambrian metamorphic rock at shallow depths. This Precambrian rock is exposed at several places in and around the Lake (Hintze, 1980). West of the Wasatch fault zone the small, intense magnetic highs and exposures of Precambrian rock continue northward about to Brigham City (figs. 1, 3; Zietz and others, 1976). This broad belt of small, intense magnetic highs constitutes transverse anomaly M1 of figure 3.

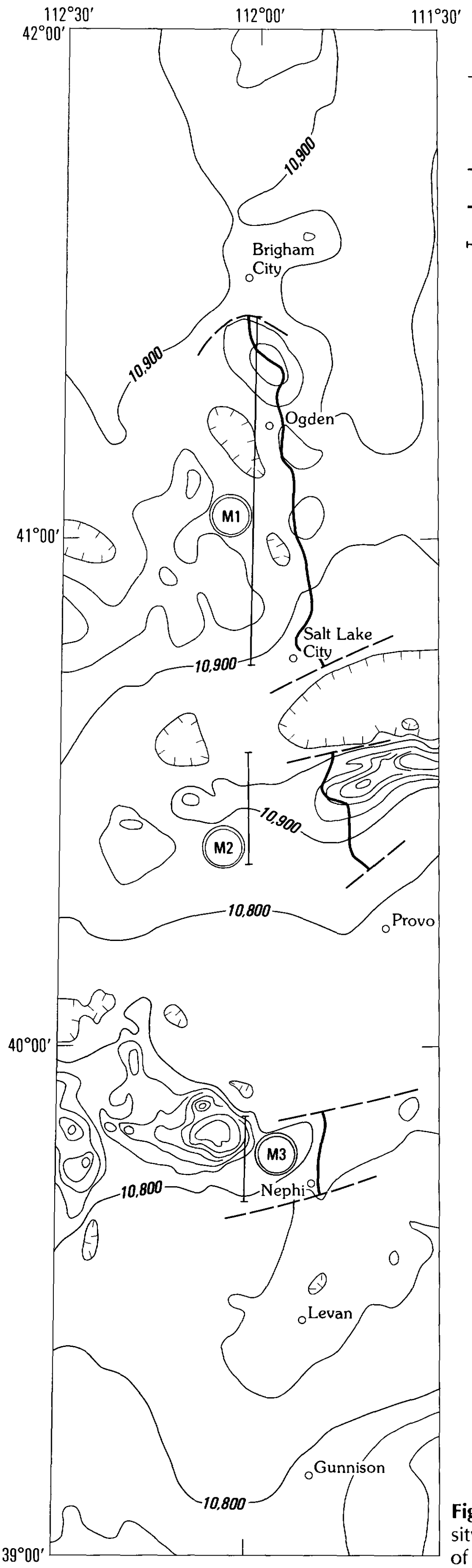

EXPLANATION

—10,800— Contour, in gammas, on total magnetic intensity, traced and simplified from map of Zietz and others (1976). Contour interval is 100 gammas relative to arbitrary datum. Hachures identify contour around closed magnetic low. Where contours are close together north of Provo and northwest of Nephi, parts of some are omitted for clarity

— — — Part of north or south edge of a transverse anomaly, drawn by inspection of map of Zietz and others (1976)

——— Part of trace of Wasatch fault zone that is intercepted by north and south edges of a transverse anomaly

(M1) Location of transverse anomaly M1 as projected from Wasatch fault zone east or west onto long 112° W.

0 10 20 30 MILES

0 10 20 30 KILOMETERS

Figure 3. Transverse anomalies (M) identified from total aeromagnetic intensity. For more detail, see colored map of Zietz and others (1976), most parts of which have contour intervals of 20 gammas.

Farther south, two other transverse anomalies are defined by narrow, east-trending belts of small, intense magnetic highs that are attributed to Tertiary intrusive and extrusive rocks (Mabey and others, 1964; Cook and Montgomery, 1972; Stewart and others, 1977, fig. 5). The Oquirrh-Uinta belt of Cook and Montgomery (1972) (Bingham-Park City zone of Mabey, 1987) crosses the Wasatch fault zone at about lat 40.5° N., and the Deep Creek-Tintic belt of the same authors (Tintic zone of Mabey, 1987) abuts the fault zone from the west at about lat 39.8° N. (fig. 3).

The north and south edges of these three belts of magnetic highs were mapped by Stewart and others (1977). We transferred these six east-trending edges to the more detailed magnetic map of Zietz and others (1976) and redrew them to conform to the more detailed magnetic contours of that map and the map of Mabey and others (1964). The east-trending edges meet the Wasatch fault zone at points, which we projected west onto a north-south line at long 112° W.

The magnetic data were collected along flight lines oriented east-west and spaced 2–4 mi (3.2–6.4 km) apart (Mabey and others, 1964; Zietz and others, 1976). Matching errors between adjacent east-trending flight lines can introduce east-trending artifacts into the mapped data. However, the east-trending belts that constitute the three transverse anomalies probably are not artifacts of matching errors between flight lines, for the following reasons. First, each belt is wide enough to involve several flight lines, and the edges of the belts cross flight lines obliquely in places. Second, belts are defined by closed magnetic highs with magnetic relief of 200–500 gammas, which is large enough to survive matching errors. Third, such closed highs are abundant inside the magnetic belts, but scarce outside the belts, indicating a real difference between magnetic susceptibilities, depths of burial of magnetic rocks, or both, inside and outside the belts.

The Wasatch Front lies at middle magnetic latitudes, so magnetic inclination causes a magnetic high to appear south of a magnetized rock body that causes the high (Vacquier and others, 1951, fig. 3; Nettleton, 1971, p. 74–77, figs. 55–57). Model calculations by T.G. Hildenbrand (oral commun., 1985) for a simple magnetic source with steep sides and uniformly induced magnetization (Vacquier and others, 1951, p. 3–15) indicate that this offset is about 8 km. For magnetic models that are equidimensional in map view and for the southward offset of 8 km, the dimensionless diagrams of Vacquier and others (1951, figs. A53–A60, A67–A70) imply depths to magnetic rock of 0–6 km, which could represent small intrusions that are exposed or buried beneath several kilometers of graben-filling sediments. For sources that are elongate east-west, implied depths are 6–14 km, which could represent upper- or mid-crustal igneous bodies from which shallow or now-exposed intrusions rose. These depths are consistent with local geology. Accordingly, locations of transverse anomalies were offset 8 km northward to approximate the true locations of causative rock masses and structures.

Results

Six points along long 112° W. represent the latitudes of the intersections of the Wasatch fault zone with the north and south edges of the three belts of magnetic highs (fig. 3, table 2). On inspection of the magnetic map of Zietz and others (1976), we found no other magnetic features that could constitute transverse anomalies in the study area. We estimate the accuracy of the distances shown in table 2 to be within 2–4 km, or 8–16 percent of the median width of the transverse anomalies, based on shapes and orientations of magnetic contours and on orientations and spacings of flight lines.

The transverse anomalies of table 2 meet the seven criteria listed above. First, the transverse anomalies and segment boundaries are similar enough in size that all could be represented on maps of the same scale (figs. 1, 3). The edges of the transverse anomalies have estimated locational accuracies of 2–4 km, which is accurate enough to detect segment boundaries.

Second, aeromagnetic data delineate the geometries of magnetic bodies of rock, and so are commonly used to identify igneous rocks and faults. Such structures are of the same sizes and at the same depths as the upper parts of faults that are likely to generate large earthquakes.

Third, the aeromagnetic data are likely to record the presence of a segment boundary in some explainable way. For example, transverse anomaly M1 (table 2) extends from about Salt Lake City to about Brigham City (fig. 3). Mabey and others (1964) attributed the small, intense magnetic highs within M1 to Precambrian metamorphic rock that is exposed (Hintze, 1980) or buried at shallow depths. Then the east-trending magnetic gradient that defines the south edge of M1 might arise from a fault, south of which the Precambrian rocks are dropped down. Such a fault might have formed during Tertiary extension, as a lateral ramp during Cretaceous thrusting of the Precambrian rocks, or earlier. Whatever its age and origin, the gradient extends eastward to the Wasatch fault zone, and so could record segmentation of the hanging wall of the fault. Similar explanations could apply to the more poorly expressed northern edge of M1. Similarly, the other two transverse anomalies are attributed to buried and exposed igneous rocks of Tertiary age (Mabey and others, 1964; Stewart and others, 1977; Hintze, 1980). Localization of igneous activity in elongated belts might indicate that the crust there was

Table 2. Locations of transverse anomalies interpreted from aeromagnetic data
[n.a., not applicable. Study area is 332 km long, north to south]

Transverse anomaly number	North end of transverse anomaly[1]	South end of transverse anomaly[1]	Transverse anomaly width (km)	Distance to next transverse anomaly to south (km)
M1	54	130	76	18
M2	148	173	25	54
M3	227	246	19	[2]86
Sum	n.a.	n.a.	120	158

[1]Distance south of Utah-Idaho border, in kilometers. Values are offset 8 km northward to correct for effect of magnetic declination.

[2]Distance to south edge of study area at lat 39° N.

unusually weak and perhaps fractured to depths at which magma was generated. If so, then at these two transverse anomalies the hanging wall of the Wasatch fault zone might still be weak and thus be segmented.

Fourth, the aeromagnetic data reflect processes that operate over times that allow inferences to be drawn about near-future seismicity, because the transverse anomalies can be interpreted to identify faults or other fractures that could still exist as weak zones and could divide the hanging wall of the Wasatch fault zone into blocks that might slip independently in the next large earthquakes.

Fifth, the transverse anomalies are reproducible because they were all identified by Mabey and others (1964), Stewart and others (1977), and us.

Sixth, the transverse anomalies in the aeromagnetic data were derived solely from the aeromagnetic maps of Mabey and others (1964), Zietz and others (1976), and Stewart and others (1977). This lack of influence from other data types holds even though the transverse aeromagnetic anomalies, once identified, were verified by comparison with gravity, geological, and mineral-deposit data (Mabey and others, 1964; Stewart and others, 1977; Hintze, 1980).

Seventh, the transverse anomalies were derived without reference to the proposed segment boundaries of Schwartz and Coppersmith (1984), because the transverse anomalies were identified by Mabey and others (1964) and Stewart and others (1977) before Swan and others (1980) and Schwartz and Coppersmith (1984) applied the segmentation hypothesis to the Wasatch fault zone and selected their particular proposed boundaries; Schwartz and Coppersmith (1984) do not mention magnetic data in their analysis of the fault zone.

EARTHQUAKE EPICENTERS

Introduction

Smith (1972, 1974) observed that two parts of the Wasatch Front that lie north and south of Salt Lake City had fewer earthquakes than did the parts that lie north of Ogden, around Salt Lake City, and south of Utah Lake (fig. 1). Cook and Smith (1967), Sbar and others (1972), and Smith and Sbar (1974) had noted the southern gap in seismicity, but Smith documented both gaps. Smith (1972) mapped epicenters of earthquakes with magnitudes of 3 or greater that occurred from 1961 to 1969. Smith (1974) mapped epicenters of earthquakes with magnitudes greater than 2 that occurred from July 1962 to September 1974 and showed a space-time plot of those epicenters that fell near the Wasatch fault zone. All three figures show both gaps, as do more recent epicentral maps and space-time plots for various time intervals from 1962 to July 1986 (Arabasz and others, 1980; Arabasz, 1984; Smith and Richins, 1984; W.J. Arabasz, oral communs., 1986).

We use the term gap in seismicity, because such gaps are what is observed in the figures cited here. We do not use the term seismic gap, because it connotes a seismically quiescent part of a fault zone that is more likely to yield in a large earthquake than are adjacent, more seismically active parts of the same fault zone.

Earthquake epicenters can be examined along and near the Wasatch fault zone for anomalies. The four ends of the two gaps in seismicity are candidates for anomalies and mark places in the fault zone across which the level of earthquake activity near the zone changed markedly.

Procedures

Seven versions of the two gaps in seismicity show the gaps to be centered about 100 km and about 200 km south of the Utah-Idaho border (fig. 4). Arabasz and others (1980) mapped epicenters from an earthquake catalogue that was revised from the one available to Smith (1972, 1974). Arabasz and others (1980) summarized the two gaps as originally shown by Smith (1974). Column 1 of figure 4 and Smith's (1972, 1974) three versions of the gaps all match the more recent versions and will not be used further. The similarity between all these versions of the ends of the gaps indicates that the existences and locations of anomalies Se1–Se4 are insensitive to differences between authors, earthquake catalogues, time intervals, and whether epicenters are plotted on a map or in a space-time diagram.

Each column in figure 4 represents the anomalies as points, but the anomalies have widths of several kilometers, and these widths can be estimated. The anomalies separate parts of the Wasatch Front that have had different rates of earthquake occurrence, at least over the two decades of record. If these differences in occurrence rates reflect differences in longer term rates of seismic slip, then the anomalies could represent changes in the amounts of seismic slip on the Wasatch fault zone, which might occur on cross faults. Any departures of the cross faults from east-west strikes, vertical dips, and perfectly planar shapes will give the anomalies widths exceeding zero. If the anomalies do not represent cross faults, then they might represent strained or complexly faulted rocks that link hanging wall blocks that have dropped down different amounts. In this case, the anomalies would also have widths exceeding zero. Therefore, the range in locations of a particular anomaly in columns 2–7 of figure 4 may be taken to represent some combination of the width of the anomaly and locational uncertainty of anomaly ends.

One or more of columns 2–7 might overestimate the width of a gap. Overestimation would happen if no earthquakes occurred near but outside a gap during the time interval on which one of columns 2–7 is based (fig. 5*A*). Then the gap and the associated anomaly would appear wider than they are. Alternatively, one or more columns might underestimate the width of a gap, because the gaps are not completely aseismic; several of the epicenter maps and space-time plots show isolated earthquakes that occurred within gaps. Even with these isolated earthquakes, the gaps remain markedly less seismically

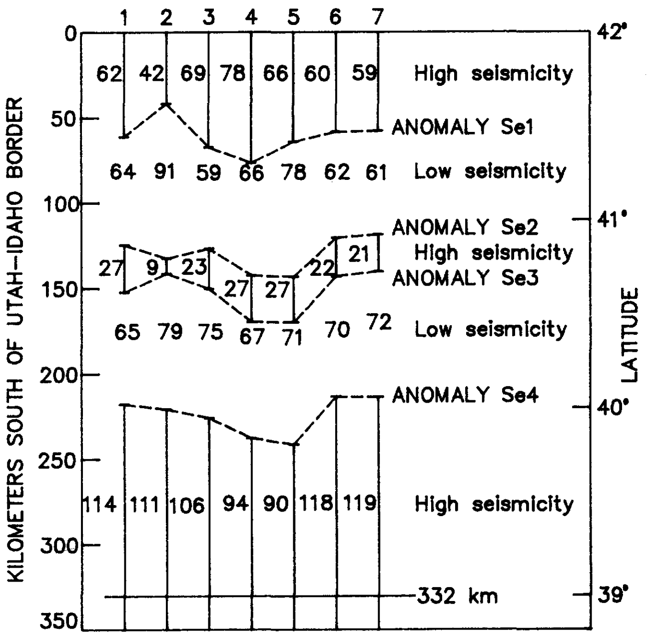

Figure 4. Changes in earthquake abundance along Wasatch Front, from north (top) to south (bottom). The seven vertical, broken lines depict seven estimates of the locations of changes in abundance of instrumental earthquakes. Solid lines show parts of the Front with many earthquakes located on or near the trace of the Wasatch fault zone, and gaps in these lines show parts of the Front with few or no earthquakes. Numerals to left of the solid lines and in the gaps show lengths of these parts of the fault zone, in kilometers, as projected onto a north-south line along long 112° W. Dashed lines connect the seven different estimates of the locations of each anomaly (change in earthquake abundance; Se).

Large numerals above the solid lines give sources of the seven estimates. 1, map of epicenters of earthquakes with magnitudes greater than 2, for July 1962–September 1974, as shown by Smith (1974, fig. 4) and interpreted by Arabasz and others (1980, fig. 3). 2, map of epicenters for October 1974–June 1978, as shown by Arabasz and others (1980, fig. 3) and interpreted by us. 3, revised map of epicenters for July 1962–September 1974, as shown by Arabasz and others (1980, fig. 4) and interpreted by us. 4, space-time plot of epicenters within 10 km of trace of Wasatch fault, for July 1962–June 1978, as shown and interpreted by Arabasz and others (1980, fig. 5). 5, same as 4 except interpreted by us. 6, map of epicenters for July 1978–December 1983, as shown by Arabasz (1984, fig. 5) and interpreted by us. 7, space-time plot of epicenters within 10 km of trace of Wasatch fault, for July 1962–December 1983, as shown by Smith and Richins (1984, fig. 10) and interpreted by us.

active than the surrounding parts of the fault zone. However, if such an isolated earthquake occurred in a gap but near its end, then an earthquake catalogue for a few years that contained the time of the isolated earthquake could underestimate the width of the gap (fig. 5*B*). If the resulting column in figure 5 were combined with other columns that did not include such isolated earthquakes within gaps, the anomaly at the end of the gap would appear wider than it should.

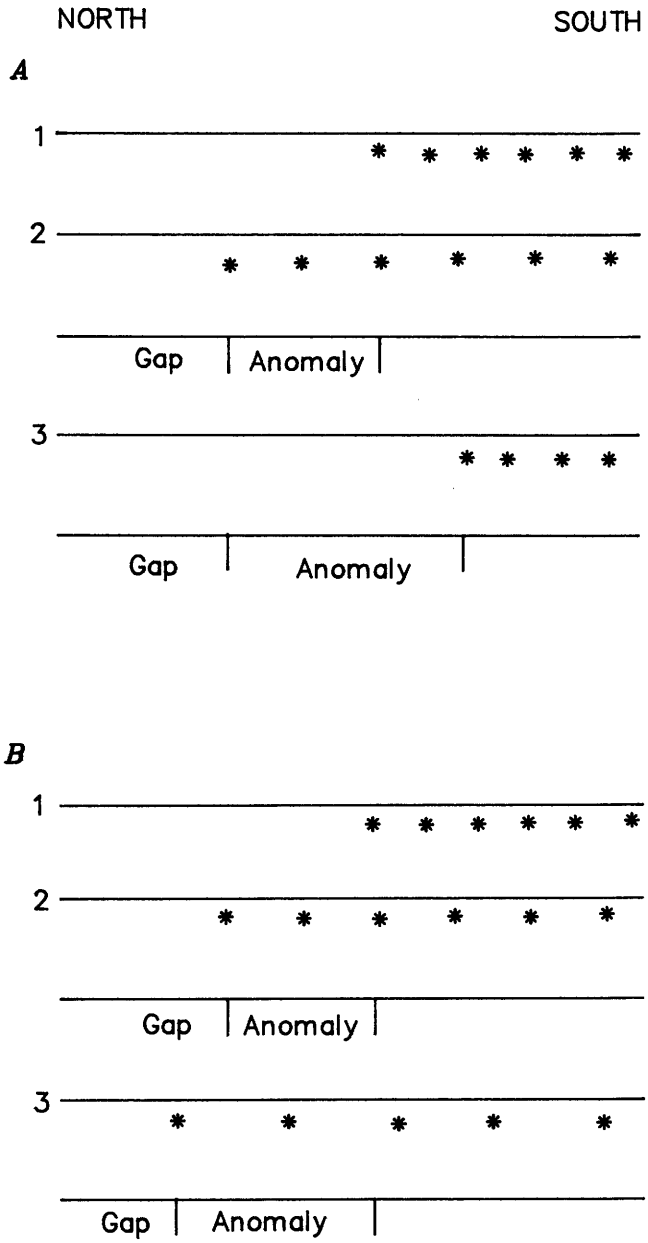

Figure 5. Overestimation and underestimation of widths of gap in seismicity and their effects on anomaly width. *A*, Overestimation of gap width causes overestimation of anomaly width. Schematic vertical cross-sections along Wasatch Front show locations of earthquakes (asterisks) during time intervals 1, 2, and 3. Gaps and anomalies inferred from these sequential locations are represented below 2 and 3. Time intervals 1 and 2 produce two different estimates of location of south end of gap. Assume these estimates are correct. The range of these estimates is the true width of the anomaly, as shown below 2. During the later time interval (3) no earthquakes are detected in the northern end of the seismically active part of the Wasatch Front, so the south end of the gap appears to be too far south and the gap appears wider than it is. The width of the anomaly is overestimated from 1, 2, and 3, as shown below 3. *B*, Similarly, underestimation of gap width also causes overestimation of anomaly width. During the later time interval (3) an isolated earthquake is detected inside the previously inactive gap, near its south end. The south end of the gap appears to be too far north and the gap appears narrower than it is. 1, 2, and 3 cause the width of the anomaly to be overestimated, as shown below 3.

Thus, both overestimation and underestimation of gap width cause anomalies to appear wider than they should. To guard against such errors we deleted any estimates of the location of the anomaly that make the anomaly seem unusually wide. These aberrant estimates were identified by inspecting histograms of the six estimates for each anomaly. For each anomaly, one or two estimates fall far above or below the others, are separated from them by a wide interval that contains no intermediate estimates, and would double or nearly double the anomaly width if the aberrant estimate or estimates were retained. For example, columns 2–7 place anomaly Se1 at 42, 59, 60, 66, 69, and 78 km south of the Utah-Idaho border (fig. 4). The value of 42 km is from column 2. The other five estimates are more tightly clustered, and give a width of 19 km for anomaly Se1. Adding the estimate from column 2 would widen the anomaly another 17 km, so this estimate is deleted and anomaly Se1 is taken as 19 km wide. Similarly, anomalies Se2–Se4 are taken to be 13, 10, and 13 km wide, respectively, by deleting the estimates of columns 4 and 5.

Once aberrant estimates of the location of an anomaly have been deleted, the remaining estimates define not only the width of the anomaly but also its north and south ends. For example, for anomaly Se1 five estimates remain after deleting that of column 2. The five estimates span 59–78 km south of the Utah-Idaho border, because column 7 places the north end of the anomaly a minimum of 59 km south of the border and column 4 places the south end at a maximum of 78 km (fig. 4).

Results

The ends of seismic anomalies (table 3) were identified from earthquakes that have occurred since 1962 and mostly since 1974. The location of each anomaly end was estimated from one of the columns of figure 4. Each column's estimate of the location of the end of a gap in seismicity was controlled by one or a few epicenters. Arabasz and others (1980, p. 1482) estimated from various tests that calculated locations of epicenters might be in error by 5 km or less. Accordingly, values in table 6 are assumed to be accurate to within 5 km, or within 38 percent of the median anomaly width.

The anomalies of table 3 meet the seven criteria listed above. First, the epicentral locations have estimated accuracies small enough to give them the resolution to

Table 3. Locations of seismological anomalies
[n.a., not applicable. Study area is 332 km long, north to south]

Anomaly number	North end of anomaly[1]	South end of anomaly[1]	Anomaly width (km)	Distance to next anomaly to south (km)
Se1	59	78	19	42
Se2	120	133	13	8
Se3	141	151	10	62
Se4	213	226	13	[2]106
Sum	n.a.	n.a.	55	218

[1]Distance south of Utah-Idaho border, in kilometers.

[2]Distance to south edge of study area at lat 39° N.

detect something the size of a segment boundary. Second, the earthquakes occurred from 1962 to 1983 and were mostly of magnitude 4 or smaller (Arabasz and others, 1980; Arabasz, 1984; Smith and Richins, 1984). These ranges of time and magnitude are large enough, and the epicentral locations are numerous and accurate enough, that the epicentral patterns of small earthquakes along the Wasatch Front are capable of delineating the locations and map shapes of whatever structures are likely to be responsible for large earthquakes. We do not require that the observed earthquakes actually are related to likely causative structures of large earthquakes, but only that the observed earthquakes be able to delineate the causative structures if a relationship exists. Third, spatial and temporal patterns of instrumental epicenters are likely to change in some way across segment boundaries. The ends of the gaps in seismicity could represent segment boundaries by recording differences in rates of seismic slip or in ratios of seismic to aseismic slip between fault blocks that constitute adjacent segments. Fourth, the instrumental earthquake data span about two decades, and the gaps appear consistently in catalogues that cover 1962–1974, 1974–1978, and 1978–1983 (fig. 4). This duration and stationarity of the gaps indicates that the gaps are likely to persist at least for the next few decades. Fifth, the gaps are reproducible, because they have been recognized by several workers. Sixth, the gaps were derived from epicentral locations alone, without reference to any other data type of this report. Seventh, the gaps were derived without reference to the proposed segment boundaries because the gaps were noted by Smith (1972, 1974) before segmentation was proposed for the Wasatch fault (Swan and others, 1980) and before Schwartz and Coppersmith (1984) proposed their boundaries, and also because suggested locations of gap ends have changed little since 1972 (fig. 4).

SALIENTS

Introduction

At four places along the Wasatch fault zone large projections of exposed footwall bedrock extend westward into the hanging wall. These projections are called salients (fig. 6; spurs of Gilbert, 1928; Zoback, 1983, p. 9; Bruhn, Gibler, and Parry, 1987; Bruhn, Gibler, Houghton, and Parry, 1987). The Pleasant View and Salt Lake salients consist of fault-bounded blocks that have dropped down with respect to the main part of the footwall that flanks them on the east, but have dropped less than has the hanging wall that flanks them on the west. At the Traverse Mountains salient the fault zone bulges sharply westward, with a partly down dropped block adjacent to the bulge on the southwest. The Payson salient consists of two south-trending ridges across which fault slip is distributed discontinuously as the fault zone steps southwestward across the ridges.

At these four salients the trace of the Wasatch fault zone departs from its usual aspect of a single, comparatively narrow fault zone with a straight or simply curved trace that runs along the west foot of the range front of the Wasatch Range (figs. 1, 6). King (1983) suggested that fractured rocks around sharp bends or forks in faults could initiate or halt seismic ruptures. At the salients the fault trace bends or forks, and rock exposed in the salients is broken by unusually abundant small

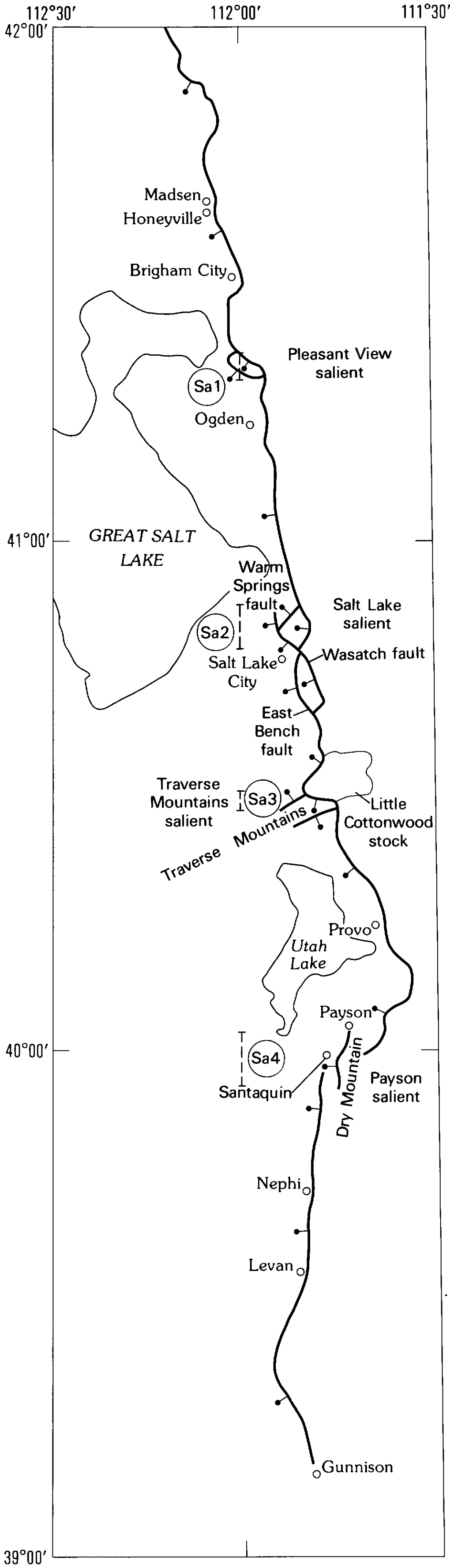

EXPLANATION

Mapped or inferred normal fault, bar and ball on downthrown side. Traced and simplified from Hintze (1980), with modifications after Van Horn (1972), Miller (1980, 1982), Zoback (1983, figs. 1, 4, p. 9), Davis (1983a, b, 1985), Crittenden and Sorensen (1985), Scott and Shroba (1985), Bruhn, Gibler, Houghton, and Parry (1987), and M.N. Machette (oral commun., 1986)

Sa1 Westward projection of anomaly Sa1 into long 112° W.

Geologic contact of Little Cottonwood stock, from Hintze (1980)

0 10 20 30 MILES

0 10 20 30 KILOMETERS

Figure 6. Salients (Sa) of the Wasatch fault zone.

faults (fig. 6 and maps and papers cited there). Accordingly, the geometry of the Wasatch fault in map view is a type of data that can be examined for anomalies. The salients are candidates for these anomalies.

Procedures

The four salients are large enough that the 1:500,000-scale Geologic Map of Utah (Hintze, 1980) shows them. Larger scale maps and topical reports provide details of the fault geometries in and around the salients. The expressions of salients in fault geometry and in exposed bedrock geology are distinctive enough that probably no large exposed salients have been missed. Support for this statement comes from consideration of three other westward-projecting footwall spurs that Gilbert (1928) discussed together with the salients of figure 6. The Madsen spur (Gilbert, 1928) nestles in a small reentrant of the range front and covers about 5 km^2 (Davis, 1985). Evidence for the existence of a fault-bounded bedrock salient at the Madsen spur is the issuance of hot springs from beneath an outcrop of limestone conglomerate or of mixed limestone and conglomerate, about 3 km west of the range front (Gilbert, 1928; Davis, 1985). From this observation Gilbert inferred the presence of breccia on a fault at the west end of the Madsen spur. However, mapping by C.G. Oviatt of pre-Cenozoic bedrock and Cenozoic sediments at and around the spur led Oviatt to conclude that the spur is a large rockslide (Oviatt, 1985, p. 53; C.G. Oviatt, written and oral communs., 1985, 1986). The geomorphic expression of the Honeyville spur led Gilbert (1928) to conclude that it is probably a landslide, covering less than 2 km^2, instead of a bedrock salient. Recent mapping confirms this (C.G. Oviatt, written commun., 1986; S.F. Personius, oral and written communs., 1985). Finally, Gilbert (1928) mentioned a small unnamed spur about 5 km north of Ogden. The spur, which exposes gneiss over most of its extent, is about 0.5 km wide and extends about 0.5 km west from the range front; the mapped trace of the Wasatch fault bulges westward around the west side of the spur (Crittenden and Sorensen, 1985). This spur is too small to constitute a salient in the sense of anomalies Sa1–Sa4 of figure 6. Therefore, these three other spurs are either too small or too likely to be of surficial origin to be grouped with the four salients shown in figure 6.

However, other salients might be hidden beneath the upper Cenozoic sediments that bury most of the hanging wall of the Wasatch fault zone. For example, Cook and Berg (1961, plate 13) inferred from a west-facing gravity gradient that the Warm Springs fault (fig. 6) extends north about 14 km from the west tip of the Salt Lake salient before rejoining the main trace of the Wasatch fault. Similarly, Van Horn (1972; see also review by Scott and Shroba, 1985) suggested that for the past 5,000 yr most faulting south of Salt Lake City has occurred on the East Bench fault instead of on the Wasatch fault along the range front (fig. 6). Thus, the Salt Lake salient might be flanked by two other unrecognized salients, one on the north that has dropped down too far to be expressed in exposed bedrock geology and one on the south that is too young for such expression. Such hidden salients might eventually be detected by combined use of gravity, seismic reflection or refraction, and geologic data. Such combined investigations are beyond the scope of this report. Also, the statistical analysis of Wheeler and Krystinik (1987a, d) requires that the different data types that are used must be examined independently of each other, in order that anomalies in any one data type are independent of anomalies in any other data type.

Results

Anomaly Sa1 (fig. 6, table 4) is the Pleasant View salient of Eardley (1944), also called the Pleasant View spur by Gilbert (1928) and the Warm Springs salient by Morisawa (1972, p. D13). This salient is nearly surrounded by mapped and inferred normal faults. It exposes Cambrian rocks over 3–4 km^2 that are separated from the Wasatch Range by a 1–2-km-wide cover of Quaternary sediments (Gilbert, 1928; Davis, 1985; Crittenden and Sorensen, 1985; Personius, 1986). The thin veneer of sediment that covers most of the salient contains an unusually wide zone of numerous short, discontinuous, poorly expressed fault traces, scarps, grabens, photolineaments, and related features all of diverse orientations (Cluff and others, 1970; Miller, 1980; Crittenden and Sorensen, 1985).

Anomaly Sa2 is the Salt Lake salient of Eardley (1944), also called the City Creek spur by Gilbert (1928) and the Ensign Peak salient by Snay and others (1984, p. 1115), and termed another Warm Springs salient by Morisawa (1972, p. D13). This salient is mostly bounded by mapped and inferred normal faults. Within the salient, Cambrian to Eocene rocks are exposed almost continuously to their eastern fault contact with the Wasatch Range (Gilbert, 1928; Hintze, 1980; Davis, 1983a; Bryant, 1984). Scarps of latest Quaternary age (Scott and Shroba, 1985) are present in two areas on the south side of the salient and are interspersed with less prominent scarps and inferred fault traces elsewhere around the salient (Cluff and others, 1970; Miller, 1980).

Anomaly Sa3 is the Traverse Mountains salient, also called the Traverse spur by Gilbert (1928), at which upper Paleozoic sedimentary rocks and Eocene to Oligocene intrusive rocks in the footwall (Hintze, 1980; Davis, 1983b) adjoin upper Cenozoic basin-filling sediments

Table 4. Locations of anomalies interpreted from fault geometry
[n.a., not applicable. Study area is 332 km long, north to south]

Anomaly number	North end of anomaly[1]	South end of anomaly[1]	Anomaly width (km)	Distance to next anomaly to south (km)
Sa1	70	76	6	48
Sa2	124	134	10	31
Sa3	165	169	4	48
Sa4	217	230	13	[2]102
Sum	n.a.	n.a.	33	229

[1]Distance south of Utah-Idaho border, in kilometers.

[2]Distance to south edge of study area at lat 39° N.

(M.N. Machette, unpublished mapping, 1986) across the Wasatch fault zone. The fault zone bows sharply west to pass around the Little Cottonwood stock (Lone Peak salient of Gilbert, 1928) in the footwall. Traverse Mountains salient itself is bounded by faults on the northwest and southeast sides and is in fault contact on its northeast with the Little Cottonwood stock of the Wasatch Range. Where the Wasatch fault crosses bedrock at the salient, the fault becomes degraded (Cluff and others, 1973) and loses the steep, little-modified scarps that led Anderson and Miller (1979) to suggest a Holocene age for scarps of the Wasatch fault zone north and south of the salient.

Anomaly Sa4 is here named the Payson salient, which Gilbert (1928) and Loughlin (1913) observed to comprise a pair of north-trending, north-sloping bedrock ridges west of Dry Mountain, south of Payson and south of Santaquin. Between the ridges and north and south of them the Wasatch fault zone is continuous and has well-defined scarps of Holocene age (Cluff and others, 1973; Anderson and Miller, 1979; Machette, 1984). The ridges expose complexly faulted, folded, and tilted rocks of Precambrian through Tertiary ages. Four to five kilometers southwest of Santaquin bedrock exposures are nearly continuous across the northward projection of the Wasatch fault zone (Hintze, 1980; Davis, 1983b). The nearly continuous exposures reveal the presence of a partly buried bedrock ridge trending southwest from Santaquin, similar to the Traverse Mountains salient. Different authors drew the trace of the main fault through the bedrock in the two ridges and under the adjacent Quaternary sediments in markedly different ways (reconnaissance map of Morisawa, 1972, fig. 1; compilation of Anderson and Miller, 1979; bedrock geologic map of Metter, 1955, as compiled by Davis, 1983b; M.N. Machette, unpublished mapping, 1986).

The locations of anomaly ends (table 4) are uncertain for two reasons. First, cartographic errors from drafting and measurement during our compilation might move each anomaly end as much as 1 km north or south. Second, larger uncertainties in the locations of north and south ends of anomalies arise from ignorance of the subsurface geometries of the salients. However, these uncertainties can be estimated. Because the faults that bound the salients formed in extension, dip slip has been normal and the faults are unlikely to dip inwards under the salients. The north-south widths of the anomalies in the subsurface will be no smaller than the exposed widths of table 4, but they could be larger. Smith and Richins (1984, p. 97, figs. 9, 11) estimated that large normal-faulting earthquakes of the Basin and Range province nucleate at depths of about 15 km. If planar salient-bounding faults dip 45°–60°, their down-dip lengths must be 17–21 km to reach depths of 15 km. In map view large changes in fault geometry can take place over horizontal distances of 17–21 km (fig. 6). If such large geometric changes can also take place down the dips of the faults that bound the salients, then it would be difficult to estimate the subsurface widths of the salients from exposed widths.

However, down-dip changes in geometry of the Wasatch and related faults likely are smaller than along-strike changes. From oil well, seismic reflection, gravity, and topographic data at six places along the Wasatch fault zone, Zoback (1983, fig. 6) estimated that minimum structural relief across the fault zone is 2.6–4.0 km. Parry and Bruhn (1986, 1987) examined fluid inclusions in fault rock at the southern and western edges of the Little

Cottonwood stock and a stratigraphic reconstruction, and they concluded that uplift on the fault zone was at least 11 km. Dips of 45°–60° and uplifts of 2.6–4.0 km and of 11 km would require dip slip of 3–16 km. Dip slips this large might have broken asperities and otherwise smoothed some irregularities in the down-dip geometry of the Wasatch fault zone. Little such smoothing of the along-strike geometry is likely to have occurred, because the irregular shape of much of the fault trace around the salients (fig. 6) argues against large amounts of strike slip. Thus, the fault zone is likely to change its geometry less down its dip than along its strike. Accordingly, it is worthwhile to estimate subsurface widths of salients from exposed widths.

The Pleasant View salient nestles in a southwest-facing embayment in the footwall of the Wasatch fault zone. The north and south ends of the embayment are about 5 km beyond the ends of the salient (Davis, 1985; Crittenden and Sorensen, 1985). If the salient at depth merges smoothly into the ends of the embayment, then the salient could be as much as 10 km wider at depth than its exposed width of 6 km. With cartographic errors of 1 km or less at each end, the Pleasant View salient might be as narrow as 4 km or as wide as 18 km.

The Salt Lake salient might be several times as wide in the subsurface as at ground level. Van Horn (1972), Scott and Shroba (1985), and earlier workers mapped the East Bench fault on the south side of the salient (fig. 6) about 5 km west of the main trace of the Wasatch fault and extending southward about 15 km beyond the south end of the salient. Van Horn (1972) estimated that the East Bench fault moved within the last 5,000 yr. Scott and Shroba (1985, p. 8–9) give evidence for middle to late Quaternary movement on this fault. From a shallow seismic-reflection profile, Crone and Harding (1984, p. 249–252) estimated that the East Bench fault had as much as 85 m of dip slip during Quaternary time. For the north side of the salient, Pavlis and Smith (1980) compiled several estimates of the northward extent of the Warm Springs fault (fig. 6). The compilation indicates that the Warm Springs fault might extend in the subsurface about as far north of the salient as the East Bench fault extends south of it. Therefore, the Salt Lake salient might be bounded on north and south by two blocks that have dropped down enough that they are buried today. The two buried blocks and the comparatively high salient might act together to control large seismic ruptures. If each buried block has a north-south width of 15 km, then with cartographic uncertainties the Salt Lake salient might be as narrow as 8 km or as wide as 42 km in the subsurface.

The Traverse Mountains salient is bounded by border faults that dip northwest and southeast (fig. 6). Zoback (1983, p. 9) inferred the existence of the fault on the northwest side of the salient from a steep, northwest-facing gravity gradient and from drilled depths to consolidated rock (Mattick, 1970). Hunt and others (1953, p. 38, plate 1) mapped a fault along the southeast side of the salient. M.N. Machette (unpublished mapping, 1986) found neither fault to be exposed nor to show evidence of late Pleistocene slip. Southwest-plunging slip vectors on the Wasatch fault zone north of the salient, together with the northeast strike of the northwest-dipping border fault, constrain the border fault to dip steeply (Bruhn, Gibler, Houghton, and Parry, 1987; Bruhn, Gibler, and Parry, 1987). Dip magnitude of the southern border fault is unknown. We assume that both border faults dip 45°–60°, to obtain a conservatively large estimate of the maximum subsurface width of the salient. The northern border fault strikes N. 61° E., and the southern border fault strikes N. 68° W. (Miller, 1982; Davis, 1983b). For these strikes and dips, both faults would reach depths of 15 km between 9 and 15 km northwest or southeast of their traces. By projecting these distances into a north-south line, the northern border fault is calculated to reach a depth of 15 km between 8 and 13 km farther north than the point at which the trace of the border fault meets the trace of the Wasatch fault (fig. 6). Similarly, the southern border fault could extend at depth 8–14 km farther south than its outcrop at the Wasatch fault. With cartographic uncertainties the northern end of anomaly Sa3 might be as much as 14 km farther north than shown in figure 6, and the southern end might be as much as 15 km farther south than shown. Anomaly width could then be as small as 2 km or as large as 33 km.

At the Payson salient, geologic maps (Metter, 1955; Hintze, 1980; Davis, 1983b) show small normal faults that extend south along the west side of Dry Mountain, with bedrock exposed on both sides of the small faults. Stratigraphic separation on the largest of these faults decreases southward. Within 5 km south of the southern edge of the anomaly some of the normal faults are lost in a thick, undifferentiated mass of Pennsylvanian and Permian strata, and the other normal faults bend southwestward to merge with the main strand of the Wasatch fault zone. North of Payson, these normal faults disappear under the Quaternary sediments around Utah Lake. The north end of the anomaly is taken as the north end of the large normal fault on the west side of Dry Mountain (fig. 6). Mapping by M.N. Machette (oral commun., 1986) shows that this fault extends northeast in Quaternary sediments to the southeastern outskirts of Payson, where it turns toward the north and borders a bedrock-cored ridge. Thus, the anomaly is 13 km wide along a north-south line. To protect against unmapped faults at the south end of the anomaly and buried fault tips at both ends, we arbitrarily assumed that the anomaly might extend another 10 km beyond its ends as shown in figure 6. Then, with cartographic uncertainty of 1 km, the anomaly could be 2 km narrower or 22 km wider than shown in table 4, for a width of 11–35 km.

The geometric anomalies meet the seven criteria listed above. First, the data can detect something the size of a segment boundary, because the four salients are of about the same sizes as are the segment boundaries of Schwartz and Coppersmith (1984). The salients are recognized from the geologic compilation of Hintze (1980), which depicts and distinguishes many features as small as 1 km.

Second, the data are able to reflect whatever structures are responsible for large earthquakes along the Wasatch Front. The salients are defined by the shapes of the traces of the Wasatch and related faults, which have structural reliefs of hundreds to thousands of meters (for example, Zoback, 1983, fig. 6). Motion on these faults was mostly seismic, because young scarps are present along most of the fault traces, and because where measured in trenches across such faults, vertical displacements of ancient ground surfaces are typically about 2 m per scarp-forming event along the Wasatch fault zone (Schwartz and Coppersmith, 1984). A compilation of characteristics of historic surface faulting in the Basin and Range province (Bucknam and others, 1980) indicates that most surface ruptures in the province have been associated with earthquake magnitudes of at least 6, and usually of at least 7. The smallest historic surface rupture was produced by an earthquake of magnitude 5.6. Surface offsets greater than 1.0 m are known only from earthquakes whose magnitudes exceeded or probably exceeded 7 (Bucknam and others, 1980; Crone and Machette, 1984), so the earthquakes that formed the salients incrementally were mostly large.

Third, the data are likely to reflect the presence of a segment boundary by an explainable anomaly. For example, a segment boundary might produce a salient as a nonconservative barrier to rupture propagation: each salient involves large bends or forks in the trace of the Wasatch and related faults. If slip vectors change orientations across such geometric irregularities, the bends and forks are termed nonconservative barriers (King and Yielding, 1984). King (1983) used geometric arguments to conclude that nonconservative barriers should be embedded in networks of small interlocking faults of many orientations. King and Nabelek (1985) called these networks process zones. Process zones form soft volumes of shattered rock that absorb the energy of incoming ruptures by dispersing it among many small faults. Where the small faults intersect larger faults, motions on the small faults offset the larger faults. The offsets lock the larger faults to form asperities and destroy the throughgoing continuity of the larger faults. Then the incoming ruptures cannot find easy paths through the process zones, so these soft rock volumes have high fracture toughness. Accordingly, large seismic ruptures should tend to stop at nonconservative barriers. When small earthquakes within a process zone have broken the asperities, one or a few asperities at a time, a later large rupture can initiate in the edge of the process zone and propagate beyond the zone. Thus, large seismic ruptures should tend to be restricted to lengths of a fault between nonconservative barriers. Such lengths would be segments, and the nonconservative barriers would be segment boundaries. King and Yielding (1984) and King and Nabelek (1985) gave examples of strike-slip and reverse faults that are, or appear to be, segmented by bends that are interpreted as nonconservative barriers. Bruhn, Gibler, Houghton, and Parry (1987) and Bruhn, Gibler, and Parry (1987) applied these ideas to the Wasatch fault zone and interpreted the Salt Lake and Traverse Mountains salients as nonconservative barriers. Bruhn and coworkers measured orientations of slip vectors for the fault strands that meet in forks at the south end of the Salt Lake salient and the north end of the Traverse Mountains salient, and showed that these slip vectors change orientations across the forks. They interpreted the forks as nonconservative barriers; the barriers could be segment boundaries.

Fourth, the data reflect faulting processes that have operated continually over the past few million years. There is no geological reason to expect these processes to change their long-term behavior over the next few millenia; probably salients will stay where they are.

Fifth, the anomalies are reliable and probably reproducible. Gilbert (1928) recognized the four salients of figure 6 and no others that are comparably large and deeply rooted. Neither we nor the reports and maps cited earlier change this list of four large salients.

Sixth, the anomalies were derived without reference to any other data types in this report. Gravity data were used to support estimates of the northward extent of the Warm Springs fault (Pavlis and Smith, 1980) and of the amount of dip slip on the Wasatch fault zone (Zoback, 1983, fig. 6), but were not used to identify the anomalies themselves.

Seventh, the anomalies were derived without reference to the segment boundaries of Schwartz and Coppersmith (1984), because the anomalies were derived solely from maps and descriptions of the trace of the Wasatch and related faults and of the Cenozoic and older bedrock geology that is exposed along and near these faults.

TOPOGRAPHIC DATA

Introduction

Schwartz and Coppersmith (1984, fig. 10, p. 5688–5689) examined elevations at 37 points along the crest of the Wasatch Range and San Pitch Mountains (fig. 1) and observed that crestal elevation changes across their proposed segment boundaries. They suggested that segment boundaries divide the footwall of the west-dipping Wasatch fault zone into blocks that have experienced different amounts of uplift and presumably different seismic histories. However, Wheeler (1984) showed that the changes in crestal elevation across the proposed segment boundaries are not significantly larger than changes between the boundaries. The implication is that spot elevations might be influenced too much by local variations in lithology and erosion rates to reflect clearly any segmentation that might be present along the fault zone.

However, Wheeler (1984) suggested that other representations of topography might be able to reflect segmentation. A footwall block that has been uplifted more than its neighbors to the north or south should be higher than the neighboring blocks, wider, or both. The topographic expression of differential uplift can be obscured by many local factors, including irregular fault geometry, lithologic variation between and within stratigraphic units, variation in the structure of the thrust sheets and related folds that make up most of the footwall, variation in erosion rates, and streams that cut through the high ground of the footwall. Accordingly, the topography should be generalized in some way, to try to smooth out effects of these obscuring factors. A simple way to generalize topography is to inspect a small-scale topographic map with a large contour interval (U.S. Geological Survey, 1976), to select and trace a few contours that most clearly summarize the overall shape of the footwall block and to smooth the selected contours during tracing by omitting small irregularities caused by minor drainages (fig. 7). Places where elevation or width of the high ground appears to change along the Wasatch Range and San Pitch Mountains are candidates for anomalies that might coincide with the proposed segment boundaries of Schwartz and Coppersmith (1984).

Procedures

Generalizing topography to produce figure 7 was subjective. To minimize this subjectivity, we selected every fourth 500-ft topographic contour, instead of unevenly spaced contours. In smoothing contours to eliminate small irregularities caused by small drainages, we used about the same degree of smoothing everywhere and for each selected contour. The distortion introduced in generalizing topography is probably less than the variability among the 12 persons who examined the smoothed topography for anomalies, as described next.

Topographic anomalies were identified by interpreting figure 7, but the interpretation was subjective. To minimize effects of subjectivity and to demonstrate reproducibility of any interpretations, 12 independent interpreters (not including us) were given copies of the topographic map of figure 7 containing only topography, legend, scale bar, and latitude-longitude marks. The three panels of the figure were taped together into a single strip map. The interpreters were asked to pick places where the height, width, or both of the Wasatch Range or San Pitch Mountains appeared to change abruptly northward or southward. Interpreters were asked to ignore features that looked like river valleys that cross the ranges and interrupt their overall height and width.

Interpretations differed markedly. No change was picked by all 12 interpreters. Fourteen changes were each picked by one or more interpreters. Five of the 12 interpreters are familiar with various aspects of the geology of the Wasatch Front and with the segmentation hypothesis (fig. 8*A*). The other seven have little or no such familiarity (fig. 8*B*). A Chi-squared test showed that the two groups do not differ significantly ($P=0.56$) in numbers of interpreters that picked each of the 14 changes, so results from the two groups of interpreters were combined (fig. 8*C*).

Despite the variations between interpreters, the 14 changes fall into two distinct groups according to their popularities (fig. 8*C*). Only two of the 14 changes were picked by half or more of the interpreters, and these two are taken as anomalies in the sense of this report.

Only three of the 12 interpreters picked these two changes and no others. Thus, the two anomalies of figure 7 might seem obvious now, but no one interpreter could have demonstrated in advance that these two changes, and only these two, should be chosen.

Results

Perusal of the topographic map from which figure 7 was derived (U.S. Geological Survey, 1976) indicates that values in table 5 are accurate to within about 2 km, or about 24 percent of the median anomaly width.

The topographic data and anomalies meet the seven criteria set out previously. First, figure 7 has sufficient resolution to detect a segment boundary. Local uncertainties of the original topographic map are less than those introduced by tracing contours to produce figure 7. These tracing errors are less than 3 km and generally less than 1 km. The errors consist mostly of smoothing irregular contours that reflect numerous small drainages. In contrast, the proposed segments are tens of kilometers long and their boundaries are several kilometers or more wide (Schwartz and Coppersmith, 1984, fig. 1, p. 5688). Thus, segments and their boundaries are larger than the likely errors and the limit of resolution of the topographic map.

Second, figure 7 can record the presence of likely causative structures of large earthquakes, because topography can record long-term differences in uplift between adjacent parts of the footwall of the Wasatch fault zone.

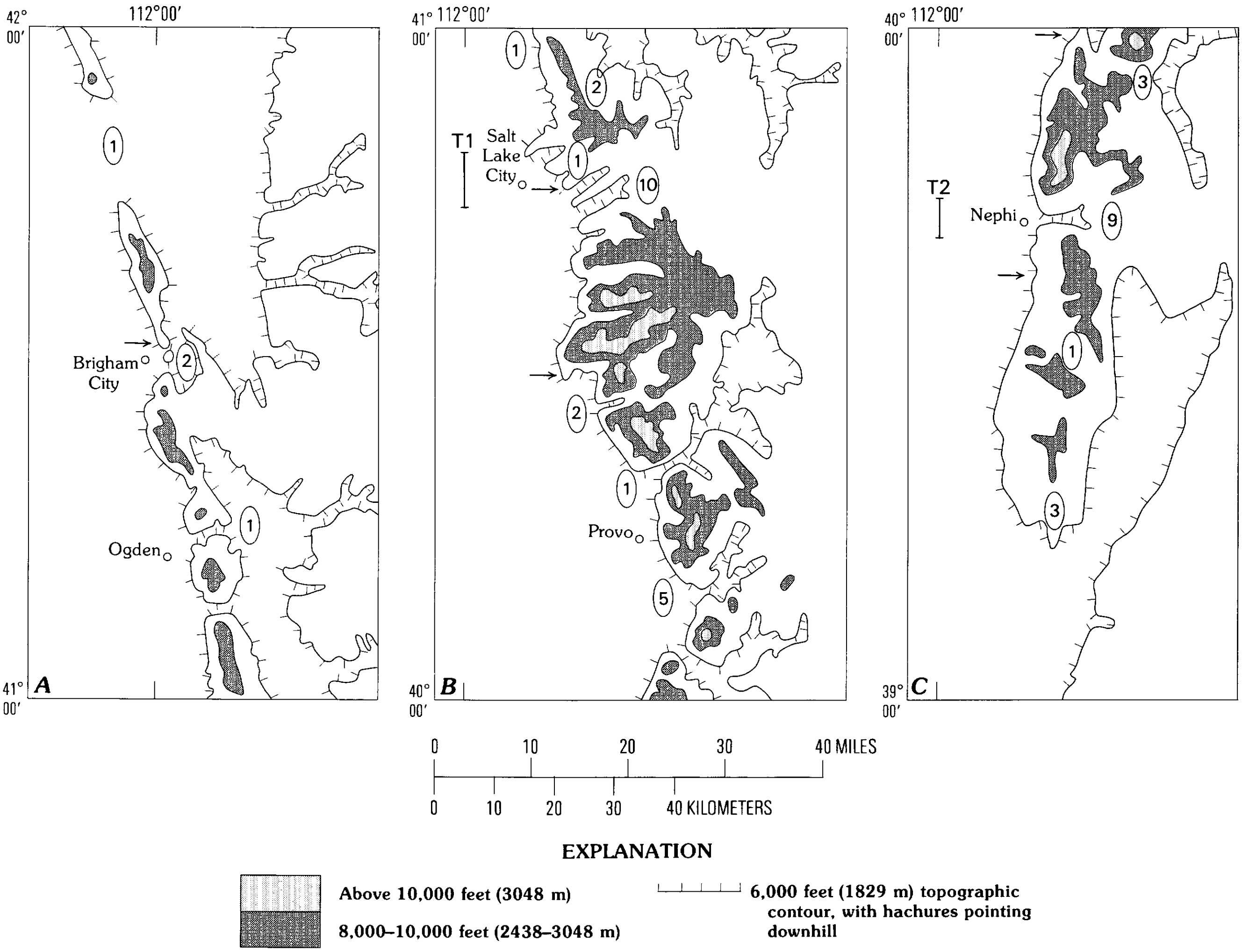

Figure 7. Strip map showing simplified topography of footwall of the Wasatch fault zone. Three panels of figure show northern (*A*), central (*B*), and southern (*C*) parts of Wasatch Front. Fault zone passes through or near cities shown in the figure and is generally below the 6,000-ft contour. Footwall of the west-dipping normal fault includes the high ground (Wasatch Range and San Pitch Mountains) east of the cities. Selected topographic contours were traced from map with contour interval of 500 ft and scale of 1:500,000 (U.S. Geological Survey, 1976). Numerals that are enclosed by ovals show 14 places where one or more of 12 independent interpreters picked a change in elevation, width, or both of the Wasatch Range or San Pitch Mountains. Numeral inside each oval shows how many of the 12 interpreters picked that change. Changes picked by at least three-quarters of the interpreters are taken as topographic anomalies. Two vertical bars labeled T1 and T2, west of Salt Lake City and Nephi, respectively, show anomalies as projected into a north-south line along long 112° W. Five east-pointing arrows locate the segment boundaries of Schwartz and Coppersmith (1984, fig. 1).

Presumably this uplift was partly or mostly seismic, so the uplift differences could record long-term differences in seismicity, including occurrences of large earthquakes, along the Wasatch Front.

Third, figure 7 is likely to show an explainable anomaly at a segment boundary. One expression of a boundary could be an uplift difference between footwall blocks that border the boundary. Such a difference could be large enough to be expressed as differences in heights and widths of parts of the Wasatch Range and San Pitch Mountains. Differences in uplift are large enough along the Wasatch fault zone to be expressed topographically: topographic relief is almost 2 km greater in the center of the Wasatch Range than at the north end or in the San Pitch Mountains (U.S. Geological Survey, 1976). Similarly, measured and estimated depths of the sediment-filled valleys that flank the ranges on the west are greatest in the center of the Wasatch Front (Zoback, 1983, fig. 6). Therefore, structural relief varies along the Wasatch fault zone by amounts that are large enough to be shown by topographic data. If these changes in structural relief are concentrated in zones as narrow as segment boundaries, then the zones are likely to be detectable with topographic data.

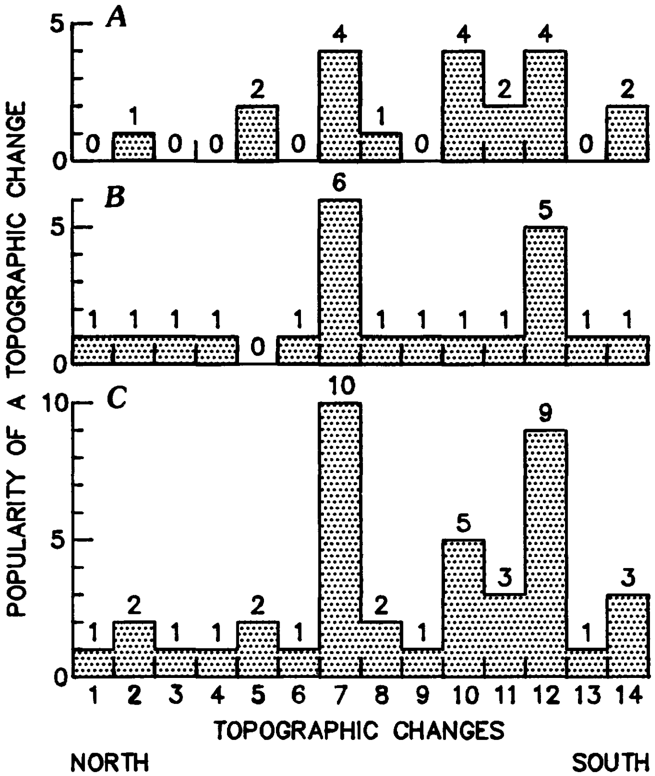

Figure 8. Degrees of reproducibility of 14 topographic changes of figure 7. From left to right are numbered the 14 changes that are shown as numerals enclosed in ovals in figure 7. Popularity of a change is the number of interpreters who picked the change, which is shown by the numerals atop each bar. *A*, Results for five interpreters who are familiar with the geology of the Wasatch Front and with the segmentation hypothesis. *B*, Results for seven interpreters who lack such familiarity. *C*, Combined results for all 12 interpreters.

Fourth, the topographic data record processes that operate over times that allow inferences to be drawn about expected near-future seismicity. The high ground (fig. 7) arose from normal slip on the Wasatch fault zone. Naeser and others (1983) used fission-track ages of apatite to estimate that normal slip between Ogden and the vicinity of Salt Lake City has continued for 10 m.y. or more, at a long-term rate of 0.4 m/ka. Slip rates for various parts of late Quaternary time near Brigham City (Personius, 1985) and between Provo and Nephi (Machette, 1984) vary from 0.12 m/ka to 1.8 m/ka or more (Machette, 1984; Personius, 1985). If these values are taken as estimates of the rate of seismic slip and as illustrations of the variability of this rate, then the implication is that such rates and associated seismicity have been occurring for 10 m.y. or longer, and so are likely to persist for the next few millenia. However, within these next millenia, rates and associated seismicity could vary, perhaps from about one-third to as much as four or five times the long-term average.

Fifth, the anomalies are reproducible, because each anomaly has been picked by nine or ten of twelve independent interpreters.

Sixth, the anomalies were derived from topographic data alone without reference to any other data type of this report.

Seventh, the anomalies were derived without apparent reference to the proposed segment boundaries of Schwartz and Coppersmith (1984). Interpreters familiar with the segmentation hypothesis did not produce significantly different anomalies than did interpreters without such familiarity.

PRE-CENOZOIC STRUCTURES

Introduction

The Wasatch fault zone formed in a part of the earth's crust that had already been damaged by a long series of compressional and extensional deformations, mainly episodes of Precambrian rifting and Late Cretaceous thrusting.

Table 5. Locations of topographic anomalies
[n.a., not applicable. Study area is 332 km long, north to south]

Anomaly number	North end of anomaly[1]	South end of anomaly[1]	Anomaly width (km)	Distance to next anomaly to south (km)
T1	130	140	10	107
T2	247	254	7	[2]78
Sum	n.a.	n.a.	17	185

[1]Distance south of Utah-Idaho border, in kilometers.

[2]Distance to south edge of study area at lat 39° N.

During Late Proterozoic time, rifting and associated crustal extension and thinning formed a north-trending, west-facing, passive continental margin that extended from Alaska through Utah to Mexico (Stewart, 1972). The sediments of the Cordilleran miogeocline accumulated on the extended and thinned continental crust of this margin (Stewart and Poole, 1974). By analogy with modern passive margins that rim the North Atlantic Ocean, the Red Sea, and similar oceans and seas, the extension and thinning probably formed a network of extensional faults in the upper crust throughout a belt that was tens to hundreds of kilometers wide (Bollinger and Wheeler, 1982, p. 22–23). Stewart and Poole (1974, p. 52) suggested that the thinning and extension occurred as far east as the Wasatch Front. If so, then the faults that accomodated extension and thinning would also have formed this far east.

The Late Proterozoic passive margin cut across an older, east-trending depositional trough of Middle Proterozoic age (Stewart, 1972). The trough lay on the site of what would later become the Uinta Mountains (fig. 9). We follow Forrester (1937, p. 635, fig. 1) in calling the trough and its Phanerozoic successors the Uinta trough. Stewart and Poole (1974) reported an oral suggestion by Paul Hoffman in 1971 that the Uinta trough might have been a Proterozoic aulacogen. Burke and Dewey (1973), Crittenden and Wallace (1973), and Sears and Price (1978) regarded the trough as one of several aulacogens in western North America that formed as precursors to the Late Proterozoic rifting.

After Proterozoic rifting and deposition of the subsequent miogeoclinal sediments, in Late Cretaceous time north-trending, east-verging thrust sheets of the Sevier orogeny reached the Wasatch Front from the west (Armstrong, 1968). Presumably the thrust sheets overrode and buried the older passive margin. By analogy with other complexes of thrust sheets, this thrust complex can be expected to contain numerous faults of diverse strikes, dips, and degrees of interconnection (Boyer and Elliott, 1982; Perry and others, 1984), although most faults strike northerly and dip at low angles. Oil well, seismic-reflection, and stratigraphic data along the Wasatch Front indicate that the thrust complex is typically 5–10 km thick (for examples, see Smith and Bruhn, 1984), although Bruhn and others (1983) review petrological evidence from which they suggest that the deepest thrust sheets of northern Utah might have extended as deep as 16 km, somewhere west of the trace of the Wasatch fault zone.

We assume that these tectonic events produced a crust that still contains numerous faults of diverse orientations, histories, and mechanical properties. Beginning in Cenozoic time, this damaged crust was extended to produce the Wasatch and other faults of the Basin and Range province.

The various pre-Cenozoic faults might control earthquakes along the Wasatch Front. Almost all small earthquakes in the area of the Wasatch fault zone occur at depths shallower than 20 km, and most are shallower than 10 km (Arabasz and others, 1980, p. 1493, fig. 8A). By analogy with large, normal-faulting earthquakes that have occurred in the Basin and Range province, Smith and Richins (1984, p. 97, figs. 9, 11) suggested that a large earthquake on the Wasatch fault zone would nucleate at a depth of about 15 km, at or near the base of the brittle upper crust (Smith and Bruhn, 1984, fig. 18). Such depths lie beneath or in the base of the thrust complex. Therefore, Arabasz (1984) and Arabasz and Julander (1986) suggested that most small, and perhaps some large, earthquakes along the Wasatch Front might be controlled by thrust-belt structures. Control could take the form of modern extensional reactivation of Cretaceous compressional faults or of earthquakes being constrained to occur within specific thrust sheets. However, large earthquakes might also occur by modern extensional reactivation of faults in structural basement beneath the thrust sheets. These subthrust faults might be north-striking, Late Proterozoic normal faults of the ancient passive margin. Extensional reactivation of such faults should produce mostly normal slip. Near the Uinta Mountains, subthrust faults might also include east-striking faults of the suggested Uinta aulacogen. Extensional reactivation of faults of the aulacogen should produce mostly strike slip.

The suggestion that subthrust faults might be reactivated in modern extension has precedents elsewhere. Winslow (1981) suggested reverse reactivation of subthrust faults for the southern Andes Mountains in and near Tierra del Fuego. The subthrust faults formed before the thrusting occurred, as normal faults associated with rifting. Reverse reactivation of the subthrust faults is inferred from folds, faults, and thickness variations of Jurassic to Tertiary strata (Winslow, 1981, p. 522–523), so is not known to have been seismic. However, seismic, compressional reactivation of subthrust faults that originally formed as normal faults during prethrusting rifting is inferred from focal mechanisms and geological data for southwestern Iran (Jackson and others, 1981; Ni and Barazangi, 1986), and from focal mechanisms, well-constrained hypocentral depths, and geological data for southwestern Virginia and eastern Tennessee (Bollinger and Wheeler, 1982, 1983; Bollinger and others, 1985; Munsey and Bollinger, 1985).

If subthrust faults that formed during prethrusting extension can be reactivated in compression, then reactivation in extension should be even easier, for two reasons. First, rocks are typically weaker in extension than in compression. Second, extensional reactivation of old normal faults would be aided by gravity, because any dip slip would involve the hanging wall dropping down. Compressional reactivation would be resisted by gravity because any dip slip would involve the hanging wall moving up.

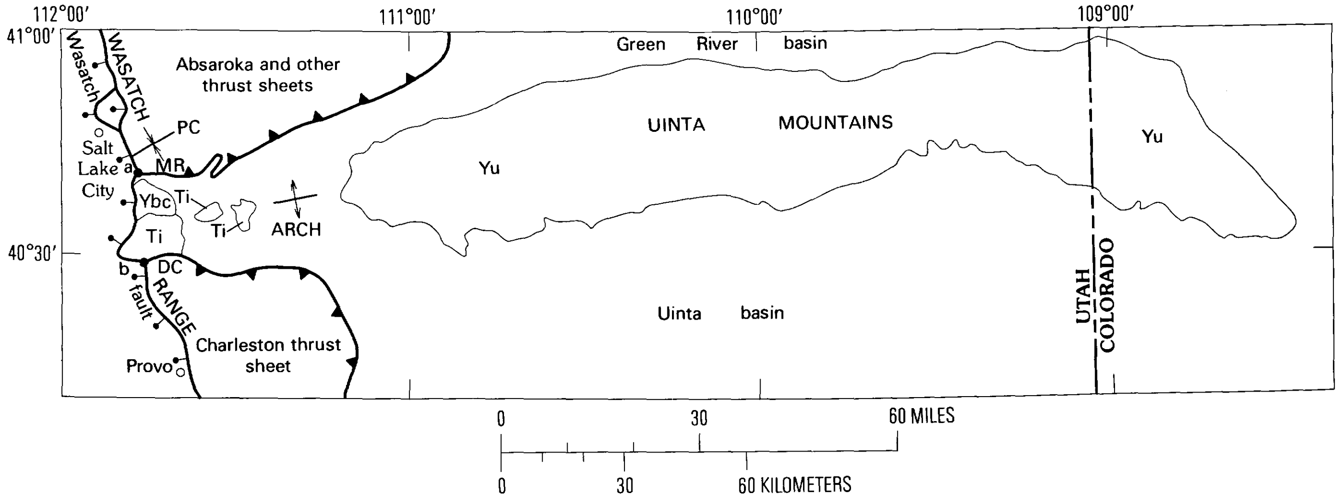

Figure 9. Map of selected tectonic elements of the Uinta aulacogen, east of the Wasatch fault zone. Line representing the trace of the north-striking Wasatch fault has bars and balls on downthrown side (footwall). Upthrown block on east side of fault zone forms Wasatch Range. The present Uinta Mountains are roughly coextensive with area that is labeled Yu. Outcrops of east-directed thrust faults, and inferred subcrops of these faults beneath Upper Cretaceous and Tertiary rocks and sediments, have sawteeth on hanging walls. Westward projection of Uinta Mountains to Wasatch fault is bounded by Parleys Canyon syncline (PC) and by Mount Raymond fault (MR) and Deer Creek fault (DC) that connect with and presumably are parts of the larger thrust faults that bound the Absaroka and Charleston thrust sheets. Points a and b correspond to a and b of figure 10. Location of aulacogen is shown by locations of exposures of Tertiary intrusives (Ti), of aulacogen-filling, Middle Proterozoic Uinta Mountain Group (Yu), of correlative Big Cottonwood Formation (Ybc), and of east-trending arch that separates Absaroka and Charleston thrust sheets. Simplified from Hintze (1980) and Tweto (1979).

In summary, compressional faults of Mesozoic age and probably deeper extensional faults of Proterozoic age permeate the rock volume within which the Wasatch fault zone formed. Cenozoic extensional reactivation of some of these faults is likely. The geometries of the reactivated faults could have controlled the nucleation, growth, and linking of large seismic ruptures that integrated to form the Wasatch fault zone. In particular, changes along the fault zone in the geometries of pre-Cenozoic faults could localize the nucleation points of large extensional earthquakes, could guide the propagation of ruptures, and could limit the lengths of surface ruptures, the areal dimensions of ruptures (and thus the magnitudes of earthquakes), or both. That is, pre-Cenozoic faults could impose segmentation on the Wasatch fault and its large earthquakes (Zoback, 1983, p. 9–12; Smith and Bruhn, 1984, p. 5740–5741; Wheeler, 1984). The Borah Peak earthquake of Idaho appears to illustrate at least some aspects of such segmentation of modern extension imposed by old faults in the Basin and Range province (Crone and Machette, 1984; Skipp and Harding, 1985; Wheeler and Krystinik, 1987d).

Accordingly, structures of the Cretaceous thrust complex and of the rifted crust that probably underlies the thrust complex can be examined along the Wasatch fault zone for along-strike changes (structural anomalies) that might coincide with the proposed segment boundaries of Schwartz and Coppersmith (1984). The pre-Cenozoic structures of most interest are faults, but folds and other features will be useful to the degree that they indicate the presence and geometries of buried faults.

Procedures

Four considerations guide the following summary of pre-Cenozoic structures. First, Smith and Bruhn (1984, p. 5740–5741, fig. 4) and Bruhn and Smith (1984) have already observed that the proposed segment boundaries of Schwartz and Coppersmith (1984) appear to coincide with large changes along strike in the geometries of thrust-belt and older structures. This observation constitutes prior inspection of the segment boundaries. If we used the structural changes that were noted by Smith and Bruhn, such prior inspection would distort results of the statistical analysis of Wheeler and Krystinik (1987a). Therefore, we must summarize pre-Cenozoic structures in enough detail, and with enough citations of reports that predate publication of the segmentation hypothesis, to make it clear that our choice of structural anomalies is not influenced by prior inspection.

Second, the thrust belt of central Utah is structurally and stratigraphically complex, is the subject of a voluminous literature that is partly proprietary, and contains abundant candidates for structural anomalies of many sizes. Therefore, we make no attempt to summarize all structures. Instead, we show that the structural anomalies chosen are reliable, reproducible, and derivable without reference to the other data types or to the proposed segment boundaries.

Third, only large structural anomalies are chosen, because only large anomalies are likely to extend to the depths at which large earthquakes are thought to nucleate in the Basin and Range province (about 15 km: Smith and Richins, 1984). Here, a large anomaly is defined as one with map dimensions exceeding 5-10 km, for two reasons. The upper crust along the Wasatch Front is a thrust belt, and thrust-related structures smaller than 5-10 km are unlikely to penetrate the thrust sheets to the nucleation depths of large earthquakes. Also, a shock of magnitude 7 might occur on a rectangular fault as short as 22 km in map view, as calculated from values of shear modulus, slip, hypocentral depth, and fault dip that are typical of large earthquakes in the Basin and Range province. A map dimension of 5-10 km is considerably less than 22 km. A practical guide for us is that any structural anomalies must be visible at the 1:500,000 scale of the geologic map of Hintze (1980). For example, Wheeler (1984) suggested that a small lateral ramp exists about 8 km east-northeast of the proposed boundary between the Provo and Nephi segments (fig. 1). A ramp is a part of a thrust fault on which the fault changes stratigraphic level (Butler, 1982). At frontal ramps, which strike parallel to the strike of the thrust belt, the change in level takes place across strike, so that the ramp undergoes reverse slip. At lateral or oblique ramps, which cut across the strike of the thrust belt, the change in level takes place along or oblique to strike, so that the ramp undergoes strike slip or oblique slip. Lateral ramps are one kind of structural anomaly that might control segmentation (Wheeler, 1984). However, this lateral ramp is too small for our purposes.

Fourth, the following discussion concentrates on the exposed footwall of the Wasatch fault zone, near the fault-zone trace. Structures of thrust belts change markedly across strike, so that thrust-belt structures more than about 30 km east or west of the trace of the fault zone are unlikely to bear directly on structures at seismogenic depths near the trace. For example, Lamerson (1982) described a large lateral ramp about 100 km east of the fault zone. The ramp is large enough for consideration here but is too far east of the trace of the fault zone for our use. However, the west-striking faults that bound the Uinta Mountains are considered, even though they lie many tens of kilometers east of the Wasatch fault zone, because these faults might continue westward in the subsurface to the fault zone.

The following sections summarize four groups of faults that might form structural anomalies.

Uinta Aulacogen

Evidence for Existence of the Aulacogen

The region occupied by the east-trending Uinta Mountains (fig. 9) has been the locus of repeated deformation since Late Archean or Early Proterozoic time. Forrester (1937) called this region the Uinta trough. The trough lies along the east-trending southern edge of an Archean craton (Bryant, 1985). The edge appears to have formed in Late Archean time, because at least 4–7 km of miogeoclinal rocks accumulated there as the Late Archean to Early Proterozoic Red Creek Quartzite. This thick sequence was thrust northward onto the Archean craton by latest Early Proterozoic time (Hansen, 1965, p. 22–32; Sears and others, 1982, p. 993–994; Bryant, 1985).

In Middle Proterozoic time the red, medium- to coarse-grained sandstones and quartzites with shales and conglomerates of the Uinta Mountain Group accumulated unconformably on the Red Creek Quartzite; these Middle Proterozoic rocks now constitute most of the exposed rocks in the Uinta Mountains (fig. 9; Hansen, 1965, p. 32–38). The Uinta Mountain Group is thick: in the eastern Uinta Mountains, Hansen (1965, p. 33) measured a partial thickness of 6.3 km and estimated its total thickness at slightly over 7.3 km. Richard (1986) reported a thickness of about 1.7 km in a well drilled about 44 km southeast of exposed Uinta Mountain Group rocks in Colorado. From wells and seismic-reflection profiles in the same area, Stone (1986) estimated partial thicknesses of 4.6–6.1 km, 1.7 km, and 0.8 km of the group in successively more easterly buried fault blocks. In the western Uinta Mountains, Wallace and Crittenden (1969, p. 120) measured thicknesses of 3.8–4.1 km in incomplete sections, and Crittenden and others (1967, p. I8, I22) used aeromagnetic data to estimate a total thickness for the group of 6.1 km. Farther west, in the footwall of the Wasatch fault zone, the correlative Middle Proterozoic Big Cottonwood Formation (Crittenden and others, 1972; Crittenden and Wallace, 1973; Crittenden, 1976) is about 4.9 km thick (fig. 9; Hansen, 1965, p. 33). The depositional patterns and great thickness of coarse clastic material in the Uinta Mountain Group led Hansen (1965, p. 34–38, 167) and Wallace and Crittenden (1969) to conclude that the clastic material was eroded from a nearby source of high relief in and northeast of the present Uinta Mountains. The material was transported southward and accumulated in the rapidly subsiding Uinta trough. Woodward (1976, p. 89) noted that the Big Cottonwood Formation (fig. 9) contains more mature sediments than does the Uinta Mountain Group, and that this difference is consistent with both units having been derived from a northeastern source. Wallace and Crittenden (1969) concluded that a strandline and hinge line trended east-west, about along the present center of the Uinta Mountains, and that the lines separated the exposed metamorphic and plutonic rocks of the northeastern source area from the rapidly subsiding trough. Lower parts of the Uinta Mountain Group were deposited in a shallow marine environment, but gradually these conditions yielded to westward-flowing rivers throughout the trough.

Bryant and Nichols (in press) compiled thicknesses of Late Proterozoic strata that are exposed in and near the footwall of the Wasatch fault zone. The Big Cottonwood Formation (fig. 9) is overlain by about 1.2 km of Late Proterozoic strata that contain unconformities. About 20 km south the thickness is about 700 m. However, nine other localities within 60 km north and south of these two expose less than 100 m of beds of correlative rocks (Hintze, 1980; Davis, 1983a, b, 1985). Thus, in Late Proterozoic time the trough of the Uinta Mountain Group might have continued to subside, at least where it crossed the future site of the Wasatch fault zone (Bryant and Nichols, in press). At the eastern end of the Uinta trough, Stone (1986) concluded from oil well and seismic-reflection data that the Uinta Mountain Group dropped down along the south edge of its present-day subcrop by Late Proterozoic to Cambrian, north-facing, normal faulting. From angular discordance between the group and overlying strata, Hansen (1986) inferred south-facing normal faulting of the same age, on the north edge of the trough. The inward-facing normal faulting at both edges of the east end of the Uinta trough indicates extension and probably subsidence at about the same time that the west end of the trough might also have been subsiding.

Forrester's (1937) isopach map of combined Paleozoic and Mesozoic strata shows the Uinta trough as an eastward projecting arm of the north-trending Cordilleran miogeocline, with greater thicknesses in the trough than in adjoining areas to the north, south, and east. However, isopach, lithofacies, and paleogeologic maps of shorter time intervals show more complex behavior of the trough.

The area of the trough formed a linear high in Cambrian time (Lochman-Balk, 1976), the Uinta peninsula of Lochman-Balk (1972). However, tectonic activity of the Uinta trough during Ordovician to Mississippian time is less clearly established. Ross (1976, figs. 5, 9, 11) thought that the site of the trough was exposed in Ordovician time, when a westward extension of the Uinta penninsula into eastern Nevada was inferred to have been high (Tooele arch of Webb, 1958; Uinta-Gold Hill arch of Roberts, 1960; Cortez-Uinta axis of Roberts and others, 1965, p. 1928). However, Foster (1972) showed the Tooele arch trending northeast during Ordovician time and lying well south of the westward projection of the Uinta Mountains, separated from the Uintas by areas of more typical thicknesses of Ordovician strata. During Devonian time the site of the Uintas was exposed (Craig, 1972), and a Late Devonian unconformity was interpreted as defining a wide, flat-topped high that extended 70–80 km west of the present Wasatch fault zone, on trend with the Uinta Mountains (Rigby, 1958, 1959; Roberts, 1960; Morris and Lovering, 1961; Baars, 1972; Sandberg and others, 1982, figs. 8 and 9, p. 704). However, the size, shape, and orientation of this Late Devonian high might not have fit those of a linear westward projection of the Uintas. Maps of Rigby (1959, figs. 1, 3), Morris and Lovering (1961, fig. 33), and Baars (1972) can be interpreted as showing that the Late Devonian uplift consisted of one small, north-trending high 60–80 km west of the Wasatch fault zone and a second, much larger high that was a tilted block, sloping southward, with the site of the Uinta Mountains lying along its northern edge. Sandberg and others (1982, p. 704–707) inferred earliest Mississippian uplift and erosion at the west end of the Uinta trough. The Uinta trough received sediments in Late Mississippian time (Hansen, 1965, fig. 14; Craig, 1972; Welsh, 1979, p. 103, 105; Sandberg and others, 1982, p. 714, fig. 17), although this trough might have been just one part of a larger trough that covered much of northeastern Utah then (Craig, 1972; Rose, 1976, figs. 9, 10). West of the present Wasatch fault zone during Late Mississippian time, the westward projection of the Uinta Mountains separated two deepening basins (Roberts and others, 1965, p. 1931 and 1934; Chamberlain, 1984).

Tectonic activity of the Uinta trough is better established for times after the Mississippian. In Pennsylvanian and Permian time, the Uinta trough was low again, being shallow, east-trending, and west-deepening (Hansen, 1965, p. 39, figs. 16, 17, 20). However, the westward projection of this trough continued to separate two lobes of the deep Oquirrh basin, as it had during Late Mississippian time (Roberts and others, 1965, figs. 7, 16). Finally, in Late Jurassic to Early Cretaceous time, the eastern part of the Uinta trough was a depocenter with a well-defined, east-trending south edge and east end but with an unknown northward extent (Hansen, 1965, fig. 30).

After the Early Cretaceous, uplift changed the site of the Uinta Mountains from a sink to a source of sediments. Conglomerates, dated unconformities, and south-directed paleocurrents led Hansen (1965, p. 108), Crittenden (1976, p. 378), Bruhn and others (1983, p. 70), and Bradley (1984) to suggest that uplift began in latest Cretaceous time. For the northeastern Uintas, Hansen (1965, p. 108) concluded that there were 2.4–3.4 km of uplift by early Paleocene time. Sedimentological, stratigraphic, oil well, seismic-reflection, and other data show major uplift along the length of the Uinta Mountains in Paleocene and especially Eocene time (Hansen, 1965, p. 108; Robinson, 1972; Gries, 1983, p. 13, fig. 7;

Bruhn and others, 1983, p. 72–74; Clement, 1983). Oligocene time saw stocks emplaced and volcanics erupted in the gap between the western Uinta Mountains and the Wasatch fault zone (fig. 9; Crittenden and others, 1973; Hintze, 1980), as well as elsewhere in Utah (Hintze, 1980). In late Oligocene time the eastern Uinta Mountains underwent north-south extension. The Oligocene Bishop Conglomerate was tilted inward toward the center of the range to form an east-trending basin in which the late Oligocene and Miocene Browns Park Formation was deposited (Hansen, 1984).

Thus, the stratigraphic record shows that the Uinta Mountains lie on the east-trending site of repeated tectonic activity, perhaps localized by structures of a rifted margin of an Archean continent. The concept of a Uinta aulacogen arose from consideration of this stratigraphic record. Specifically, the characteristics of the Uinta Mountain Group led Stewart and Poole (1974, p. 34), Burchfiel and Davis (1975, p. 365), Stokes (1976, p. 15), Bruhn and others (1983, p. 63, 85), Zoback (1983, p. 10–11), and Pricha and Gibson (1985) to interpret the group as having been deposited in a Middle Proterozoic aulacogen. Thus, the aulacogen would have been connected on the west to a Middle Proterozoic continental margin, whose location and orientation remain unknown. Presumably the same stratigraphic evidence led Burke and Dewey (1973), Sears and Price (1978), Welsh (1979, p. 93), Sears and others (1982, p. 990), and Gries (1983, p. 11) to call the Uinta trough an aulacogen, although these reports cite no evidence to justify this inference.

Evidence for Faults in the Aulacogen

Whether an aulacogen underlies the Uinta Mountains is of more than semantic interest, because of the implications for the generation of large earthquakes. An aulacogen is a marginal cratonic trough that is known or inferred to be bounded by faults (Gary and others, 1972; Hoffman, 1973; Hoffman and others, 1973; Burke and Dewey, 1973), and indeed Bates and Jackson (1980) gave graben and rift as synonyms for aulacogen. The great thicknesses of aulacogen fillings imply large amounts of dip slip on the bounding faults. These faults could penetrate to the base of the brittle upper crust where large earthquakes are likely to be generated (Meissner and Strehlau, 1982; Sibson, 1982, 1984; Chen and Molnar, 1983; Smith and Bruhn, 1984). The large map sizes of aulacogens means that their bounding faults are likely to be long enough in map view to generate long ruptures and large earthquakes. The repeated activity of the Uinta aulacogen, from Middle Proterozoic and perhaps Archean through Oligocene time, suggests that any such faults might still be weak enough to slip, or to decouple parts of the Wasatch fault zone from each other to form independent segments. The Oligocene intrusions between the western Uinta Mountains and the Wasatch fault zone, the correlation of the Big Cottonwood Formation with the Uinta Mountain Group, and the stratigraphic evidence of repeated uplift or depression along the westward projection of the Uinta Mountains, west of the Wasatch fault zone, all combine to show that the inferred aulacogen intersects the fault zone.

Accordingly, the next paragraphs will argue three things: first, that the Uinta aulacogen probably is bounded by deep faults; second, that the inferred faults are too poorly defined to be used in this report as structural anomalies in themselves; and third, that what is known of the aulacogen and thrust belt structures near it allows us to define one usable structural anomaly.

The repeated rises and falls of the crustal block that carries the Uinta Mountains could occur by regional or local flexing of the crust in isostatic compensation or by movement on faults. The block is too narrow for local isostatic compensation to be likely (Behrendt and Thiel, 1963, p. 860–861). The contours and contacts that define the block on paleogeologic, isopach, and lithofacies maps show that the edges of the block are too narrow for the vertical motions to have occurred by regional flexing. The sharp boundaries of the uplifts and downdrops that are revealed on the maps suggest that the block is bounded by faults.

Other evidence also suggests that the aulacogen is fault bounded. Mapping, well data, and seismic-reflection profiles have shown the exposed Precambrian core of the Uinta Mountains to be bounded on the north and south by inward-dipping reverse faults (for examples, see Hansen, 1965, p. 38, 137–138; Ritzma, 1969; Campbell, 1975; Hintze, 1980, section GH; Sears and others, 1982; Gries, 1983; Bruhn and others, 1983; Clement, 1983; Osmond, 1986; Stone, 1986; Hansen, 1986). Most of these data deal with faults that are exposed or faults that are shallower than the Precambrian floors of the basins north and south of the Uinta Mountains (8–11 km deep: Gries, 1983) and with Cenozoic motion on these faults. However, Sears and others (1982, p. 995) documented as much as 10 km of Early Proterozoic dip slip on faults along the northeast corner of the present range. Along the edge of the southwestern Uinta Mountains, faults experienced at least 1.8 km of dip slip before Late Devonian time (Wallace and Crittenden, 1969, p. 128, 140) and mostly between deposition of the Middle Proterozoic Uinta Mountain Group and Middle Cambrian time (Bryant, 1985, p. 117).

Behrendt and Thiel (1963) mapped Bouguer gravity and residual magnetic intensity over the Uinta Mountains. Both potential fields show steep gradients above the northern and southern edges of the range, suggestive of large buried faults. Steenland (1969) interpreted an aeromagnetic low over the range, and steep aeromagnetic gradients at the north and south edges of the range, as reflecting a fault-bounded basin that underlies the range and contains at least 11 km of the Uinta Mountain Group. Smith and Cook (1985) mapped Bouguer gravity over northeastern Utah and modeled free-air gravity along two north-south profiles across the Uinta Mountains. The models include vertical to steeply inward dipping faults at the north and south edges of the range, bounding a basin that contains 8–11 km of the Uinta Mountain Group.

Therefore, the term aulacogen adequately characterizes the depositional setting of the Uinta Mountain Group and the structural setting of the present Uinta Mountains. The implied bounding faults are probable but not certain along most of the north and south edges of the range and westward to the Wasatch fault zone. However, the number, locations, orientations, and sizes of the bounding faults remain too poorly known for the faults by themselves to constitute structural anomalies, for seven reasons.

First, the paleogeologic, isopach, and lithofacies maps that comprise most of the evidence for the aulacogen and its repeated activity lack the control to define individual faults or fault zones.

Second, published well and seismic-reflection profiles define the faults in the upper several kilometers of the Uinta and Green River basins but do not yet allow the faults to be followed down to the lower part of the brittle upper crust, nor west of the basins to the Wasatch fault zone. Similarly, geologic mapping has not defined such faults in most of the 40 km or so that separate the western Uinta Mountains from the Wasatch fault zone, because Cretaceous thrust sheets and Cenozoic strata cover much of this area (Hintze, 1980).

Third, Sears and others (1982) mapped Proterozoic faults in the northeastern Uinta Mountains, and Wallace and Crittenden (1969) did the same in the southwestern part of the range. Even these faults might not be simply related to the main bounding faults of the aulacogen, because the northeastern faults predate the Middle Proterozoic sedimentary filling of the aulacogen, and the southwestern faults postdate it (Sears and others, 1982, p. 995; Bryant, 1985, p. 117).

Fourth, large east-trending faults or fault zones at the north and south edges of the range can be inferred from gravity and magnetic data. These inferred faults are interpreted to limit the present northward and southward extent of the Uinta Mountain Group, but the faults are of unknown age. Therefore, they might postdate the Uinta Mountain Group and the aulacogen. If so, then the Uinta Mountain Group might originally have extended north and south beyond these inferred faults but might have been uplifted there by motion on the faults and eroded. The stratigraphic record documents such uplifts in Cambrian, Devonian, perhaps latest Cretaceous, Paleocene, and Eocene times. In fact, Stone (1986) offered this explanation for the region east-southeast of exposed Uinta Mountain Group rocks (fig. 9), where buried parts of this unit have been drilled and interpreted on seismic-reflection profiles. Reflectors of the group are truncated on the south against north-dipping faults, and internal reflectors parallel each other into the faults. The parallelism indicates that the group was eroded south of the faults as a result of postdepositional normal slip on the faults.

Fifth, the present southward extent of the Uinta Mountain Group is unknown, aside from the just-mentioned inference from gravity and magnetic maps. The sedimentological and stratigraphic descriptions and interpretations of the Uinta Mountain Group form one of the strongest arguments for the existence of a northern bounding fault that was active during deposition of the group. However, Bryant (1985, p. 117) noted that these descriptions and interpretations contain no hint of the existence of a southern limit to these strata (Hansen, 1965; Wallace and Crittenden, 1969). Sears and others (1982) mapped a graben in the northeastern Uinta Mountains, but it lies entirely on the north side of the range and so cannot bear on the southward extent of the Uinta Mountain Group. Small patches of Middle Proterozoic strata are exposed in the footwall of the Wasatch fault zone east of Provo and 13 km and 30 km north of Nephi (Hintze, 1980; Davis, 1983a; Bryant, 1985). It is not known whether these rocks represent the southward extent of the aulacogen, the eastward extent of the continental margin to which the aulacogen presumably connected, or something else.

Sixth, the Uinta Mountains and their environs might be underlain by many east-striking faults of Archean age, each responsible for some part of the evolution of the aulacogen and its several subsequent rises and falls. Bryant (1985) reviewed aeromagnetic, mapping, and other data that show or appear to show several large, east-striking faults within about 300 km north of the Uinta Mountains. Some of the faults have long histories of activity. The Red Creek Quartzite, which unconformably underlies the Uinta Mountain Group in the northeastern Uinta Mountains, is interpreted to be a miogeoclinal sequence of Archean to Early Proterozoic age (Hansen, 1965; Sears and others, 1982; Bryant, 1985). If the Red Creek Quartzite accumulated on a south-facing continental margin, then analogies with modern passive margins suggest that it should be underlain by numerous east-striking normal faults of Archean age. Such speculation suggests that the faults that might have controlled the growth of the aulacogen and its subsequent rises and falls through the Phanerozoic might be many, widespread, and geometrically complex.

Seventh, there are too few published data to force agreement on the dips, depths of penetration, relative sizes, or westward extents of the faults that are known to bound the Cenozoic uplift of the Uinta Mountains or are inferred to bound the aulacogen. The hypothesis that the bounding faults of the uplift steepen downward (for example, Campbell, 1975) has been replaced by the interpretation that these faults retain moderate inward dips, at least to depths that are illuminated by published seismic-reflection profiles (8–11 km or shallower: Gries, 1983). However, below these depths, sparse data allowed Sears and others (1982, fig. 5) to model faults of equal size on both north and south sides of the uplift as dipping inward at 25°–45°. The same data also allowed Bruhn and others (1983, p. 85–88, fig. 21) and Bruhn, Picard, and Isby (in press, fig. 9) to model the same faults differently. Bruhn and coworkers suggested that the northern fault dips south at about 10° to a depth of about 8 km, then steepens to dip about 30° down to 22–27 km depth. However, they interpreted the fault at the south edge of the Uinta Mountains to dip north at about 40°, to end against the south-dipping fault and to die out westward before reaching the Wasatch fault zone.

In summary, characteristics of the Uinta aulacogen indicate that it is large enough, and has been important enough in the geologic evolution of the region that includes the central Wasatch Front, that our structural anomalies should reflect the aulacogen. Unfortunately, faults of the aulacogen are too poorly known to be used directly.

Defining a Structural Anomaly at the Aulacogen

Other faults can be used instead of those of the aulacogen. Where the westward projection of the Uinta Mountains crosses the footwall of the Wasatch fault zone, the projection is bounded by two east-striking, outward-dipping parts of the Cretaceous thrust complex (fig. 9). On the south, the westward projection of the Uinta Mountains is separated from the Charleston thrust sheet by the south-dipping Deer Creek fault (Baker and Crittenden, 1961; Hintze, 1980, section CD). On the north, the projection is separated from the Parleys Canyon syncline in the Absaroka thrust sheet and overlying sheets by the north-dipping Mount Raymond thrust fault (Crittenden, 1965a,b; Crittenden and others, 1966). The intersections of the east-striking Deer Creek and Mount Raymond faults with the north-striking Wasatch fault are taken to bound a single structural anomaly, which represents the unknown fault system of the Uinta aulacogen.

The observed width of this anomaly at ground level is 21 km (fig. 10; Davis, 1983a,b). The width of the anomaly at seismogenic depths is uncertain because the subsurface geometry of the north and south edges of the fault system of the aulacogen is unknown. This uncertainty can be estimated by considering two extreme cases (fig. 10). At one extreme, the aulacogen and its fault system are assumed to be bounded in the upper few kilometers of the crust by the Deer Creek and Mount Raymond faults, which dip outward from the aulacogen. Examination of both faults as they appear in cross sections of Baker and Crittenden (1961), Crittenden (1965a,b), and Smith and Bruhn (1984) suggests outward dips of about 30°, typical of ramps in thrust belts. The Deer Creek and Mount Raymond faults might dip downward to the top of Precambrian gneisses and schists, or to the base of a thrust sheet, whichever is shallower. Smith and Bruhn (1984, figs. 5, 6) estimate these depths as about 6 km. Therefore, the anomaly in the upper 6 km might be as wide as 42 km (fig. 10). Any anomaly-bounding faults below 6 km are assumed to be high-angle faults beneath the thrust sheets, and to project upward about to the outcrops of the Deer Creek and Mount Raymond faults. Such high-angle faults would give smaller widths than 42 km for the anomaly at depths below 6 km.

At the second extreme, the aulacogen and its fault system are assumed to be bounded by steep extensional faults of Archean to Middle Proterozoic age, which project upward to and have controlled the positions of the outcrops of the Deer Creek and Mount Raymond faults. Such faults could dip either inward or outward, at dips of perhaps 60°, and could penetrate to the depth at which large earthquakes are suggested to nucleate (15 km: Smith and Richins, 1984). Outward dips indicate that the maximum width of the anomaly is distance gh of figure 10, which is less than cd and so is not considered further. However, inward dips indicate that the anomaly might be as narrow as 4 km. Accordingly, the anomaly that corresponds to the fault system of the Uinta aulacogen has a width of 21 km, and might range from 4 km to 42 km wide at seismogenic depths.

Faults of the Late Proterozoic Passive Margin

Normal and other extensional faults are inferred to have formed mostly during Late Proterozoic rifting, in crust that later became the passive continental margin on which the sediments of the Cordilleran miogeocline accumulated (for example, Christie-Blick, 1984; Pricha and Gibson, 1985; Christie-Blick and von der Borch, 1985). The inferred existence of such normal faults arises from analogies with modern passive margins. The inferred faults would now be buried under Cretaceous thrust sheets. The faults could be recognized in seismic-reflection profiles by determining thicknesses of sedimentary

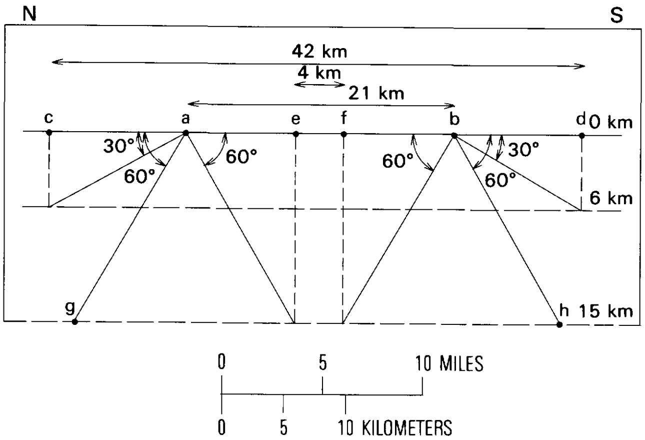

Figure 10. Schematic cross section illustrating widths of structural anomaly formed by the inferred fault system of the Uinta aulacogen. Figure represents north-south section along Wasatch fault zone, looking east into footwall block that contains the fault system of the aulacogen. Horizontal lines represent ground level (labeled 0 km) and depths of 6 and 15 km below it. East-striking Mount Raymond fault crops out at point a, and east-striking Deer Creek fault, at b. Rocks exposed north of a or south of b are involved in the thrust sheets above these two faults. Rocks that crop out between a and b include Big Cottonwood Formation and other rocks that are interpreted to be associated with the aulacogen. Lines that plunge 30° and 60° away from a and b represent extreme estimates of the subsurface geometries of faults that might form the north and south boundaries of the rocks and fault system of the aulacogen, at various depths below ground level. Deer Creek and Mount Raymond faults might dip outward 30° to depth of 6 km. Upward projections of these faults from 6 km to ground level generate points c and d. Other, deeper faults might dip inward (or outward) at 60° to 15 km depth, generating points e and f (or g and h).

sequences of Late Proterozoic to early Paleozoic age. Thicknesses should increase abruptly from footwalls to hanging walls of such faults, because the sequences would be of the same ages as the normal faulting.

For example, Pricha and Gibson (1985) suggested such a rifting origin for the north-striking ancient Ephraim fault of Moulton (1975), which lies about 30 km east of the Levan segment. Standlee (1982, fig. 14, p. 367) inferred from well and seismic-reflection data that the Ephraim fault, which dips west and offsets Cambrian to Jurassic strata, was active during but not after Middle Jurassic time. For a high-angle basement fault at about the same location, Villien and Kligfield (in press, figs. 7, 8, 11) inferred from regional relationships that the Paleozoic section is thicker in the hanging (west) wall than in the footwall. From seismic-reflection and related data Zoback (1987) suggested that south of Nephi the Wasatch fault zone is localized by a west-dipping normal fault of Late Proterozoic age, which has been reactivated in Cenozoic extension.

This inferred system of Late Proterozoic normal and other extensional faults remains too poorly documented and defined for use in this report, for two reasons. First, the faults and the stratigraphic evidence of their expected Late Proterozoic activity remain too deeply buried to be illuminated by most published seismic-reflection profiles. Second, the parts of the system of Late Proterozoic extensional faults that would be most important for defining structural anomalies are likely to be small, to strike east-west roughly parallel to most reflection profiles, or both, and so are likely to be hard to detect. This second reason is based on examination of the system of early Mesozoic extensional faults that dissects the eastern United States from Massachusetts to South Carolina (King and Beikman, 1974).

Most of these Mesozoic faults, and all of the long ones, in the eastern United States are normal faults that strike north-northeast to east-northeast, parallel to the Mesozoic-Cenozoic passive margin during whose evolution they formed. However, short cross faults or en-echelon offsets of the northeast-striking, longitudinal faults are spaced at intervals that are typically several tens of kilometers. At these cross faults and offsets, the longitudinal faults and the Mesozoic basins that they bound have three kinds of map patterns. Some longitudinal faults and basins end abruptly (for example, fig. 11, locality 1). Some longitudinal faults end and are replaced en echelon by others, so that the same basin edge extends along both faults (for example, fig. 11, locality 2). Some basins change map width abruptly across a cross fault (for example, fig. 11, locality 3). Numerous smaller examples of such fault geometries are shown on the geologic maps of New Jersey (Lewis and Kümmel, 1910–1912), Pennsylvania (Berg and others, 1980), Maryland (Cleaves and others, 1968), and Virginia (Calver and others, 1963).

For these map patterns to be visible at a scale of 1:2,500,000 (King and Beikman, 1974), the cross faults and offsets that make up the patterns must have many meters and perhaps several kilometers of structural relief. Schwartz and Coppersmith (1984) suggested that typical scarp-forming earthquakes along the Wasatch fault zone each generate about 2 m of structural relief and occur at intervals of hundreds to thousands of years. The cross faults and offsets illustrated in figure 11 have enough structural relief that their formation occupied many such intervals. Map patterns like those represented in figure 11 indicate that the longitudinal normal faults on which the Mesozoic extension occurred were segmented by cross faults and en-echelon offsets. If most of the faulting occurred seismically, then the cross faults and offsets might have acted as stress concentrators, nucleation sites, and propagation barriers for seismic ruptures, as appears to have occurred during the Borah Peak earthquake (Crone and Machette, 1984; Skipp and Harding, 1985; Wheeler and Krystinik, 1987d).

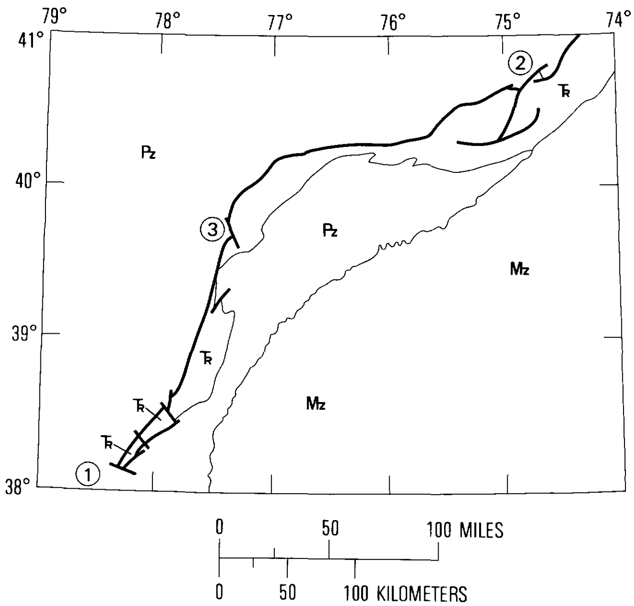

Figure 11. Map of Mesozoic extensional faults that bound Triassic sedimentary filling of Newark-Gettysburg basin in eastern United States. Heavy lines denote faults and light lines denote unfaulted contacts. Triassic basin filling (Ŧr) and Paleozoic (Pz) rocks are overlapped from southeast by Mesozoic (Mz) strata of Coastal Plain province. Circled numerals identify localities cited in text. Traced and simplified from King and Beikman (1974).

Therefore, an analogy between the Mesozoic extensional faults of the eastern U.S. and the inferred Late Proterozoic extensional faults beneath the thrust sheets of the Wasatch Front suggests that the Late Proterozoic faults might be segmented by short cross faults and by en-echelon offsets of north-striking normal faults. For defining structural anomalies the most important parts of the inferred system of Late Proterozoic extensional faults will be cross faults and offsets. The analogy with the eastern U.S. suggests that beneath the Wasatch Front, most such cross faults and offsets should be small compared to the longitudinal faults and should strike more or less east. However, published seismic-reflection profiles also strike roughly east at high angles to the Wasatch fault zone (most profiles lie entirely east of the fault zone), the thrust sheets, and the Late Proterozoic passive margin. These profiles are unlikely to show most of the expected cross faults or offsets, at least until the reflection data become much more numerous and widely available for reprocessing than they are now.

In summary, the thrust sheets of the Wasatch Front are probably underlain by an extensional fault system of Late Proterozoic age. This system might be segmented. The parts of the system that are the most likely to cause segmentation and to control its expression in the properties of large earthquakes are unlikely to be detectable with data that are now available. To solve this problem would require such complete coverage of the Wasatch Front by expensive reflection profiles that any cross faults and offsets are likely to remain undetected for many years. Accordingly, the analysis of segmentation in this report proceeds, but we remain mindful of our ignorance of subthrust structures.

Cretaceous Thrust Faults North of the Uinta Mountains

Geometries of the Thrust Faults

Structural terminology of thrust belts varies between regions, organizations, and geologists. We use the terminology of Boyer and Elliott (1982) and Butler (1982), because it comes closer to being an accepted standard than any other terminology known to us.

North of the Mount Raymond fault and the Uinta Mountains, the footwall of the Wasatch fault zone comprises a series of thrust sheets that extend east into Wyoming and north into Idaho. These thrust sheets reached the area of the Wasatch Front from the west in Cretaceous time, as part of the eastward-propagating Sevier orogeny (Armstrong, 1968). Thrusting progressed farther eastward until Eocene time (Armstrong and Oriel, 1965; Oriel and Armstrong, 1966). The eastern thrust sheets, those not extensively deformed by Tertiary extension, have been objects of intensive petroleum exploration (Monley, 1971; Royse and others, 1975; Dixon, 1982), and proprietary well data and seismic-reflection profiles have illuminated many of their structures. Most of this exploration took place several tens of kilometers east of the Wasatch fault zone, but some profiles extend west as far as the fault zone, where they support interpretations of thrust structure there (Royse and others, 1975; Smith and Bruhn, 1984).

The oldest large thrust fault is the Willard fault (fig. 12), which bounds the base of the Cache allochthon of Crittenden (1972). This fault places Precambrian and Paleozoic rocks of the Cordilleran miogeocline over correlative rocks of the adjoining shelf, and so has carried the miogeoclinal rocks far from the west (Crittenden, 1972, 1976). The younger Absaroka thrust fault then formed in the footwall of the Willard fault and carried the Willard fault and the Cache allochthon eastward to their present positions (fig. 13). En route, the Absaroka fault cut upsection in a frontal ramp, from Precambrian basement to Cambrian shales, at about the position of the present Wasatch fault zone. When the hanging wall of the Absaroka thrust climbed this ramp, the thrusting-duplicated rocks formed a large ramp anticline with the Cache allochthon draped over its top and down its east limb (figs. 12, 13; Royse and others, 1975). The Precambrian rocks that are exposed in the core of this ramp

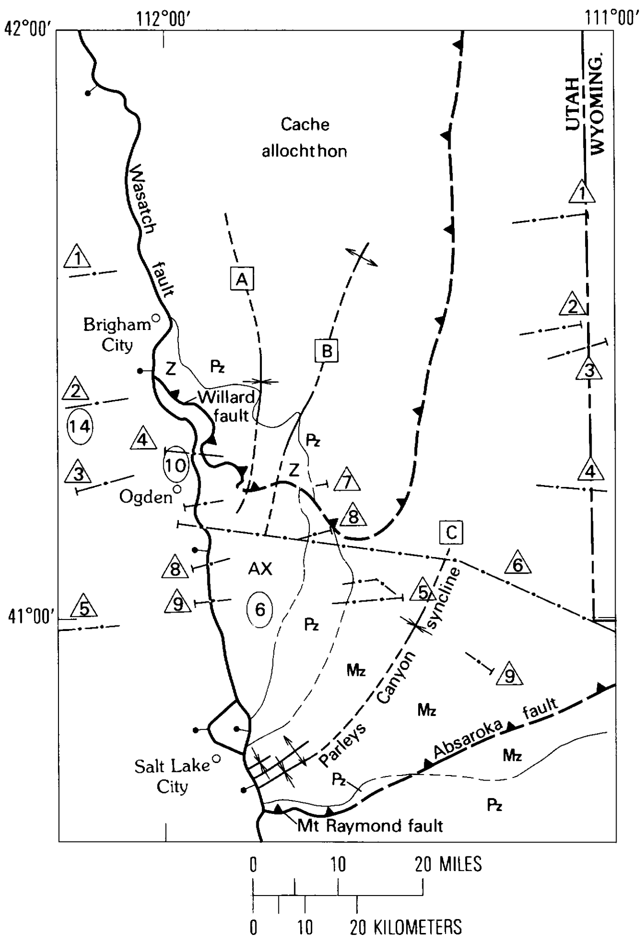

EXPLANATION

- Trace of Wasatch fault—Bar and ball on downthrown (west) side
- **Anticlinal crest or synclinal trough**—Dashed where covered by Upper Cretaceous or Cenozoic strata
- [A] **Anticline (B) or syncline (A, C) that is shown in figure 13**—Parleys Canyon syncline (C) extends northward between Utah-Wyoming border and eastern trace of Willard fault, but as a wide basin bounded on east and west by west-dipping thrust faults. Accordingly, the Parleys Canyon syncline is shown on figure 13, but its trough is too poorly defined to represent on this map much north of lat 41° N.
- **Trace of thrust fault**—Dashed where covered by Upper Cretaceous or Cenozoic strata, sawteeth on hanging wall. All thrust faults involved eastward movement of hanging walls
- **Generalized contact between Archean and Early Proterozoic Farmington Canyon Complex (AX), Late Proterozoic (Z), Paleozoic (Pz), and Mesozoic (Mz) strata**—Dashed where covered by Upper Cretaceous or Cenozoic strata
- **Approximate location of a published cross section that spans part or all of map area**—Section ends that fall within map area are located approximately by a short line that crosses and terminates the dash-dot line. Numeral in triangle identifies section. 1, section *AB* of Hintze (1980); 2, section *JJ'* of Smith and Bruhn (1984); 3, section *CC'* of Crittenden (1972); 4, section *YY'* of Royse and others (1975); 5, section *CC'* of Smith and Bruhn (1984); 6, section *AA'* of Bruhn, Picard, and Isby (in press); 7–9, sections *XX'*, *YY'*, and *ZZ'* of Schirmer (1985)
- (6) **Approximate depth in kilometers below ground level of top of west-dipping ramp in basal (Absaroka) thrust fault, as interpreted on sections 2, 4,**

Figure 12. Sketch map of selected structural elements, in and near footwall of Wasatch fault zone north of the trace of the Mount Raymond fault and Uinta Mountains. Location of east edge of Willard fault is uncertain north of about lat 41°30′ N. (for example, compare Royse and others, 1975, fig. 1, with Dover, 1983). Compiled and interpreted from Stokes (1963), Crittenden (1972, 1974), Royse and others (1975), Sorensen and Crittenden (1979), Hintze (1980), Lamerson (1982, p. 320), Bruhn and others (1983), Dover (1983), Bryant (1984), and Smith and Bruhn (1984).

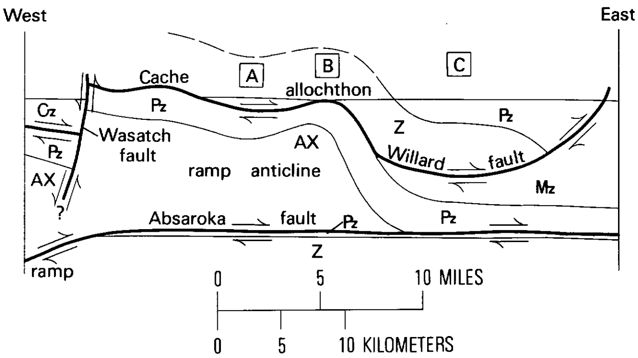

Figure 13. Sketch of cross section showing northward view through structures mapped in figure 12. Generalized and simplified from various sources, mostly down-plunge viewing of figure 12 and section YY′ of Royse and others (1975). Because sketch is generalized, it corresponds to no single line of section through figure 12, nor does it match details of mapped geology exactly along any one line of section. Structures plunge gently northward, so the rocks exposed along successively more southerly sections of figure 12 correspond to successively deeper horizontal cuts through this figure. Prethrusting rocks are Archean and Early Proterozoic (AX), late Proterozoic (Z), Paleozoic (Pz), and Mesozoic (Mz). Postthrusting strata are Cenozoic (Cz). Boxed letters A–C above section indicate approximate locations of the Parleys Canyon syncline (C) and two other large folds that trend northward toward or across the southern edge of the Cache allochthon (fig. 12).

anticline define the east edge of the northern Utah highland of Eardley (1939; Northern Utah uplift of Eardley, 1969).

Lastly, Cenozoic extension of the thrust complex produced the Wasatch and related faults. Numerous other named thrust faults are known in outcrop or subcrop farther east, but they can be regarded as eastern splays of the Willard and Absaroka thrust systems and so will not be treated here (Royse and others, 1975, sections XX′, YY′).

The thrust complex above the Absaroka thrust fault plunges gently north. Accordingly, south of Ogden the core of the ramp anticline is exposed as the Archean and Early Proterozoic Farmington Canyon Complex (Bryant, 1984). Paleozoic and Mesozoic units dip east in the front limb of the anticline. The eastern dips identify rocks that were uplifted as they were carried up the frontal ramp and were tilted east at the top of the ramp. The tilted rocks are bounded on the southeast by the northeastward extension of the Parleys Canyon syncline (figs. 12, 13). Northward the ramp anticline plunges beneath the Cache allochthon. However, the presence of the ramp anticline beneath the allochthon is revealed by a paired anticline and syncline that begin in the exposed Farmington Canyon Complex and continue northward through the Cache allochthon (figs. 12, 13).

The northward deepening of the Willard thrust fault might define a structural anomaly for this report (Bruhn, Picard, and Isby, in press, fig. 8). Bruhn and others (1983) summarized differences in metamorphic grade and structural style across the Willard fault. These differences between the hanging wall and footwall of the fault might cause the two walls to respond differently to Neogene extension, and so might have favored segmentation of the Wasatch fault zone. A structural anomaly could extend from the intersection of the traces of the Willard and Wasatch faults, northward to the latitude at which the Willard fault reaches the depth at which large normal-faulting earthquakes are suggested to nucleate (15 km, according to Smith and Richins, 1984).

However, such a structural anomaly would be too wide to be useful because the Willard fault deepens northward only gradually. The trace of the fault has been mapped at scales of 1:24,000 and 1:50,000 for a straight-line distance of about 26 km southeastward from its intersection with the trace of the Wasatch fault (Sorensen and Crittenden, 1976, 1979; Bryant, 1984; Crittenden and Sorensen, 1985). Within this mountainous area the trace of the Willard fault is sinuous and offset by steep young faults. By choosing small areas between such offsets, the orientation of the Willard fault can be determined by three-point problems. Each determination averages the orientation of the fault over about 1 km^2. Under the Willard fault is a recumbent, isoclinal syncline (Crittenden and Sorensen, 1985; Crittenden, 1972). The orientation of the axial surface of the syncline, determined as was the fault orientation, parallels the Willard fault.

West of the north-trending anticline and syncline shown in figure 12, the Willard fault is folded about an axis that plunges northwest at 6° (fig. 14). The tightness of the clustered points in figure 14 and the scatter of their source areas over a distance of about 26 km indicate that this low plunge can be used as a regional estimate of the northward deepening of the Willard fault. If the axis of the folded fault plunges northwest at 6°, the axis will reach a depth of 15 km at a point 111 km north of its outcrop. Perusal of the maps of Hintze (1980) and Stokes (1963) showed no evidence that the fault increases its northward deepening anywhere south of the Utah-Idaho border. Instead, the map patterns indicate a gradual northward deepening of the fault. This indication is consistent with estimates by Crittenden (1972) that the Cache allochthon reaches thicknesses of 35,000 ft (10.6 km) or more in northernmost Utah. The indication of gradual northward deepening is also consistent with the shapes of the ramp anticline as it is shown in the successively more northerly cross sections CC′ of Smith and Bruhn (1984), YY′ of Royse and others (1975), and JJ′ of Smith and Bruhn (1984). These sections show the ramp anticline gradually becoming wider and lower northward, which would allow the overlying Cache allochthon to plunge gradually northward also.

Therefore, the Willard fault might divide the upper crust into nearly horizontal layers with different seismogenic properties, but the fault is unlikely to dip steeply enough northward to segment either wall of the Wasatch fault zone.

Structural Anomaly at a Lateral Ramp

Near Salt Lake City the ramp anticline (fig. 13) plunges south steeply enough that a usable structural anomaly can be defined. The structural anomaly is

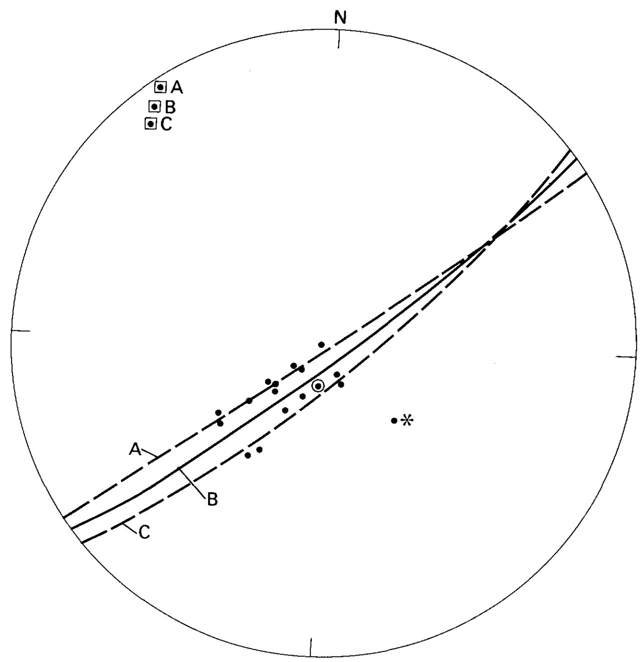

Figure 14. Equal-area, lower hemisphere projection of estimates of orientation of Willard thrust fault. Estimates are planes, although their poles are plotted here. Estimates are three-point solutions to orientation of fault (16 dots) and to orientation of axial surface of recumbent, isoclinal syncline beneath and parallel to fault (one circled dot). Great circle A was fit by eye to the nine northwestern poles, and C, to the seven southeastern poles. Pole marked with an asterisk was discarded as anomalous, because its orientation is so far from the other orientations. Boxed dots are poles to great circles A–C, with pole B determined as midpoint of an arc joining poles A and C. Great circle B was drawn from pole B, and represents the best fit to all 16 retained estimates of the fault orientation. Pole B plunges 6° toward N. 39° W. Estimates were calculated from maps of Sorensen and Crittenden (1976, 1979), Bryant (1984), and Crittenden and Sorensen (1985).

associated with the southern nose of the ramp anticline. The Archean and Early Proterozoic core of the anticline is bounded on the east by Paleozoic and Mesozoic strata and by the northeast-trending syncline that lies at the bottom of the east limb of the anticline (fig. 13). The east-dipping strata and the syncline sweep south and then west into the Parleys Canyon syncline, which bounds the nose of the anticline on the south (fig. 12). The Archean and Early Proterozoic rocks in the ramp anticline and the Mesozoic rocks in the trough of the Parleys Canyon syncline both have moved up the frontal ramp, in order to be exposed at the present ground level. If the two rock masses had moved up the ramp separately, they would be separated by a large, east-striking, strike-slip fault. No such fault is mapped (Crittenden, 1974; Davis, 1983a), so the two rock masses moved up the ramp together.

The structural anomaly could have either of two subsurface geometries, each involving a large lateral ramp (fig. 15). Both geometries can be visualized by noticing that the Precambrian core of the ramp anticline has more structural relief than does the Parleys Canyon syncline. Before the thrusting that formed both folds, the strata that are now involved in the anticline and nearby syncline were probably flat lying. Because the anticline and syncline are within about 10 km of each other, the strata involved in both folds were probably of comparable thicknesses before thrusting and remain so now. Total stratal thicknesses involved in the two folds probably differ by an amount much less than the difference in structural relief between the two folds, which Smith and Bruhn (1984, fig. 5B) estimated as at least 6 km. As an example of such a difference, strata of Late Proterozoic age are absent in the ramp anticline (Bryant, 1984) but are exposed south of the Parleys Canyon syncline (Davis, 1983a, b) and so might be present under the syncline. If the difference in structural relief exceeds likely thickness differences between the areas of the two folds, then the Absaroka thrust fault on which both areas moved up the frontal ramp together must have risen from deeper stratigraphic levels west of the ramp anticline than west of the Parleys Canyon syncline. Then the ramp west of the anticline is higher than the ramp west of the syncline.

Published cross sections that are based on seismic-reflection profiles represent the top of the frontal ramp at various locations under or a few kilometers west of the Wasatch fault zone (fig. 12). Dixon (1982, fig. 14, p. 1579) interpreted the top of the ramp to be at the western edge of a prominent reflector above the basement. If other authors have inferred the position of the top of the ramp from similar evidence, then westward-worsening quality of data and the subjectivity inherent in such inferences could explain the east-west scatter of the three circled numerals on sections 2, 4, and 5 of figure 12.

Atop the frontal ramp the Absaroka thrust fault is in Cambrian shales (Monley, 1971; Royse and others, 1975; Dixon, 1982). The ramp anticline exposes Archean and Early Proterozoic rocks (fig. 12), and so must have risen at least from this stratigraphic level (arrows 1,

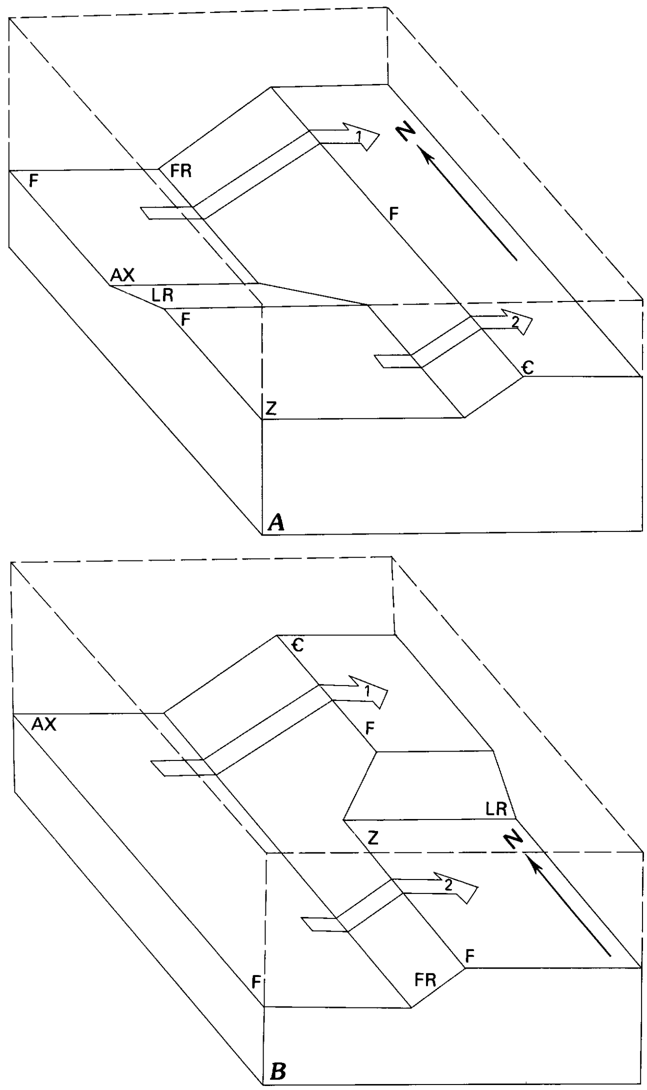

Figure 15. Unscaled block diagrams illustrating two possible geometries of lateral ramps at south nose of ramp anticline of figure 13. Projections are orthographic. Both diagrams represent geometries at the time that the Absaroka thrust fault formed, but before eastward transport had occurred. Hanging wall block is drawn dashed as if transparent. Parts of Absaroka fault are horizontal flats (F) on which motion paralleled beds, frontal ramp (FR) on which reverse motion cut upsection to east, and lateral ramp (LR) on which motion was strike slip. Lateral ramp is drawn perpendicular to frontal ramp for simplicity but might strike obliquely to frontal ramp. Stratigraphic levels of flats are in Archean and Early Proterozoic metamorphic rocks of Farmington Canyon Complex (AX), in late Proterozoic metasedimentary strata of early part of Cordilleran miogeocline (Z), and in Cambrian shales of miogeocline (Ꞓ). Open arrows represent eastward transport of parts of hanging wall block up frontal ramp. Arrow 1 represents motion of ramp anticline that is cored by W rocks, and arrow 2, of rocks in and under Parleys Canyon syncline (figs. 12, 13). *A*, Lateral ramp is west of frontal ramp. *B*, Lateral ramp is east of frontal ramp.

figs. 15*A*, *B*). Because rocks in the Parleys Canyon syncline have moved up less of a ramp than have rocks in the ramp anticline, this lesser ramp has either a shallower bottom (arrow 2, fig. 15*A*) or a deeper top (arrow 2, fig. 15*B*). The first alternative requires a lateral ramp west of the frontal ramp (fig. 15*A*). The second requires a lateral ramp east of the frontal ramp (fig. 15*B*). The flat at intermediate depth (labeled Z in fig. 15) could be in late Archean and Early Proterozoic rocks or in Late Proterozoic strata of the Cordilleran miogeocline. In the case shown in figure 15*A*, the Absaroka thrust would have ramped from an Archean level to a Late Proterozoic level somewhere west of arrow 2 and the area represented by the block diagram. In the case shown in figure 15*B*, ramping from Late Proterozoic level to Cambrian level would have taken place somewhere east of arrow 2 and the block diagram.

We favor the model of figure 15*A* over that of figure 15*B*, because of a tilted frontal ramp that is exposed along the trace of the Mount Raymond fault over a distance of about 12 km eastward from the Wasatch fault zone (R.L. Bruhn, oral commun., 1984; Crittenden, 1965b, c; Crittenden and others, 1966; Bruhn, Picard, and Isby, in press, figs. 5, 6; Bradley, 1986). Exposed strata range from Late Proterozoic to Jurassic in age and dip steeply northward off the dome that was formed by Oligocene (Crittenden and others, 1973) intrusion of the Little Cottonwood stock (figs. 9, 12). Thus, map view is nearly a cross-sectional view of pre-Oligocene structure. Down-plunge viewing of geologic maps (Crittenden, 1965b, c; Crittenden and others, 1966; Bruhn, Picard, and Isby, in press) reveals that for about 6 km eastward from the Wasatch fault zone, the Mount Raymond thrust fault is in footwall rocks of the shaly Middle Cambrian Ophir Formation and Mississippian limestones and dolomites. Below this part of the thrust fault lies an unbroken sequence of Middle and Late Proterozoic and Lower Cambrian strata. Eastward, however, the thrust fault cuts progressively up section, so that its footwall exposes successively younger rocks ending in Middle Jurassic Twin Creek Limestone. Where the fault cuts up section, the angle between the fault and undragged beds in the footwall is about 30°, as calculated from mapped bed orientations and fault traces of Crittenden (1965b). The doming has uplifted and exposed a cross section of a frontal ramp, on which the Mount Raymond thrust fault has ramped from Cambrian up to Jurassic levels. Also exposed is part of the flat that lies at the western foot of the frontal ramp, in the Cambrian and Mississippian strata; the flat lies south along trend from the nose of the ramp anticline (fig. 12).

The Mount Raymond thrust fault is interpreted to be part of the basal thrust fault, the Absaroka fault (fig. 12; Crittenden, 1974; Hintze, 1980; Bradley, 1986). The Absaroka fault underlies the ramp anticline at Cambrian level (Royse and others, 1975) and is at Cambrian level at the Mount Raymond fault. The ramp anticline and Mount Raymond fault are separated by only 10–20 km, a distance that includes the Parleys Canyon syncline, so presumably the deepest thrust fault under the Parleys Canyon syncline is also at Cambrian level. If the deepest thrust fault atop the frontal ramp lies in Cambrian rocks under the ramp anticline, under the Parleys Canyon syncline, and at the Mount Raymond fault, then the model of figure 15*A* must be preferred over that of figure 15*B*.

Thus, the structural anomaly that has caused the southern nose of the ramp anticline is best interpreted to be a north-dipping lateral ramp that extends westward from the frontal ramp, and which underlies the hanging (west) wall of the Wasatch fault zone. This conclusion is consistent with independent interpretations of Smith and Bruhn (1984, section DD′) and Schirmer (1985, p. 136–137).

The location of the lateral ramp can be estimated from the southward decrease in structural relief of the ramp anticline, by recalling that structural relief increases with the height of the frontal ramp that produced the relief. The south end of the anticlinal nose should be east of the top of the lateral ramp of figure 15*A*. Between the anticlinal nose and the Parleys Canyon syncline lies a small anticline-syncline pair (fig. 12). The south end of the nose of the ramp anticline is the north limb of the syncline of the fold pair. The bottom of the lateral ramp is harder to locate, because the shape of the ramp anticline is obscured by Tertiary cover, the complex internal structure of the Archean and Early Proterozoic rocks, and extensional faults (Bryant, 1984). A dip of about 30° is common among ramps, so the lateral ramp is assumed to dip 30° north. Such a ramp would reach a depth of 15 km at about 26 km north of the small syncline. Perusal of the map pattern of the ramp anticline (Stokes, 1963; Bryant, 1984) suggests that the nose of the anticline might extend as far as 38 km north of the small syncline, so the lateral ramp might dip shallowly enough north (22°) to be 38 km wide in map view. Accordingly, the structural anomaly is taken as 26 km wide, with its south edge at the trough of the small syncline. The width of the anomaly is uncertain and could be as much as 38 km, assuming that the south edge of the anomaly is fixed at the synclinal trough.

Cretaceous Thrust Faults South of the Uinta Mountains

Geometries of the Thrust Faults

South of the Deer Creek fault and the Uinta Mountains, the footwall of the Wasatch fault zone exposes a thrust complex much like that in northern Utah. The best exposed thrust sheet in central Utah is the Charleston thrust sheet (fig. 16). Like the Cache allochthon of northern Utah, the Charleston sheet contains rocks of the Cordilleran miogeocline that moved eastward over rocks of the coeval shelf facies (Crittenden, 1961, 1972, 1976; Tooker, 1983). From thrust offsets of isopachs of lower Paleozoic, Mississippian, and Pennsylvanian to Permian units, Crittenden (1961) estimated eastward transport of about 40 mi (64 km) each for the Cache allochthon and Charleston sheet. From a balanced cross section through the northern part of the Charleston sheet, Riess (1985, p. 21) estimated 41 km of eastward transport. Paleontological, stratigraphic, and structural data have established that most thrusting was of Cretaceous age in both northern and central Utah (Armstrong and Oriel, 1965; Oriel and Armstrong, 1966; Royse and others, 1975; Standlee, 1982; Fouch and others, 1983; Villien and Kligfield, in press; Lawton, 1985; Heller and others, 1986; Bryant and Nichols, in press; Bruce Bryant, oral and written communs., 1985).

The Charleston sheet is bounded in map view by traces of the Deer Creek, Charleston, Strawberry Valley,

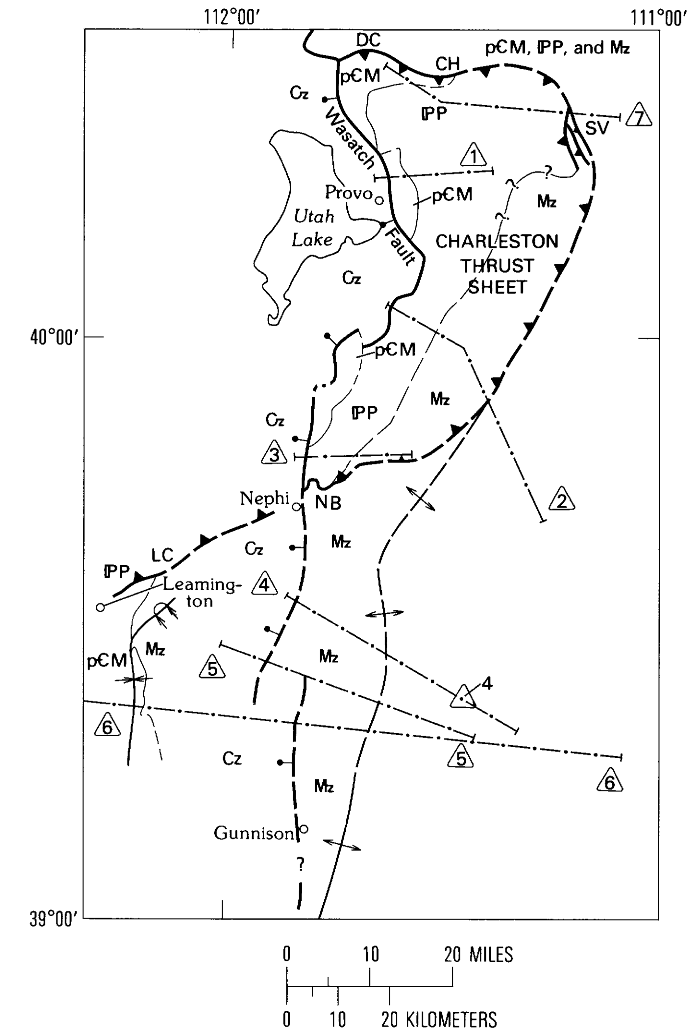

EXPLANATION

Trace of Wasatch fault—Dashed where uncertainly located. Bar and ball on downthrown (west) side

Anticlinal crest or synclinal trough—Dashed where covered by Upper Cretaceous or Cenozoic strata

Overturned syncline

Trace of thrust fault—Dashed where covered by Upper Cretaceous or Cenozoic strata, sawteeth on hanging wall. All thrust faults involved eastward movement of hanging walls. DC, Deer Creek fault; CH, Charleston fault; NB, Nebo fault; LC, Leamington Canyon fault; SV, Strawberry Valley fault.

Generalized contact between Precambrian to Mississippian (pC̶M), Pennsylvanian to Permian (IPP), and Mesozoic (Mz) strata that are involved in thrusting—Dashed where covered by postthrusting Upper Cretaceous or Cenozoic strata (Cz). Location of eastern edge of youngest thrust strata is uncertain and is taken as about at the easternmost structures shown here. East of these structures, rocks are mostly Mesozoic and Cenozoic. Structures not compiled for northwest or southwest parts of map area

1 **Approximate location of a published cross section**—Numeral in triangle identifies section. 1, section *EE′* of Smith and Bruhn (1984); 2, section *DD′* of Lawton (1985); 3, section *FF′* of Smith and Bruhn (1984); 4, section *CC′* of Lawton (1985); 5, section in figure 14 of Standlee (1982); 6, section *AA′* of Villien and Kligfield (in press); 7, section *AA′A″* of Riess (1985, plate II). Section 6 extends west beyond edge of figure

Figure 16. Sketch map of selected structural elements, in and near the footwall and part of the hanging wall of the Wasatch fault zone, south of the Deer Creek fault. Compiled and interpreted from Christiansen (1952), Stokes and Madsen (1961), Stokes (1963), Hintze (1980), Standlee (1982), Smith and Bruhn (1984), Villien and Kligfield (in press), and Lawton (1985).

Deer Creek fault bounds Charleston thrust sheet on the north and connects eastward to Charleston thrust fault, but underwent Tertiary extensional motion over about 10 km of its length east of the Wasatch fault zone (Baker and Crittenden, 1961, section AA′; Riess, 1985). This Tertiary extension on the Deer Creek fault might have reactivated an east-striking lateral ramp that formed during Cretaceous thrusting on the Charleston fault, but such reactivation is not proven. Here the Deer Creek fault is drawn as an extension of the Charleston fault for simplicity. Geometry of connection between Strawberry Valley and Nebo faults is uncertain (Lawton, 1985, figs. 2, 6, p. 1156). Northwestward dip of Leamington Canyon fault and its connection with Nebo fault are controversial (Higgins, 1982; Sprinkel and others, 1982, p. 303–306), as discussed in text.

and Nebo faults, and by their mapped and inferred connections. At the Wasatch fault zone, along the west edge of the exposed part of the thrust sheet, one or two large ramp anticlines expose east-dipping Precambrian and Paleozoic strata and have been dismembered by the irregular trace of the Wasatch fault zone. Tertiary extensional reactivation of some Mesozoic thrust faults (Royse, 1983; Hopkins and Bruhn, 1983; Riess, 1985) might have contributed to this dismemberment.

The thrust sheet has internal structural complexities (Smith and Bruhn, 1984, p. 5740–5741; Wheeler, 1984; Lawton, 1985), but its north and south edges stand out as candidates for structural anomalies. At the north edge, the Deer Creek fault has already been used to define the south end of an anomaly that is associated with the Uinta aulacogen. At the south edge, the Nebo fault has been inferred to extend southwest as the Leamington Canyon fault (Christiansen, 1952; Morris and Shepard, 1964; Morris, 1983; Smith and Bruhn, 1984, p. 5741; Bruhn, Picard, and Isby, in press, fig. 8). The Nebo and Leamington Canyon faults are southern limits of exposures of thick, Pennsylvanian and Permian rocks of the miogeocline. The Nebo and perhaps the Leamington Canyon faults transported these basin-facies rocks eastward, overriding or deforming Upper Cretaceous synorogenic strata (Christiansen, 1952, plate 1; Jefferson, 1982; Sprinkel and others, 1982, p. 303–306; Lawton, 1985). Both faults can be regarded as parts of the same northeast-striking oblique ramp (Smith and Bruhn, 1984, p. 5741), up which the Charleston sheet moved as its basal thrust fault cut up section eastward.

Several map relations are consistent with this interpretation. On the southeast side of the Leamington Canyon fault, the north end of a large syncline bends to the northeast (fig. 16). Where this syncline trends north, beds in the west limb are upright and dip moderately east, but where trends swing to the northeast, the northwest limb is overturned (Christiansen, 1952, plate 1; Higgins, 1982, fig. 7). Where trends change from north to northeast in the west limb of the syncline, several small strike-slip faults cut Cambrian units at high angles (Higgins, 1982, fig. 7, p. 54). The angles at which these small faults cut beds in map view, and the senses of the offsets of the faults, indicate that the faulting would have caused the overturned limb of the syncline to undergo northeast-southwest extension. The northeastward bend of the syncline, the overturning of the northwest limb, and the northeastward extension are all consistent with the hypothesized overriding of the north end of the syncline by the Charleston thrust sheet as it moved up an oblique ramp, and with deformation of the north end of the syncline by drag in the footwall of the ramp.

However, other map relations are inconsistent with the interpretation that the Leamington Canyon and Nebo faults are parts of the same oblique ramp. In its few small exposures the Leamington Canyon fault dips southeast instead of northwest (Morris, 1983, p. 77; Higgins, 1982, fig. 7). Slickenlines and hinges of small folds record northwestward or southeastward movement on the Leamington Canyon fault (Higgins, 1982, p. 50, fig. 12), but Higgins does not mention the sense of this movement. If the sense of movement was northwestward, then the southeast-dipping Leamington Canyon fault might be a small backthrust (Sprinkel and others, 1982, p. 305–306), subsidiary above some larger, east- or southeast-directed thrust fault. If so, then apparently this hypothetical larger fault is not exposed anywhere. If the sense of movement on the Leamington Canyon fault was southeastward, then the southeast dips of this fault might indicate that the fault has been folded within a ramp anticline that formed as a younger, deeper, unexposed thrust fault moved up the hypothesized oblique ramp.

Examination of the maps and sections of Higgins (1982) and Christiansen (1952) suggest these and other structural interpretations of these apparently contradictory relations, but all such interpretations are speculative. It remains unclear whether the Leamington Canyon fault is the main thrust fault northeast of Leamington, which way the main fault dips or moved, and whether the main fault and the Nebo fault are part of the same oblique ramp. Accordingly, the following calculations assume only that there is an oblique or lateral ramp in the Nebo fault where it crosses the Wasatch fault; the calculations are independent of whether the Leamington Canyon and Nebo faults are connected.

Structural Anomaly at a Lateral Ramp

The width of the structural anomaly near Nephi must be estimated from map relations there, excluding relations near Leamington. Near the intersection of the Nebo and Wasatch faults, the Charleston thrust sheet (above the Nebo fault) has been interpreted to have been distorted by evaporite diapirism of Cretaceous to Tertiary age, which was intense locally (Witkind, 1982; 1983, fig. 4) but not regionally in the thrust sheet (Standlee, 1982; Lawton and others, 1982). Map patterns of the trace of the Nebo fault and of vertical to overturned units in its hanging wall (Johnson, 1959; Black, 1965) can be interpreted to indicate that diapiric distortion is confined south of a point that lies 7 km north of Nephi. The effect of the distortion takes the form of a south-facing half window in the thrust sheet (fig. 16). However, cross sections of Johnson (1959) and Black (1965) can also be interpreted to attribute this half window to irregularities in the original shape of the Nebo thrust fault, perhaps locally accentuated by diapirism. Whether the half window is attributed to diapirism, to the original shape of the Nebo fault, or to both, elsewhere the fault remains more or less horizontal where exposed in the hills 0–7 km north of Nephi. If the Nebo fault dips north or northwest on a lateral or oblique ramp, it must do so farther than 7 km north of Nephi. Because the thrust sheet is distorted only south of this point, the top of the ramp is assumed to lie 7 km north of Nephi.

If the ramp is lateral, it strikes east. If it is oblique, it probably strikes N. 70° E., to pass along the south edges of exposures of basin-facies Pennsylvanian to Permian rocks southwest of Nephi (Hintze, 1980). A lateral ramp that dips north at 30° would reach a depth of 15 km at a point 26 km north of the top of the ramp. An oblique ramp would reach this depth 24 km north of its top. The mean of these two estimates is 25 km, measured along a north-south line.

Thus, a structural anomaly that represents a lateral or oblique ramp in the Nebo fault most likely spans the area between 7 and 32 km north of Nephi. Cartographic errors and the 2-km difference between the northward extents of lateral and oblique ramps combine to indicate that parts of the ramp might lie buried as little as 6 or as much as 34 km north of Nephi.

Southward, other thrust sheets emerge from beneath the Charleston sheet (Standlee, 1982; Villien and Kligfield, in press; Lawton, 1985). Cross sections through the other sheets are based on geologic mapping and on well and seismic-reflection data. The sections differ in the relative sizes of several structures and in the inferred eastern limit of thrusting, but not in the main features shown in the sections. Neither these sections, nor their accompanying geologic and structural maps, nor the mapped surface geology (Hintze, 1980; Stokes, 1963) shows any candidates for structural anomalies between the Nebo fault and the southern edge of the study area.

Results

Anomaly St1 corresponds to the north-dipping lateral ramp that we infer to lie west of the southern nose of a ramp anticline between Salt Lake City and Ogden (figs. 12, 15*A*). The south end of the anomaly is where the trace of the Wasatch fault zone intersects the trough of a small syncline about 5 km north of the Parleys Canyon syncline. The north end of the anomaly might be as much as 38 km north of this point, but the anomaly has a most likely width of 26 km.

Anomaly St2 corresponds to the fault system of the Uinta aulacogen. The anomaly extends 21 km along the Wasatch fault zone between its intersections with the traces of the Deer Creek and Mount Raymond faults (figs. 9, 10). North-south width could vary from 4 to 42 km. Regardless of width, the anomaly is centered on the midpoint of distance ab of figures 9 and 10.

Anomaly St3 corresponds to the north-dipping, lateral or oblique ramp that is inferred to connect to the Nebo fault (fig. 16). The anomaly spans the area from 7 to 32 km north of Nephi, and might extend as little as 6 km or as much as 34 km north of Nephi.

The three anomalies were plotted on the map of Hintze (1980) and projected west onto long 112° W. (table 6).

The anomalies meet the seven criteria set out previously. First, the anomalies were identified using geological data at various scales but were located using mapping that was published mostly at 1:24,000, which affords sufficient resolution to detect a segment boundary. Second, the structural data characterize large structures in the top part of the brittle upper crust, where large earthquakes are likely to nucleate. Third, the structural

Table 6. Locations of structural anomalies
[n.a., not applicable. Study area is 332 km long, north to south]

Anomaly number	North end of anomaly[1]	South end of anomaly[1]	Anomaly width (km)	Distance to next anomaly to south (km)
St1	112	138	26	8
St2	146	167	21	53
St3	220	245	25	[2]87
Sum	n.a.	n.a.	72	148

[1]Distance south of Utah-Idaho border, in kilometers.

[2]Distance to south edge of study area at lat 39° N.

data are likely to reflect the presence of a segment boundary by an explainable anomaly. The anomalies correspond to faults or fault systems that could divide one or both walls of the Wasatch fault zone into blocks. The faults or fault systems could have low enough strength that they could partly or entirely decouple blocks that they separate, thereby confining seismic ruptures to single blocks (as suggested independently from gravity data by Zoback (1987) for St3). Such confining would amount to segmentation, and such faults or fault systems would be segment boundaries. Alternatively, the faults that cross the Wasatch fault zone at anomalies St1–St3 could form nonconservative barriers (King and Nabelek, 1985), at which large seismic ruptures might tend to start and stop. Fourth, the structural data allow inferences about expected near-future seismicity, because the pre-Cenozoic structures involved have stopped their developments and their characteristics will not change over the next decades to millenia. Fifth, the structural anomalies are reproducible because Smith and Bruhn (1984) and Bruhn and Smith (1984) have independently observed apparent spatial associations of anomalies St1–St3 and other structures with the segment boundaries that were proposed by Schwartz and Coppersmith (1984). Also, the anomalies have been described in enough detail that an independent reader should be able to reproduce them by reference to the cited sources. Sixth and seventh, the structural anomalies were derived from structural, stratigraphic, and other geological data, but without reference to any other data types of this report or to the proposed segment boundaries of Schwartz and Coppersmith (1984).

SUMMARY AND QUESTIONS

The six data types discussed above have 2–10 anomalies each and together form 26 anomalies along the length of the Wasatch fault zone in Utah (fig. 17*A*). The distribution of anomalies along the fault zone defines a pattern of clustered anomalies. The north and south ends of each anomaly in the pattern have various locational uncertainties, which are small compared to anomaly widths and do not greatly distort most aspects of the anomaly pattern (figs. 17*B*, *C*).

Each data type and its anomalies have been shown to satisfy criteria that insure that the anomalies are pertinent to identifying segment boundaries. Each anomaly was identified by methods that are partly or wholly subjective. Subjectivity introduces operator variability, which can decrease the reliability of results, so the criteria also insure that the individual anomalies and their locations are reliable enough to be worth interpreting.

Each anomaly might indicate the presence of a segment boundary. Where several anomalies in different data types fall at about the same place along the fault

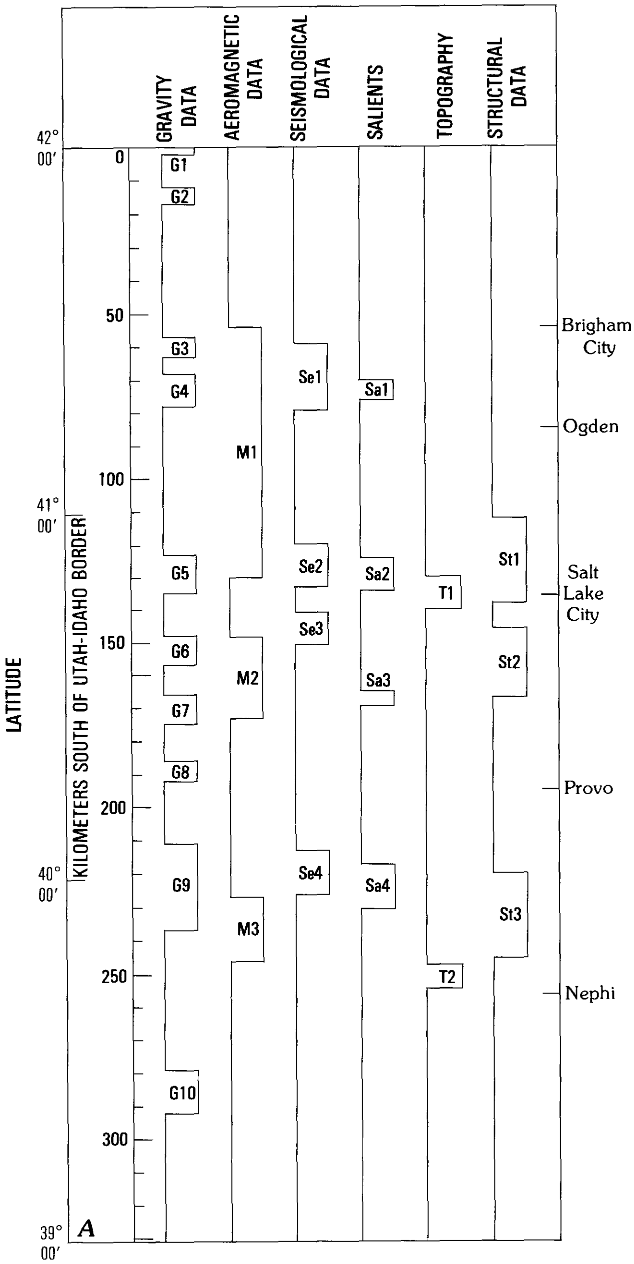

Figure 17(above and facing page). Distribution of anomalies along Wasatch fault zone. Length of anomaly pattern is 332 km, southward from Utah-Idaho border. Anomaly locations were projected east or west from trace of fault zone into lat 112° W. Locations of anomaly ends along this meridian and anomaly names are from tables 1–6. Columns show anomalies in six data types discussed in text. Solid line in each column steps to right edge of column where there is an anomaly in the corresponding data type, and steps to left edge between anomalies. *A*, Each anomaly is drawn with its measured width (tables 1–6). *B*, Each anomaly is drawn with the minimum width that is allowed by the locational uncertainties of its edges. This procedure would give anomaly Se3 a width of 0 km, so its minimum width is arbitrarily set at 1 km. Uncertainties are described in the "Results" sections of the six parts of this report that describe the data types. C, Each anomaly is given its maximum allowable width. Anomalies Se2 and Se3 overlap by 2 km, as do St1 and St2.

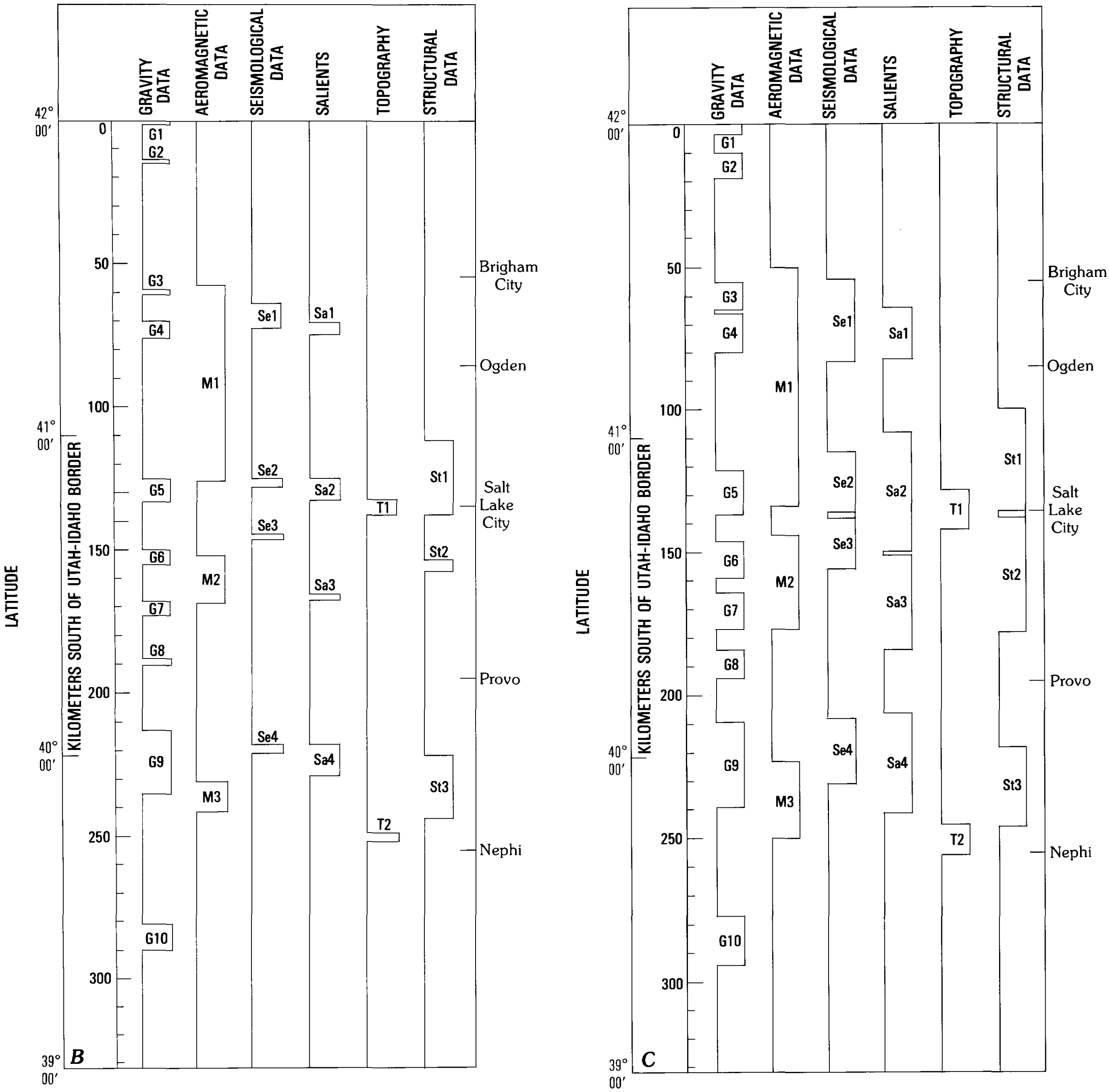

zone, a segment boundary is a reasonable interpretation, provided other causes of the coinciding anomalies can be ruled out. For example, at and near km 70 (fig. 17*A*) anomalies G4, M1, Se1, Sa1, and perhaps G3 appear to coincide. Near km 230 anomalies G9, M3, Se4, Sa4, St3, and perhaps T2 similarly appear to coincide. Over a broad zone between km 110 and 180 as many as 12 anomalies might coincide. These three parts of the fault zone might each contain one or more segment boundaries.

However, subjective evaluation of figure 17 can take us little farther than this. Probably most interpreters would agree that G3 coincides with M1 and Se1, and G4 with M1, Se1, and Sa1, but might disagree about whether G3 coincides with Sa1 or G4. Does T2 coincide with the five anomalies that lie immediately north of it (G9, M3, Se4, Sa4, and St3)? Probably most interpreters would consider M3 to coincide with G9 and St3, and G9 and St3 to coincide with Se4 and Sa4; does this mean that M3 coincides with Se4 and Sa4? Should the cluster of 12 anomalies between km 100 and 180 (fig. 17*A*) be subdivided? If so, how? More subtly, how much of the visual impact of figure 17 is caused by the order in which the data types are listed from left to right?

Chance also creates a problem for interpretation of the observed anomaly pattern. Anomalies are abundant enough and wide enough that two or more might coincide by chance, even if the coincident anomalies share no underlying geological cause like a segment boundary. Experiments with anomalies that are scattered randomly along a fault zone show that chance coincidences can be surprisingly common and can look disturbingly convincing (Wheeler and Krystinik, 1987a). Anomaly coincidences that have a high probability of having arisen by chance should not be considered worth interpreting. How many anomalies in different data types must coincide before we may confidently assume that the pattern of coincidences is worth interpreting?

Development and application of methods to answer these questions lie well beyond the scope of this report, which is restricted to data summaries, analyses, and interpretations. However, Wheeler and Krystinik (1987a) derived and described such methods, and Wheeler and Krystinik (1987b, c, d) applied them to the anomaly pattern of figure 17 and the values of tables 1–6.

REFERENCES CITED

Algermissen, S.T., Perkins, D.M., Thenhaus, P.C., Hanson, S.L., and Bender, B.L., 1982, Probabilistic estimates of maximum acceleration and velocity in rock in the contiguous United States: U.S. Geological Survey Open-File Report 82–1033, 99 p., 6 folded plates.

Anderson, L.W., and Miller, D.G., 1979, Quaternary fault map of Utah: Long Beach, Calif., Fugro, Inc., 35 p., 1 folded plate, scale 1:500,000.

Arabasz, W.J., 1984, Earthquake behavior in the Wasatch Front area—Association with geologic structure, space-time occurrence, and stress state, *in* Hays, W.W., and Gori, P.L., eds., Workshop on "Evaluation of regional and urban earthquake hazards and risk in Utah", Salt Lake City, Utah, August 14–16, 1984, Proceedings: U.S. Geological Survey Open-File Report 84-763, p. 310–339.

Arabasz, W.J., and Julander, D.R., 1986, Geometry of seismically active faults and crustal deformation within the Basin and Range-Colorado Plateau transition in Utah: Geological Society of America Special Paper 208, p. 43–74.

Arabasz, W.J., Smith, R.B., and Richins, W.D., 1980, Earthquake studies along the Wasatch Front, Utah—Network monitoring, seismicity, and seismic hazards: Bulletin of the Seismological Society of America, v. 70, p. 1479–1499.

Armstrong, R.C., and Oriel, S.S., 1965, Tectonic development of Idaho-Wyoming thrust belt: American Association of Petroleum Geologists Bulletin, v. 49, p. 1847–1866.

Armstrong, R.L., 1968, Sevier orogenic belt in Nevada and Utah: Geological Society of America Bulletin, v. 79, p. 429–458.

Baars, D.L., 1972, Devonian system, *in* Mallory, W.W., ed.-in-chief, Geologic atlas of the Rocky Mountain region: Denver, Colo., Rocky Mountain Association of Geologists, p. 90–99.

Baker, A.A., and Crittenden, M.D., Jr., 1961, Geology of the Timpanogos Cave quadrangle, Utah: U.S. Geological Survey Geologic Quadrangle Map GQ–132, scale 1:24,000, 1 sheet.

Bates, R.L., and Jackson, J.A., eds., 1980, Glossary of geology, 2d ed.: Falls Church, Va., American Geological Institute, 749 p.

Behrendt, J.C., and Thiel, Edward, 1963, A gravity and magnetic survey of the Uinta Mountains: Journal of Geophysical Research, v. 68, p. 857–868.

Berg, T.M., Edmunds, W.E., Geyer, A.R., Glover, A.D., Hoskins, D.M., MacLachlan, D.B., Root, S.I., Sevon, W.D., and Socolow, A.A., compilers, 1980, Geologic map of Pennsylvania: Pennsylvania Topographic and Geologic Survey Map 1, scale 1:250,000, 3 sheets.

Black, B.A., 1965, Nebo overthrust, southern Wasatch Mountains, Utah: Brigham Young University Geology Studies, v. 12, p. 55–89.

Bollinger, G.A., Teague, A.G., Munsey, J.W., and Johnston, A.C., 1985, Focal mechanism analyses for Virginia and eastern Tennessee earthquakes (1978–1984): U.S. Nuclear Regulatory Commission NUREG/CR-4288, 86 p., 8 microfiches.

Bollinger, G.A., and Wheeler, R.L., 1982, The Giles County, Virginia, seismogenic zone—Seismological results and geological interpretations: U.S. Geological Survey Open-File Report 82-585, 142 p.

______1983, The Giles County, Virginia, seismic zone: Science, v. 219, p. 1063–1065.

Boyer, S.E., and Elliott, David, 1982, Thrust systems: American Association of Petroleum Geologists Bulletin, v. 66, p. 1196–1230.

Bradley, M.D., 1984, Demarcation of a duplex zone—Rockport Lake area, Utah [abs.]: American Association of Petroleum Geologists Bulletin, v. 68, p. 932–933.

______1986, Thrust splay correlation in the Absaroka thrust system of northcentral Utah: Geological Society of America Abstracts with Programs, v. 18, no. 5, p. 343.

Bruhn, R.L., Gibler, P.R., Houghton, Wendy, and Parry, W.T., 1987, Structure of the Salt Lake segment, Wasatch normal fault zone—Implications for rupture propagation during normal faulting, *in* Gori, P.L., and Hays, W.W., eds., Assessment of regional earthquake hazards and risks along the Wasatch Front, Utah: U.S. Geological Survey Open-File Report 87-585, v. I, p. H1–H57.

Bruhn, R.L., Gibler, P.R., and Parry, W.T., 1987, Rupture characteristics of normal faults—An example from the Wasatch fault zone, Utah, *in* Coward, M.P., Dewey, J.F., and Hancock, P.H., eds., Continental extensional tectonics: Geological Society of London Special Publication No. 28, p. 337–353.

Bruhn, R.L., Picard, M.D., and Beck, S.L., 1983, Mesozoic and early Tertiary structure and sedimentology of the central Wasatch Mountains, Uinta Mountains and Uinta Basin, *in* Gurgel, K.D., ed., Geologic excursions in the overthrust belt and metamorphic core complexes of the Intermountain region: Utah Geological and Mineral Survey Special Studies 59, p. 63–105.

Bruhn, R.L., Picard, M.D., and Isby, J.S., in press, Tectonics and sedimentology of the Uinta arch, western Uinta Mountains and Uinta basin, *in* Petersen, James, ed., Sedimentation and tectonics in the Rocky Mountain region:

American Association of Petroleum Geologists Special Publication.

Bruhn, R.L., and Smith, R.B., 1984, Relation of Wasatch fault zone to ancient thrust belt structures—Implications for normal fault geometry and maximum expectable earthquake magnitudes [abs.]: Transactions of the American Geophysical Union, v. 64, no. 45, p. 842.

Bryant, Bruce, 1984, Reconnaissance geologic map of the Precambrian Farmington Canyon Complex and surrounding rocks in the Wasatch Mountains between Ogden and Bountiful, Utah: U.S. Geological Survey Miscellaneous Investigations Map I-1447, scale 1:50,000, 1 sheet.

______1985, Structural ancestry of the Uinta Mountains, *in* Picard, M.D., ed., Geology and energy resources, Uinta basin of Utah: Utah Geological Association Publication 12, p. 115–120.

Bryant, Bruce, and Nichols, D.J., in press, Late Mesozoic and early Tertiary reactivation of an ancient zone of crustal weakness along the Uinta arch and its interaction with the Sevier orogenic belt, *in* Schmidt, C.J., and Perry, W.J., Jr., eds., Interaction of the Rocky Mountain foreland and the frontal Cordilleran thrust belt: Geological Society of America Special Paper.

Bucknam, R.C., Algermissen, S.T., and Anderson, R.E., 1980, Patterns of late Quaternary faulting in western Utah and an application to earthquake hazard evaluation, *in* Andriese, P.D., compiler, Earthquake hazards along the Wasatch-Sierra Nevada frontal fault zones, 1979, Proceedings: U.S. Geological Survey Open-File Report 80-801, p. 299–314.

Burchfiel, B.C., and Davis, G.A., 1975, Nature and controls of Cordilleran orogenesis, western United States—Extensions of an earlier synthesis: American Journal of Science, v. 275-A, p. 363–396.

Burke, Kevin, and Dewey, J.F., 1973, Plume-generated triple junctions—Key indicators in applying plate tectonics to old rocks: Journal of Geology, v. 81, p. 406–433.

Butler, R.W.H., 1982, The terminology of structures in thrust belts: Journal of Structural Geology, v. 4, p. 239–245.

Calver, J.L., Hobbs, C.R.B., Jr., Milici, R.C., Spiker, C.T., and Wilson, J.M., 1963, Geologic map of Virginia: Virginia Division of Mineral Resources, scale 1:500,000, 2 sheets.

Campbell, J.A., 1975, Structural geology and petroleum potential of the south flank of the Uinta Mountain uplift, northeastern Utah: Utah Geology, v. 2, p. 129–132, 2 folded plates, approximate scales 1:703,000, 1:43,640, and 1:69,800.

Chamberlain, A.K., 1984, Shallow-water clastic sediments of Great Blue Formation and Manning Canyon Shale, Oquirrh basin, Utah [abs.]: American Association of Petroleum Geologists Bulletin, v. 68, p. 934.

Chen, W.-P., and Molnar, Peter, 1983, Focal depths of intracontinental and intraplate earthquakes and their implications for the thermal and mechanical properties of the lithosphere: Journal of Geophysical Research, v. 88, no. B5, p. 4183–4214.

Christiansen, F.W., 1952, Structure and stratigraphy of the Canyon Range, central Utah: Geological Society of America Bulletin, v. 63, p. 717–740.

Christie-Blick, Nicholas, 1984, Latest Proterozoic and Early Cambrian rifting in California, Nevada and Utah—Support for Early Cambrian continental separation: Geological Society of America Abstracts with Programs, v. 16, no. 6, p. 471.

Christie-Blick, Nicholas, and von der Borch, C.C., 1985, Sequence boundaries in Proterozoic successions—A comparison of the Brigham Group (Utah) and Wilpena Group (South Australia), with implications for sea-level change and global correlation: Geological Society of America Abstracts with Programs, v. 17, no. 7, p. 546.

Cleaves, E.T., Edwards, Jonathan, Jr., and Glaser, J.D., 1968, Geologic map of Maryland: Maryland Geological Survey, scale 1:250,000, 1 sheet.

Clement, J.H., 1983, North flank of the Uinta Mountains, Utah, *in* Bally, A.W., ed., Seismic expression of structural styles—A picture and work atlas: American Association of Petroleum Geologists Studies in Geology Series No. 15, v. 3, p. 3.2.2-29 to 3.2.2-32.

Cluff, L.S., Brogan, G.E., and Glass, C.E., 1970, Wasatch fault, northern portion—Earthquake fault investigation and evaluation: Oakland, Calif., Woodward-Clyde and Associates unpublished report to Utah Geological and Mineral Survey, 109 p.

______1973, Wasatch fault, southern portion—Earthquake fault investigation and evaluation: Oakland, Calif., Woodward-Lundgren and Associates unpublished report to Utah Geological and Mineral Survey, 179 p.

Cluff, L.S., Glass, C.E., and Brogan, G.E., 1974, Investigation and evaluation of the Wasatch fault north of Brigham City and Cache Valley faults, Utah and Idaho: Oakland, Calif., Woodward-Lundgren and Associates unpublished report to U.S. Geological Survey, 232 p.

Cluff, L.S., Hintze, L.F., Brogan, G.E., and Glass, C.E., 1975, Recent activity of the Wasatch fault, northwestern Utah, U.S.A.: Tectonophysics, v. 29, p. 161–168.

Cluff, L.S., and Slemmons, D.B., 1972, Wasatch fault zone—Features defined by low-sun-angle photography, *in* Hilpert, L.S., ed., Environmental geology of the Wasatch Front, 1971: Utah Geological Association Publication 1, p. G1–G9.

Cook, K.L., and Berg, J.W., Jr., 1961, Regional gravity survey along the central and southern Wasatch Front, Utah: U.S. Geological Survey Professional Paper 316–E, p. 75–89, 1 folded plate, scale 1:500,000.

Cook, K.L., and Montgomery, J.R., 1972, East-west transverse structural trends in eastern Basin and Range province as indicated by gravity data: Geological Society of America Abstracts with Programs, v. 4, no. 5, p. 315.

______1974, Crustal structure and east-west transverse structural trends in eastern Basin and Range province as indicated by gravity data: Geological Society of America Abstracts with Programs, v. 6, no. 3, p. 158.

Cook, K.L., Montgomery, J.R., Smith, J.T., and Gray, E.F., 1975, Simple Bouguer gravity anomaly map of Utah: Utah Geological and Mineral Survey Map 37, scale 1:1,000,000, 1 sheet.

Cook, K.L., and Smith, R.B., 1967, Seismicity in Utah, 1850 through June 1965: Bulletin of the Seismological Society of America, v. 57, p. 689–718, 1 folded plate.

Craig, L.C., 1972, Mississippian system, *in* Mallory, W.W., ed.-in-chief, Geologic atlas of the Rocky Mountain region: Denver, Colo., Rocky Mountain Association of Geologists, p. 100–110.

Crittenden, M.D., Jr., 1961, Magnitude of thrust faulting in northern Utah: U.S. Geological Survey Professional Paper 424–D, p. D128–D131.

______1965a, Geology of the Dromedary Peak quadrangle, Utah: U.S. Geological Survey Geologic Quadrangle Map GQ–378, scale 1:24,000, 1 sheet.

______1965b, Geology of the Mount Aire quadrangle, Salt Lake County, Utah: U.S. Geological Survey Geologic Quadrangle Map GQ–379, scale 1:24,000, 1 sheet.

______1965c, Geology of the Sugar House quadrangle, Salt Lake County, Utah: U.S. Geological Survey Geologic Quadrangle Map GQ–380, scale 1:24,000, 1 sheet.

______1972, Willard thrust and the Cache allochthon, Utah: Geological Society of America Bulletin, v. 83, p. 2871–2880.

______1974, Regional extent and age of thrusts near Rockport Reservoir and relation to possible exploration targets in northern Utah: American Association of Petroleum Geologists Bulletin, v. 58, p. 2428–2435.

______1976, Stratigraphic and structural setting of the Cottonwood area, Utah, *in* Hill, J.G., ed., Geology of the Cordilleran hingeline: Denver, Colo., Rocky Mountain Association of Geologists, p. 363–379.

Crittenden, M.D., Jr., Calkins, F.C., and Sharp, B.J., 1966, Geologic map of the Park City West quadrangle, Utah: U.S. Geological Survey Geologic Quadrangle Map GQ–535, scale 1:24,000, 1 sheet.

Crittenden, M.D., Jr., and Sorensen, M.L., 1985, Geologic map of the North Ogden quadrangle and part of the Ogden and Plain City quadrangles, Box Elder and Weber Counties, Utah: U.S. Geological Survey Miscellaneous Investigations Series Map I–1606, scale 1:24,000, 1 sheet.

Crittenden, M.D., Jr., Stewart, J.H., and Wallace, C.A., 1972, Regional correlation of Upper Precambrian strata in western North America: International Geological Congress, 24th, Montreal, Canada, 1972, Section 1, p. 334–341.

Crittenden, M.D., Jr., Stuckless, J.S., Kistler, R.W., and Stern, T.W., 1973, Radiometric dating of intrusive rocks in the Cottonwood area, Utah: U.S. Geological Survey Journal of Research, v. 1, p. 173–178.

Crittenden, M.D., Jr., and Wallace, C.A., 1973, Possible equivalents of the Belt Supergroup in Utah: Idaho Bureau of Mines and Geology, Belt Symposium, v. 1, p. 116–138.

Crittenden, M.D., Jr., Wallace, C.A., and Sheridan, M.J., 1967, Mineral resources of the High Uintas primitive area, Utah: U.S. Geological Survey Bulletin 1230–I, 27 p., 1 folded plate, scale 1:125,000.

Crone, A.J., and Harding, S.T., 1984, Relationship of late Quaternary fault scarps to subjacent faults, eastern Great Basin, Utah: Geology, v. 12, p. 292–295.

Crone, A.J., and Machette, M.N., 1984, Surface faulting accompanying the Borah Peak earthquake, central Idaho: Geology, v. 12, p. 664–667.

Currey, D.R., 1982, Lake Bonneville—Selected features of relevance to neotectonic analysis: U.S. Geological Survey Open-File Report 82–1070, 30 p., 1 folded plate, scale 1:500,000.

Davis, F.D., compiler, 1983a, Geologic map of the central Wasatch Front, Utah: Utah Geological and Mineral Survey Map 54–A, scale 1:100,000, 2 sheets.

______1983b, Geologic map of the southern Wasatch Front, Utah: Utah Geological and Mineral Survey Map 55–A, scale 1:100,000, 2 sheets.

______1985, Geologic map of the northern Wasatch Front, Utah: Utah Geological and Mineral Survey Map 53–A, scale 1:100,000, 2 sheets.

Dixon, J.S., 1982, Regional structural synthesis, Wyoming salient of western overthrust belt: American Association of Petroleum Geologists Bulletin, v. 66, p. 1560–1580.

Dover, J.H., 1983, New data on thrusts in northeastern Utah and southwestern Wyoming: Geological Society of America Abstracts with Programs, v. 15, no. 5, p. 318–319.

Eardley, A.J., 1939, Structure of the Wasatch-Great Basin region: Geological Society of America Bulletin, v. 50, p. 1277–1310.

______1944, Geology of the north-central Wasatch Mountains, Utah: Geological Society of America Bulletin, v. 55, p. 819–894.

______1969, Willard thrust and the Cache uplift: Geological Society of America Bulletin, v. 80, p. 669–680.

Forrester, J.D., 1937, Structure of the Uinta Mountains: Geological Society of America Bulletin, v. 48, p. 631–666.

Foster, N.H., 1972, Ordovician system, *in* Mallory, W.W., ed.-in-chief, Geologic atlas of the Rocky Mountain region: Denver, Colo., Rocky Mountain Association of Geologists, p. 76–85.

Fouch, T.D., Lawton, T.F., Nichols, D.J., Cashion, W.B., and Cobban, W.A., 1983, Patterns and timing of synorogenic sedimentation in Upper Cretaceous rocks of central and northeast Utah, *in* Reynolds, M.W., and Dolly, E.D., eds., Mesozoic paleogeography of the west-central United States, Rocky Mountain paleogeography symposium 2: Denver, Colo., Rocky Mountain Section, Society of Economic Paleontologists and Mineralogists, p. 305–336.

Freedman, Davis, Pisani, Robert, and Purves, Roger, 1978, Statistics: New York, W.W. Norton and Company, 506 p.

Gary, Margaret, McAfee, Robert, Jr., and Wolf, C.L., eds., 1972, Glossary of geology: Washington, D.C., American Geological Institute, 857 p.

Gilbert, G.K., 1928, Studies of Basin-Range structure: U.S. Geological Survey Professional Paper 153, 91 p.

Gries, Robbie, 1983, North-south compression of Rocky Mountain foreland structures, *in* Lowell, J.D., and Gries, Robbie, eds., Rocky Mountain foreland basins and uplifts: Denver, Colo., Rocky Mountain Association of Geologists, p. 9–32.

Hansen, W.R., 1965, Geology of the Flaming Gorge area, Utah-Colorado-Wyoming: U.S. Geological Survey Professional Paper 490, 196 p.

______1984, Post-Laramide tectonic history of the eastern Uinta Mountains, Utah, Colorado, and Wyoming: Mountain Geologist, v. 21, no. 1, p. 5–29.

______1986, History of faulting in the eastern Uinta Mountains, Colorado and Utah, *in* Stone, D.S., ed., New interpretations of northwest Colorado geology: Denver, Colo., Rocky Mountain Association of Geologists, p. 5–17.

Hays, W.W., 1979, Program and plans of the U.S. Geological

Survey for producing information needed in national seismic hazards and risk assessment, fiscal years 1980–1984: U.S. Geological Survey Circular 816, 40 p.

Hays, W.W., and Gori, P.L., 1984, Summary and background, Workshop on "Evaluation of regional and urban earthquake hazards and risk in Utah", *in* Hays, W.W., and Gori, P.L., eds., Workshop on "Evaluation of regional and urban earthquake hazards and risk in Utah", Salt Lake City, Utah, August 14–16, 1984, Proceedings: U.S. Geological Survey Open-File Report 84–763, p. 1–47.

Heller, P.L., Bowdler, S.S., Chambers, H.P., Coogan, J.C., Hagen, E.S., Shuster, M.W., Winslow, N.S., and Lawton, T.F., 1986, Time of initial thrusting in the Sevier orogenic belt, Idaho-Wyoming and Utah: Geology, v. 14, p. 388–391.

Hicks, C.R., 1973, Fundamental concepts in the design of experiments: New York, Holt, Rinehart, and Winston, 349 p.

Higgins, J.M., 1982, Geology of the Champlin Peak quadrangle, Juab and Millard Counties, Utah: Brigham Young University Geology Studies, v. 29, Part 2, p. 40–58, 1 folded plate, scale 1:24,000.

Hintze, L.F., 1980, compiler, Geologic map of Utah: Salt Lake City, Utah, Utah Geological and Mineral Survey, scale 1:500,000, 2 sheets.

Hoffman, Paul, 1973, Evolution of an early Proterozoic continental margin—The Coronation geosyncline and associated aulacogens of the northwestern Canadian shield: Royal Society of London Philosophical Transactions, Series A, v. 273, p. 547–581.

Hoffman, Paul, Dewey, J.F., and Burke, Kevin, 1973, Aulacogens and their genetic relation to geosynclines, with a Proterozoic example from Great Slave Lake, Canada: Society of Economic Paleontologists and Mineralogists Special Publication No. 19, p. 38–55.

Hopkins, D.L., and Bruhn, R.L., 1983, Extensional faulting in the Wasatch Mountains, Utah: Geological Society of America Abstracts with Programs, v. 15, no. 5, p. 402.

Hunt, C.B., Varnes, H.D., and Thomas, H.E., 1953, Lake Bonneville—Geology of northern Utah Valley, Utah: U.S. Geological Survey Professional Paper 257-A, 99 p., 7 folded plates.

Jackson, J.A., Fitch, T.J., and McKenzie, D.P., 1981, Active thrusting and the evolution of the Zagros thrust belt, *in* McClay, K.R., and Price, N.J., eds., Thrust and nappe tectonics: Geological Society of London Special Publication No. 9, p. 371–380.

Jefferson, W.S., 1982, Structural and stratigraphic relations of Upper Cretaceous to Lower Tertiary orogenic sediments in the Cedar Hills, Utah, *in* Nielson, D.L., ed., Overthrust belt in Utah: Utah Geological Association Publication 10, p. 65–80.

Johnson, K.D., 1959, Structure and stratigraphy of the Mount Nebo-Salt Creek area, southern Wasatch Mountains, Utah: Brigham Young University Geology Studies, v. 6, no. 6, 49 p., 1 folded plate, scale about 1:29,333.

King, Geoffrey, 1983, The accomodation of large strains in the upper lithosphere of the Earth and other solids by self-similar fault systems—The geometrical origin of b-value: Pure and Applied Geophysics, v. 121, p. 761–815.

King, Geoffrey, and Nabelek, John, 1985, Role of fault bends in the initiation and termination of earthquake rupture: Science, v. 228, p. 984–987.

King, Geoffrey, and Yielding, Graham, 1984, The evolution of a thrust fault system—Processes of rupture initiation, propagation and termination in the 1980 El Asnam (Algeria) earthquake: Royal Astronomical Society Geophysical Journal, v. 77, p. 915–933.

King, P.B., and Beikman, H.M., 1974, Geologic map of the United States (exclusive of Alaska and Hawaii): U.S. Geological Survey, scale 1:2,500,000, 3 sheets.

Lamerson, P.R., 1982, The Fossil basin and its relationship to the Absaroka thrust system, Wyoming and Utah, *in* Powers, R.B., ed., Geologic studies of the Cordilleran thrust belt: Denver, Colo., Rocky Mountain Association of Geologists, p. 279–340, 13 folded plates.

Lawton, T.F., 1985, Style and timing of frontal structures, thrust belt, central Utah: American Association of Petroleum Geologists Bulletin, v. 69, p. 1145–1159.

Lawton, T.F., Dickinson, W.R., and Jefferson, W.S., 1982, Inferred eastern extent, overthrust belt, central Utah [abs.]: American Association of Petroleum Geologists Bulletin, v. 66, p. 592.

Lewis, J.V., and Kümmel, H.B., 1910–1912, Geologic map of New Jersey: New Jersey Bureau of Geology and Topography Map No. 40, scale 1:250,000, 1 sheet (revised in 1931 by H.B. Kümmel and in 1950 by M.E. Johnson).

Lochman-Balk, Christina, 1972, Cambrian system, *in* Mallory, W.W., ed.-in-chief, Geologic atlas of the Rocky Mountain region: Denver, Colo., Rocky Mountain Association of Geologists, p. 60–75.

______1976, The Cambrian section of the central Wasatch Mountains, *in* Hill, J.G., ed., Geology of the Cordilleran hingeline: Denver, Colo., Rocky Mountain Association of Geologists, p. 103–108.

Loughlin, G.F., 1913, Reconnaissance in the southern Wasatch Mountains, Utah: Journal of Geology, v. 21, p. 436–452.

Mabey, D.R., 1987, Subsurface geology along the Wasatch Front, *in* Gori, P.L., and Hays, W.W., eds., Assessment of regional earthquake hazards and risks along the Wasatch Front, Utah: U.S. Geological Survey Open-File Report 87–585, v. I, p. C1–C39.

Mabey, D.R., Crittenden, M.D., Jr., Morris, H.T., Roberts, R.J., and Tooker, E.W., 1964, Aeromagnetic and generalized geologic map of part of north-central Utah: U.S. Geological Survey Geophysical Investigations Map GP-422, scale 1:250,000, 1 sheet.

Mabey, D.R., Oliver, H.W., and Hildenbrand, T.G., 1983, Regional gravity and magnetic anomalies in the northern Basin and Range province, *in* The role of heat in the development of energy and mineral resources in the northern Basin and Range province: Geothermal Resources Council Special Report No. 13, p. 307–315.

Machette, M.N., 1984, Preliminary investigations of late Quaternary slip rates along the southern part of the Wasatch fault zone, central Utah, *in* Hays, W.W., and Gori, P.L., eds., Workshop on "Evaluation of regional and urban earthquake hazards and risk in Utah", Salt Lake City, Utah, August 14–16, 1984, Proceedings: U.S. Geological Survey Open-File Report 84–763, p. 391–406.

Mattick, R.E., 1970, Thickness of unconsolidated to semi-consolidated sediments in Jordan Valley, Utah: U.S.

Geological Survey Professional Paper 700-C, p. C119-C124.
Meissner, R., and Strehlau, J., 1982, Limits of stresses in continental crusts and their relation to the depth-frequency distribution of shallow earthquakes: Tectonics, v. 1, p. 73-89.
Metter, R.E., 1955, The geology of a part of the southern Wasatch Mountains, Utah: Columbus, Ohio, Ohio State University Ph. D. dissertation, 242 p., 2 folded plates, scale 1:24,000.
Miller, R.D., 1980, Surficial geologic map along part of the Wasatch Front, Salt Lake Valley, Utah: U.S. Geological Survey Miscellaneous Field Studies Map MF-1198, scale 1:100,000, 2 sheets, 13 p. pamphlet.
______1982, Surficial geologic map along the southern part of the Wasatch Front, Great Salt Lake and Utah Valleys, Utah: U.S. Geological Survey Miscellaneous Field Studies Map MF-1477, scale 1:100,000, 1 sheet, 14 p. pamphlet.
Monley, L.E., 1971, Petroleum potential of Idaho-Wyoming overthrust belt, *in* Cram, I.H., ed., Future petroleum provinces of the United States—Their geology and potential: American Association of Petroleum Geologists Memoir 15, p. 509-537.
Moore, D.S., 1979, Statistics—Concepts and controversies: San Francisco, W.H. Freeman and Company, 313 p.
Morisawa, Marie, 1972, The Wasatch fault zone—General aspects, *in* Hilpert, L.S., ed., Environmental geology of the Wasatch Front, 1971: Utah Geological Association Publication 1, p. D1-D17.
Morris, H.T., 1983, Interrelations of thrust and transcurrent faults in the central Sevier orogenic belt near Leamington, Utah, *in* Miller, D.M., Todd, V.R., and Howard, K.A., eds., Tectonic and stratigraphic studies in the eastern Great Basin: Geological Society of America Memoir 157, p. 75-81.
Morris, H.T., and Lovering, T.S., 1961, Stratigraphy of the East Tintic Mountains, Utah: U.S. Geological Survey Professional Paper 361, 145 p.
Morris, H.T., and Shepard, W.M., 1964, Evidence for a concealed tear fault with large displacement in the central East Tintic Mountains, Utah: U.S. Geological Survey Professional Paper 501-C, p. C19-C21.
Moulton, F.C., 1975, Lower Mesozoic and Upper Paleozoic petroleum potential of the Hingeline area, central Utah, *in* Symposium on deep drilling frontiers of the central Rocky Mountains: Denver, Colo., Rocky Mountain Association of Geologists, p. 87-97 (reprinted *in* Hill, J.G., ed., 1976, Geology of the Cordilleran hingeline: Denver, Colo., Rocky Mountain Association of Geologists, p. 219-229).
Munsey, J.W., and Bollinger, G.A., 1985, Focal mechanism analyses for Virginia earthquakes (1978-1984): Bulletin of the Seismological Society of America, v. 75, p. 1613-1636.
Naeser, C.W., Bryant, Bruce, Crittenden, M.D., Jr., and Sorensen, M.L., 1983, Fission-track ages of apatite in the Wasatch Mountains, Utah—An uplift study, *in* Miller, D.M., Todd, V.R., and Howard, K.A., eds., Tectonic and stratigraphic studies in the eastern Great Basin: Geological Society of America Memoir 157, p. 29-36.
Nettleton, L.L., 1971, Elementary gravity and magnetics for geologists and seismologists: Society of Exploration Geophysicists Monograph Series No. 1, 121 p.
Ni, James, and Barazangi, Muawia, 1986, Seismotectonics of the Zagros continental collision zone and a comparison with the Himalayas: Journal of Geophysical Research, v. 91, no. B8, p. 8205-8218.
Oriel, S.S., and Armstrong, F.C., 1966, Times of thrusting in Idaho-Wyoming thrust belt—Reply: American Association of Petroleum Geologists Bulletin, v. 50, p. 2614-2621.
Osmond, J.C., 1986, Petroleum geology of the Uinta Mountains-White River uplift, Colorado and Utah, *in* Stone, D.S., ed., New interpretations of northwest Colorado geology: Denver, Colo., Rocky Mountain Association of Geologists, p. 213-221.
Oviatt, C.G., 1985, Preliminary notes on the Paleozoic stratigraphy and structural geology of the Honeyville quadrangle, northern Wellsville Mountain, Utah, *in* Kerns, G.J., and Kerns, R.L., Jr., eds., Orogenic patterns and stratigraphy of north-central Utah and southeastern Idaho: Utah Geological Association Publication 14, p. 47-54.
Parry, W.T., and Bruhn, R.L., 1986, Pore fluid and seismogenic characteristics of fault rock at depth on the Wasatch fault, Utah: Journal of Geophysical Research, v. 91, no. B1, p. 730-744.
______1987, Fluid inclusion evidence for minimum 11 km vertical offset on the Wasatch fault, Utah: Geology, v. 15, p. 67-70.
Pavlis, T.L., and Smith, R.B., 1980, Slip vectors on faults near Salt Lake City, Utah, from Quaternary displacements and seismicity: Bulletin of the Seismological Society of America, v. 70, p. 1521-1526.
Perry, W.J., Roeder, D.H., and Lageson, D.R., compilers, 1984, North American thrust-faulted terranes: American Association of Petroleum Geologists Reprint Series No. 27, 466 p.
Personius, S.F., 1985, Preliminary assessment of late Quaternary displacement along the Wasatch fault zone near Brigham City, Utah: Geological Society of America Abstracts with Programs, v. 17, no. 4, p. 261.
______1986, The Brigham City segment—A new segment of the Wasatch fault zone, northern Utah: Geological Society of America Abstracts with Programs, v. 18, no. 5, p. 402.
Pricha, Frank, and Gibson, R.I., 1985, Cordilleran hingeline—Late Precambrian rifted margin of the North American craton and its impact on the depositional and structural history, Utah and Nevada: Geology, v. 13, p. 465-468.
Richard, J.J., 1986, Interpretation of a seismic section across the Danforth Hills anticline (Maudlin Gulch) and Axial Arch in northwest Colorado, *in* Stone, D.S., ed., New interpretations of northwest Colorado geology: Denver, Colo., Rocky Mountain Association of Geologists, p. 191-193, 2 folded unscaled plates.
Riess, S.K., 1985, Structural geometry of the Charleston thrust fault, central Wasatch Mountains, Utah: Salt Lake City, Utah, University of Utah, M.S. thesis, 73 p., 2 folded plates, scales about 1:85,000 and about 1:24,000.
Rigby, J.K., 1958, Geology of the Stansbury Mountains, eastern Toole County, Utah: Utah Geological Society Guidebook No. 13, p. 1-134.
______1959, Upper Devonian unconformity in central Utah: Geological Society of America Bulletin, v. 70, p. 207-218.

Ritzma, H.R., 1969, Tectonic resume, Uinta Mountains, *in* Lindsay, J.B., ed., Geologic guidebook of the Uinta Mountains, Utah's maverick range: Intermountain Association of Geologists, Annual field conference, 16th, September 4-6, 1969, Guidebook, p. 57-63.

Roberts, R.J., 1960, Paleozoic structure in the Great Basin [abs.]: Geological Society of America Bulletin, v. 71, p. 1955.

Roberts, R.J., Crittenden, M.D., Jr., Tooker, E.W., Morris, H.T., Hose, R.K., and Cheney, T.M., 1965, Pennsylvanian and Permian basins in northwestern Utah, northeastern Nevada and south-central Idaho: American Association of Petroleum Geologists Bulletin, v. 49, p. 1926-1956.

Robinson, Peter, 1972, Tertiary history, *in* Mallory, W.W., ed.-in-chief, Geologic atlas of the Rocky Mountain region: Denver, Colo., Rocky Mountain Association of Geologists, p. 233-242.

Rose, P.R., 1976, Mississippian carbonate shelf margins, western United States, *in* Hill, J.G., ed., Geology of the Cordilleran hingeline: Denver, Colo., Rocky Mountain Association of Geologists, p. 135-151.

Ross, R.J., Jr., 1976, Ordovician sedimentation in the western United States, *in* Hill, J.G., ed., Geology of the Cordilleran hingeline: Denver, Colo., Rocky Mountain Association of Geologists, p. 109-133.

Royse, Frank, 1983, Extensional faults and folds in the foreland thrust belt, Utah, Wyoming, Idaho: Geological Society of America Abstracts with Programs, v. 15, no. 5, p. 295.

Royse, Frank, Warner, M.A., and Reese, D.L., 1975, Thrust belt structural geometry and related stratigraphic problems, Wyoming-Idaho-northern Utah, *in* Bolyard, D.W., ed., Deep drilling frontiers of the central Rocky Mountains: Denver, Colo., Rocky Mountain Association of Geologists, p. 41-54.

Sandberg, C.A., Gutschick, R.C., Johnson, J.G., Poole, F.G., and Sando, W.J., 1982, Middle Devonian to Late Mississippian geologic history of the overthrust belt region, western United States, *in* Powers, R.B., ed., Geologic studies of the Cordilleran thrust belt: Denver, Colo., Rocky Mountain Association of Geologists, p. 691-719.

Sbar, M.L., Barazangi, Muawia, Dorman, James, Scholz, C.H., and Smith, R.B., 1972, Tectonics of the Intermountain Seismic Belt, western United States—Microearthquake seismicity and composite fault plane solutions: Geological Society of America Bulletin, v. 83, p. 13-28.

Schirmer, T.W., 1985, Basement thrusting in north-central Utah—A model for the development of the northern Utah highland, *in* Kerns, G.J., and Kerns, R.L., Jr., eds., Orogenic patterns and stratigraphy of north-central Utah and southeastern Idaho: Utah Geological Association Publication 14, p. 129-143.

Schwartz, D.P., and Coppersmith, K.J., 1984, Fault behavior and characteristic earthquakes—Examples from the Wasatch and San Andreas fault zones: Journal of Geophysical Research, v. 89, no. B7, p. 5681-5698.

Scott, W.E., and Shroba, R.R., 1985, Surficial geologic map of an area along the Wasatch fault zone in the Salt Lake Valley, Utah: U.S. Geological Survey Open-File Report 85-448, scale 1:24,000, 18 p., 1 folded plate of 2 sheets.

Sears, J.W., Graff, P.J., and Holden, G.S., 1982, Tectonic evolution of lower Proterozoic rocks, Uinta Mountains, Utah and Colorado: Geological Society of America Bulletin, v. 93, p. 990-997.

Sears, J.W., and Price, R.A., 1978, The Siberian connection—A case for Precambrian separation of the North American and Siberian cratons: Geology, v. 6, p. 267-270.

Sibson, R.H., 1982, Fault zone models, heat flow, and the depth distribution of earthquakes in the continental crust of the United States: Bulletin of the Seismological Society of America, v. 72, p. 151-163.

______1984, Roughness at the base of the seismogenic zone—Contributing factors: Journal of Geophysical Research, v. 89, p. 5791-5799.

Skipp, Betty, and Harding, S.T., 1985, Preliminary report on geology of Borah Peak area, Idaho, including interpretation of seismic and gravity data, *in* Stein, R.S., and Bucknam, R.C., eds., Workshop XXVIII On the Borah Peak, Idaho, earthquake, 3-6 October, 1984, Proceedings, v. A: U.S. Geological Survey Open-File Report 85-290, p. 657-671.

Smith, J.T., and Cook, K.L., 1985, Geologic interpretation of gravity anomalies of northeastern Utah, *in* Picard, M.D., ed., Geology and energy resources, Uinta basin of Utah: Utah Geological Association Publication 12, p. 121-146.

Smith, R.B., 1972, Contemporary seismicity, seismic gaps, and earthquake recurrences of the Wasatch Front, *in* Hilpert, L.S., ed., Environmental geology of the Wasatch Front, 1971: Utah Geological Association Publication 1, p. I1-I9.

______1974, Seismicity and earthquake hazards of the Wasatch Front, Utah: Earthquake Information Bulletin, v. 6, no. 4, p. 12-17.

Smith, R.B., and Bruhn, R.L., 1984, Intraplate extensional tectonics of the eastern Basin-Range—Inferences on structural style from seismic reflection data, regional tectonics, and thermal-mechanical models of brittle-ductile deformation: Journal of Geophysical Research, v. 89, no. B7, p. 5733-5762.

Smith, R.B., and Richins, W.D., 1984, Seismicity and earthquake hazards of Utah and the Wasatch Front—Paradigm and paradox, *in* Hays, W.W., and Gori, P.L., eds., Workshop on "Evaluation of regional and urban earthquake hazards and risk in Utah", Salt Lake City, Utah, August 14-16, 1984, Proceedings: U.S. Geological Survey Open-File Report 84-763, p. 73-112.

Smith, R.B., and Sbar, M.L., 1974, Contemporary tectonics and seismicity of the western United States with emphasis on the Intermountain Seismic Belt: Geological Society of America Bulletin, v. 85, p. 1205-1218.

Snay, R.A., Smith, R.B., and Soler, T., 1984, Horizontal strain across the Wasatch Front near Salt Lake City, Utah: Journal of Geophysical Research, v. 89, p. 1113-1122.

Sorensen, M.L., and Crittenden, M.D., Jr., 1976, Preliminary map of the Mantua quadrangle and part of the Willard quadrangle, Box Elder, Weber, and Cache Counties, Utah: U.S. Geolological Survey Miscellaneous Field Studies Map MF-720, scale 1:24,000, 1 sheet.

______1979, Geologic map of the Huntsville quadrangle, Weber and Cache Counties, Utah: U.S. Geological Survey Geologic Quadrangle Map GQ-1503, scale 1:24,000, 1 sheet.

Sprinkel, D.A., Witkind, I.J., and Baer, J.L., 1982, The overthrust belt in central Utah (road log), *in* Nielson, D.L., ed., Overthrust belt in Utah: Utah Geological Association Publication 10, p. 301-334.

Standlee, L.A., 1982, Structure and stratigraphy of Jurassic rocks in central Utah—Their influence on tectonic development of the Cordilleran foreland thrust belt, *in* Powers, R.B., ed., Geologic studies of the Cordilleran thrust belt: Denver, Colo., Rocky Mountain Association of Geologists, p. 357-382.

Steenland, N.C., 1969, An aeromagnetic survey of the Uinta Mountains, *in* Lindsay, J.B., ed., Geologic guidebook of the Uinta Mountains, Utah's maverick range: Intermountain Association of Geologists, Annual field conference, 16th, September 4-6, 1969, Guidebook, p. 47-51, 1 folded plate, approximate scales 1:192,000 and 1:290,000.

Stewart, J.H., 1972, Initial deposits in the Cordilleran geosyncline—Evidence of a late Precambrian (<850 m.y.) continental separation: Geological Society of America Bulletin, v. 83, p. 1345-1360.

Stewart, J.H., Moore, W.J., and Zietz, Isidore, 1977, East-west patterns of Cenozoic igneous rocks, aeromagnetic anomalies, and mineral deposits, Nevada and Utah: Geological Society of America Bulletin, v. 88, p. 67-77.

Stewart, J.H., and Poole, F.G., 1974, Lower Paleozoic and uppermost Precambrian Cordilleran miogeocline, Great Basin, western United States, *in* Dickinson, W.R., ed., Tectonics and sedimentation: Society of Economic Paleontologists and Mineralogists Special Publication No. 22, p. 28-57.

Stokes, W.L., 1963, compiler, Geologic map of Utah, northwest quarter: Salt Lake City, Utah, Utah State Land Board and University of Utah, scale 1:250,000, 1 sheet.

______1976, What is the Wasatch Line?, *in* Hill, J.G., ed., Geology of the Cordilleran hingeline: Denver, Colo., Rocky Mountain Association of Geologists, p. 11-25.

Stokes, W.L., and Madsen, J.H., Jr., 1961, Geologic map of Utah, northeast quarter: Salt Lake City, Utah, Utah State Land Board and University of Utah, scale 1:250,000, 1 sheet.

Stone, D.S., 1986, Seismic and borehole evidence for important pre-Laramide faulting along the Axial Arch in northwest Colorado, *in* Stone, D.S., ed., New interpretations of northwest Colorado geology: Denver, Colo., Rocky Mountain Association of Geologists, p. 19-36.

Swan, F.H., III, Schwartz, D.P., and Cluff, L.S., 1980, Recurrence of moderate to large magnitude earthquakes produced by surface faulting on the Wasatch fault zone, Utah: Bulletin of the Seismological Society of America, v. 70, p. 1431-1462.

Tooker, E.W., 1983, Variations in structural style and correlation of thrust plates in the Sevier foreland thrust belt, Great Salt Lake area, Utah, *in* Miller, D.M., Todd, V.R., and Howard, K.A., eds., Tectonic and stratigraphic studies in the eastern Great Basin: Geological Society of America Memoir 157, p. 61-73.

Tweto, Ogden, 1979, compiler, Geologic map of Colorado: U.S. Geological Survey, scale 1:500,000, 1 sheet.

U.S. Geological Survey, 1976, State of Utah: U.S. Geological Survey, scale 1:500,000, contour interval 500 feet, 1 sheet.

Vacquier, Victor, Steenland, N.C., Henderson, R.G., and Zietz, Isidore, 1951, Interpretation of aeromagnetic maps: Geological Society of America Memoir 47, 151 p., 14 folded plates.

Van Horn, Richard, 1972, Map showing relative ages of faults in the Sugar House quadrangle, Salt Lake County, Utah: U.S. Geological Survey Miscellaneous Investigations Map I-766-B, scale 1:24,000, 1 sheet.

Villien, Alain, and Kligfield, Roy, in press, Thrusting and synorogenic sedimentation in central Utah, *in* Petersen, James, ed., Sedimentation and tectonics in the Rocky Mountain region: American Association of Petroleum Geologists Special Publication.

Wallace, C.A., and Crittenden, M.D., Jr., 1969, The stratigraphy, depositional environment and correlation of the Precambrian Uinta Mountain Group, western Uinta Mountains, Utah, *in* Lindsay, J.B., ed., Geologic guidebook of the Uinta Mountains, Utah's maverick range: Intermountain Association of Geologists, Annual field conference, 16th, September 4-6, 1969, Guidebook, p. 127-141.

Webb, G.W., 1958, Middle Ordovician stratigraphy in eastern Nevada and western Utah: American Association of Petroleum Geologists Bulletin, v. 42, p. 2335-2377.

Welsh, J.E., 1979, Paleogeography and tectonic implications of the Mississippian and Pennsylvanian in Utah, *in* Newman, G.W., and Goode, H.D., eds., Basin and Range symposium and Great Basin field conference: Denver, Colo., Rocky Mountain Association of Geologists, p. 93-106.

Wheeler, R.L., 1984, A plan for evaluating hypothesized segmentation of the Wasatch fault, *in* Hays, W.W., and Gori, P.L., eds., A workshop on "Evaluation of regional and urban earthquake hazards and risk in Utah", Salt Lake City, August 1984, Proceedings: U.S. Geological Survey Open-File Report 84-763, p. 576-605.

______1985, Evaluating point concentrations on a map—Earthquakes in the Colorado lineament: Geology, v. 13, p. 701-704.

Wheeler, R.L., and Krystinik, K.B., 1987a, Evaluating coinciding anomalies along a fault trace—Simulations and statistical procedures: U.S. Geological Survey Bulletin 1802 [in press].

______1987b, Persistent segment boundaries on the Wasatch fault zone, central Utah [abs.]: Seismological Research Letters, v. 58, no. 1, p. 31.

______1987c, Persistent and nonpersistent seismic segmentation of the Wasatch fault zone, Utah: Geological Society of America Abstracts with Programs, v. 19, no. 5, p. 342.

______1987, Persistent and nonpersistent segmentation of the Wasatch fault zone, Utah—Statistical analysis for evaluation of seismic hazard, *in* Gori, P.L., and Hays, W.W., eds., Assessment of regional earthquake hazards and risks along the Wasatch Front, Utah: U.S. Geological Survey Open-File Report 87-585, v. I, p. B1-B124.

Winslow, M.A., 1981, Mechanisms for basement shortening in the Andean foreland fold belt of southern South America, *in* McClay, K.R., and Price, N.J., eds., Thrust and nappe tectonics: Geological Society of London Special Publication No. 9, p. 513-528.

Witkind, I.J., 1982, Salt diapirism in central Utah, *in* Nielson,

D.L., ed., Overthrust belt in Utah: Utah Geological Assocation Publication 10, p. 13–30.
______1983, Overthrusts and salt diapirs, central Utah, *in* Miller, D.M., Todd, V.R., and Howard, K.A., eds., Tectonic and stratigraphic studies in the eastern Great Basin: Geological Society of American Memoir 157, p. 45–59.
Woodward, L.A., 1976, Stratigraphy of younger Precambrian rocks along Cordilleran hingeline, Utah and southern Colorado, *in* Hill, J.G., ed., Geology of the Cordilleran hingeline: Denver, Colo., Rocky Mountain Association of Geologists, p. 83–90.
Zietz, Isidore, Shuey, Ralph, and Kirby, J.R., Jr., 1976, Aeromagnetic map of Utah: U.S. Geophysical Investigations Map GP–907, scale 1:1,000,000, 1 sheet.
Zoback, M.L., 1983, Structure and Cenozoic tectonism along the Wasatch fault zone, Utah, *in* Miller, D.M., Todd, V.R., and Howard, K.A., eds., Tectonics and stratigraphy of the eastern Great Basin: Geological Society of America Memoir 157, p. 3–27.
______1987, Superimposed late Cenozoic, Mesozoic, and possible Proterozoic deformation along the Wasatch fault zone in central Utah, *in* Gori, P.L., and Hays, W.W., eds., Assessment of regional earthquake hazards and risks along the Wasatch Front, Utah: U.S. Geological Survey Open-File Report 87–585, v. I, p. E1–E43.

★ U.S. GPO: 1988 573-047/66,057